THE ROLE OF LIPID SECOND MESSENGERS IN ANGIOGENESIS AND THE VASCULAR ENDOTHELIUM RESPONSE TO RADIATION

By

Amanda Gwynn Linkous

Dissertation

Submitted to the Faculty of the

Graduate School of Vanderbilt University

in partial fulfillment of the requirements

for the degree of

DOCTOR OF PHILOSOPHY

in

Cancer Biology

December, 2009

Nashville, Tennessee

Approved:

Professor Dennis Hallahan

Professor Jin Chen

Professor Michael Freeman

Professor P. Charles Lin

Professor John Oates

ACKNOWLEDGEMENTS

The work presented in this dissertation would not have been possible without the extraordinary mentorship of Dr. Dennis Hallahan. Dr. Hallahan is an outstanding researcher, and his guidance and love of science have provided constant encouragement throughout my graduate career. In addition to his role in the experimental design, Dennis continually advocated my career development through publications, grant-writing instruction, and endless opportunities to present my research at national meetings. I have been extremely fortunate to have Dr. Hallahan as my mentor and am sincerely grateful for all of his help along the way.

I would like to thank the members of my dissertation committee, Dr. Jin Chen, Dr. Charles Lin, Dr. Michael Freeman, and Dr. John Oates for their experimental advice and direction. I also wish to declare my devout appreciation to all of the members of the Hallahan laboratory. Even when experiments failed, my lab mates made each day fun and exciting, and I will cherish all of the memories that we created together.

Finally, I want to express my deepest gratitude to my family. As a two-time cancer survivor, my mother, Marcella Mullins, has been my inspiration for entering the field of cancer research. I also want to thank my father, Dallas Mullins, whose support and confidence in my abilities has been unwavering. My siblings, Dallas and Sherry, have consistently provided loving words and much needed comic relief during stressful times. Lastly, I want to thank my husband, Aaron, for embarking on this difficult, but rewarding journey with me. His constant love and understanding have been my foundation, and to him I am forever indebted.

TABLE OF CONTENTS

Page

LIST OF FIGURES

CHAPTER I

INTRODUCTION

Radioresistance

Although modifications in therapeutic protocols have improved tumor response, local recurrence in lung cancer and glioblastoma (GBM) continues to be a problem for radiation therapy (Clamon et al., 1999; DeAngelis, 2001; Lee et al., 1999; Wagner, 2000). Both tumors are highly resistant to radiation and are, therefore, classified as some of the most difficult types of cancer to treat. In an attempt to improve the outcome of GBM patients, there have been many efforts to intensify radiotherapy including brachytherapy and radioactive seeds implanted in the tumor bed that deliver an additional 60 Gy, but none have improved survival (DeAngelis, 2001; Suh and Barnett, 1999; Videtic et al., 1999). Brachytherapy has been replaced by stereotactic radiosurgery, which is noninvasive and easier to administer. However, only tumors 3 cm or less in diameter are amenable to stereotactic radiosurgery, and only if they are not located immediately adjacent to critical structures such as the optic nerve or brain stem (Tokuuye et al., 1998). Despite aggressive treatment, most patients die of the disease, with median survival of about one year for glioblastoma.

A similar scenario exists for lung cancer. Although modest survival benefit has been observed with surgery and radiotherapy, an efficacy plateau has been reached (Amir et al., 2008). Despite surgery and radiation treatment, approximately 30 to 40% of patients with non–small-cell lung cancer (NSCLC) who have discrete lesions and histologically negative lymph nodes die of recurrent disease (Brock et al., 2008; Hoffman et al., 2000; Martini et al., 1995; Mountain, 1997). It has become

obvious, therefore, that additional treatments are needed in order to provide an improved survival benefit for these patients (Amir et al., 2008). Currently, the most common approach to improve the outcome of radiotherapy is to combine radiation with chemotherapeutic agents (Dietz et al., 2008; Forastiere et al., 2006; Iranzo et al., 2008; McGinn et al., 1996; Stratford, 1992). However, many of the platinum-based chemotherapeutic agents used as standard treatment for cancer exhibit toxicity within normal tissues (Arany and Safirstein, 2003; Berns and Ford, 1997; Goldstein and Mayor, 1983; Mackall, 2000; Wang et al., 2004). Therefore, the development of non-toxic, yet effective molecular-targeted radiosensitizers is essential for improvement of the therapeutic ratio.

Vascular endothelial response to radiation

Understanding the response of the tumor microenvironment to ionizing radiation is important for the development of efficient radiosensitizing agents (Levy et al., 1995b; Shweiki et al., 1995; Wachsberger et al., 2003). The effectiveness of radiotherapy is often limited by the response of tumor vascular endothelium (Wachsberger et al., 2003; Yazlovitskaya, 2008). Several studies have demonstrated that clinically relevant doses of ionizing radiation (2-5 Gy) elicit the activation of both PI3K/Akt and MAPK pro-survival signaling pathways in tumor endothelium (Dent et al., 2003a; Yazlovitskaya, 2008; Zhan and Han, 2004; Zingg et al., 2004). The result of such activation is increased radioresistance within the tumor blood vessels. Since destruction of the tumor vascular network enhances the treatment of cancer (Folkman, 1971; Strijbos et al., 2008), radiosensitizers that target these survival pathways could improve the outcome of cancer.

Upon irradiation, signal transduction is generated during the interaction of ionizing radiation with cellular membranes (Haimovitz-Friedman et al., 1994; Valerie et al., 2007). In chapter III, we demonstrate that ionizing radiation interacts with vascular endothelial cell membranes to activate cytosolic phospholipase A2 ($cPLA_2$) and produce a biologically active lysophospholipid known as lysophosphatidylcholine (LPC). This LPC generation results in increased cellular viability and contributes to the overall radioresistance of vascular endothelial cells.

Cytosolic phospholipase A2 and lysophosphatidylcholine production

$cPLA_2$ is an 85-kDa Ca^{2+}-sensitive protein that belongs to a superfamily of PLA_2 enzymes. On the basis of biological properties, mammalian PLA_2 can be classified into 3 major categories: cytosolic PLA_2 ($cPLA_2$), intracellular Ca^{2+} independent PLA_2 ($iPLA_2$), and secretory PLA_2 ($sPLA_2$). This family of enzymes is responsible for the hydrolysis of the sn-2 acyl bond of glycerophospholipids on the cell membrane. As a result of this hydrolysis, both free fatty acid and lysophospholipids are generated. Calcium binding to the amino-terminal CalB domain of $cPLA_2$ promotes the translocation of the ubiquitously distributed $cPLA_2$ from the cytosol to the cell membrane (Clark et al., 1991). Once there, $cPLA_2$ then specifically cleaves the acyl ester bond of phosphatidylcholine (PC) (Farooqui et al., 2006; Grewal et al., 2005; Herbert et al., 2007; Nakanishi and Rosenberg, 2006) to produce lysophospholipids and release arachidonic acid (AA) (1). This cytosolic form of PLA_2 has been implicated in diverse cellular responses such as mitogenesis, differentiation, and inflammation (Yazlovitskaya, 2008). Radiation-induced activation of $cPLA_2$ in vascular endothelial cells resulted in the increased production of LPC, a lipid-derived second messenger which triggered Akt and ERK1/2 phosphorylation (Yazlovitskaya,

2008). LPC activates a wide range of cell types within the vascular system and can regulate a variety of biological functions including cytokine synthesis, chemotaxis, and endothelial growth factor expression (Fujita et al., 2006; Marathe et al., 2001). According to our data and others, LPC could induce signal transduction through a variety of receptors. The result of this signaling cascade is an increase in endothelial cell proliferation and survival (Fujita et al., 2006; Yazlovitskaya, 2008).

Autotaxin and lysophosphatidic acid production

In addition to its transactivation of downstream receptors, LPC may also be hydrolyzed into lysophosphatidic acid (LPA) which has been shown to stimulate cell proliferation, migration, and survival and has been implicated in tumor progression (Ptaszynska et al., 2008; Ren et al., 2006). Signaling of LPA is primarily mediated through classic G protein-coupled receptors belonging to the endothelial differentiation gene (EDG) family (LPA_1/EDG-2, and LPA_2/EDG-4). LPA can also exert its role through other receptors such as LPA_3/EDG-7, LPA_4/GPR23, and LPA_5/GPR92. The primary enzyme responsible for the hydrolysis of LPC to LPA is autotaxin (Hama et al., 2004; Jansen et al., 2005; Tokumura et al., 1986; Umezu-Goto et al., 2002). Autotaxin is a member of the ectonucleotide pyrophosphatase and phosphodiesterase family of enzymes, but unlike other members of this group, autotaxin possesses robust lysophospholipase D activity (Jansen et al., 2005; Ptaszynska et al., 2008). It is synthesized as a 103 kDa secreted protein and is upregulated in a variety of malignancies, including lung cancer and glioblastoma (Jansen et al., 2005; Kishi et al., 2006). Although initially purified from melanoma cells as a potent chemoattractant (Stracke et al., 1992), autotaxin has since been

shown to stimulate cell proliferation and enhance tumor invasion and metastasis (Tanaka et al., 2006).

Tumor angiogenesis

Recent data suggests that autotaxin facilitates tumor progression by promoting angiogenesis (Nam et al., 2001; Tanaka et al., 2006). In autotaxin-null mouse embryos, early blood vessels formed normally, but failed to develop into mature vessels (Tanaka et al., 2006). Thus, autotaxin appears to play a role in the stabilization and maturation of preformed vasculature. Judah Folkman first illuminated the crucial role of tumor angiogenesis by hypothesizing that tumor growth was dependent upon the formation of a functional vascular network (Dewhirst et al., 2008; Folkman, 1971). Early works by Folkman and others helped demonstrate that tumors require angiogenesis in order to maintain a constant nutrient supply. Such experiments became the foundation for the concept that angiogenesis inhibition can prevent tumor progression by maintaining tumors in a state of quiescence. It is now well-established that angiogenesis occurs in the majority of human solid tumors. However, this new blood vessel formation is often inefficient and frequently leads to defective delivery of oxygen and nutrients to the tumor. These inadequacies within the tumor vasculature help facilitate a vicious cycle of unsatisfied nutrient demand by the tumor, which drives continued aberrant angiogenesis (Dewhirst et al., 2008). On the basis of this concept, the *in vivo* results from the autotaxin-null embryos raise the possibility that, in addition to stimulating tumor cell proliferation and motility, autotaxin supports an invasive microenvironment for vascular endothelial cells as well as tumor cells. Because LPC and LPA are regulators of migration and cellular growth in a variety of cell systems, these lipid mediators may be the effectors of the

motogenic actions of autotaxin. Therefore, lipid second messengers may play a critical role in angiogenesis as well as the tumor vascular response to ionizing radiation. In chapter VI, we address the roles of $cPLA_2$ and lysophospholipids in tumor angiogenesis.

Summary

Despite advances in cancer treatment protocols, lung cancer and glioblastoma continue to be some of the most difficult malignancies to treat. This resistance to therapeutic agents is often determined by the response of the tumor blood vessels. The combined findings in this dissertation demonstrate key regulatory roles for cytosolic phospholipase A2 and lysophospholipids in tumor angiogenesis and the tumor vasculature response to radiation (**Figure 1**). In addition, these results suggest that $cPLA_2$ may serve as an effective, novel molecular target for anti-angiogenesis therapy and tumor sensitization to radiation therapy.

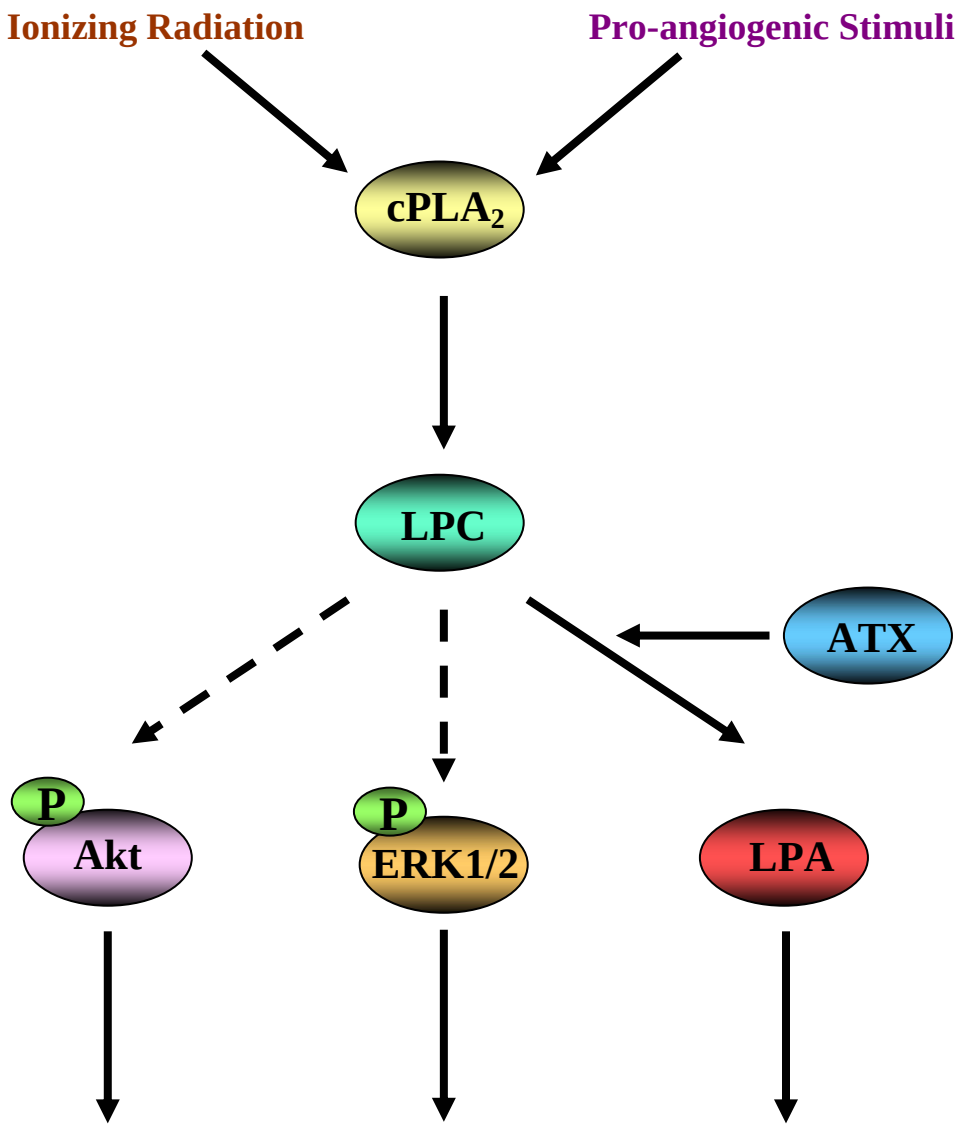

Radioresistance and Tumor Angiogenesis

Figure 1. Proposed role of $cPLA_2$ in tumor angiogenesis and the vascular endothelial response to radiation. Pro-angiogenic stimuli and ionizing radiation (3 Gy) trigger the activation of $cPLA_2$ which leads to increased production of LPC in vascular endothelial cells. Increased LPC generation initiates the downstream phosphorylation of pro-survival signaling molecules, including Akt and ERK1/2. Alternatively, LPC may be converted into LPA by Autotaxin which is expressed by tumor cells as well as vascular endothelial cells. LPA then activates pro-survival signal transduction in a GPCR-mediated mechanism. The result of these molecular events is enhanced radioresistance within vascular endothelium and increased tumor angiogenesis.

CHAPTER II

MATERIALS and METHODS

Chemicals

Organic solvents and PLA_2 inhibitors ($AACOCF_3$ and MAFP, cytosolic $cPLA_2$ inhibitors; $PACOCF_3$, Ca^{2+}-independent PLA_2 inhibitor; cyclic (2-naphthylAla-Leu-Ser-2-naphthylAla-Arg), secreted $sPLA_2$-IIA inhibitor I) were purchased from EMD Biosciences (San Diego, CA, USA). 4-[2-[5-Chloro-1-(diphenylmethyl)-2-methyl-1*H*-indol-3-yl]-ethoxy]benzoic Acid (CDIBA) was synthesized by the Vanderbilt Chemical Synthesis Core. Tridecanoyl LPC (13 : 0), palmitoyl LPC (16 : 0); stearoyl LPC (18 : 0); oleoyl LPC (18 : 1); arachidoyl LPC (20 : 0); phosphatidylcholine (PC); phosphatidic acid (PA); lysophosphatidic acid (LPA), and sphingomyelin (SM) were purchased from Avanti Polar Lipids (Alabaster, AL, USA). L-α-lysophosphatidylcholine (LPC) and arachidonic acid (AA) were purchased from Sigma (St. Louis, MO, USA).

Cell culture

Murine lewis lung carcinoma (LLC) cells, human large cell lung cancer H460 cells, A549 lung cancer cells, and murine vascular endothelial cells (3B11) were purchased from American Type Culture Collection (Manassas, VA). Mouse glioblastoma (GL261) cells were obtained from Dr. Yancie Gillespie (University of Alabama-Birmingham, Birmingham, AL). 3B11, LLC, and GL261 cells were maintained in DMEM plus 10% fetal bovine serum and 1% penicillin/streptomycin (Life Technologies, Gaithersburg, MD) in a 37°C and 5% CO_2 environment. H460

and A549 cells were cultured in RPMI 1640 (Life Technologies) supplemented with 10% fetal bovine serum and 1% penicillin-streptomycin. Embryonic fibroblasts from cPLA$_2\alpha^{+/+}$ and cPLA$_2\alpha^{-/-}$ mice (MEF$^{cPLA2\alpha\ +/+}$ and MEF$^{cPLA2\alpha\ -/-}$) were kindly provided by Dr. JV Bonventre (Renal Unit, Brigham Women's Hospital, Harvard Medical School, Boston, MA, USA). MEFs were maintained in Dulbecco's modified Eagle's medium/F-12 (1/1) with 10% FBS and 1% penicillin/streptomycin (Life Technologies, Gaithersburg, MD, USA). MEFs from passages 2–5 were used in this study. Murine Pulmonary Microvascular Endothelial Cells (MPMEC) were isolated from 1-3 month-old mice and were maintained in EGM-2-MV (Cambrex, East Rutherford, NJ). Human Umbilical Vein Endothelial Cells (HUVEC) were obtained from Cambrex (East Rutherford, NJ, USA) and were maintained in EGM-2-MV. HUVEC from passages 2-5 were used. For the irradiation of cells, a Therapax DXT 300 X-ray machine (Pantak Inc., East Haven, CT, USA) delivering 2.04 Gy/min or Mark I 137Cs irradiator (JL Shepherd and Associates, San Fernando, CA, USA) delivering 1.84 Gy/min was used. Due to the high sensitivity of HUVECs to temperature and pH, cells were transported to and from the irradiator in a gas/temperature-controlled chamber (5% CO_2, 37°C).

Isolation of mouse lung endothelial cells

Primary cultures of MPMEC were isolated as described previously (Pozzi et al., 2000). Briefly, 1-3 month-old C57/BL6 mice were anesthetized, and the lung vasculature was perfused with PBS and 2 mmol/L EDTA followed by 0.25% trypsin and 2 mmol/L EDTA via the right ventricle. The heart and lungs were excised and incubated at 37°C for 20 min. The visceral pleura were removed, and the perfusion was repeated. Primary vascular endothelial cells were recovered and grown on tissue

culture plates coated with 0.2% gelatin for approximately 2 weeks in EGM-2-MV containing 5% FCS. Endothelial cell purity was greater than 95% as determined by expression of von Willebrand Factor, an endothelial cell marker.

Mouse tumor models, treatment and tumor growth delay studies

Institutional Animal Care and Use Committee (IACUC) guidelines were followed when handling and treating all mice used in this study (IACUC-approved protocols M/04/013 and M/07/358). For radiosensitization studies, 10^6 of LLC or H460 cells were implanted into the hind limbs of C57/BL6 mice and nude mice, respectively. Once tumors exceeded 2 mm in diameter, the mice were stratified into groups of 5 to 6 animals representing similar distributions of tumor sizes. Tumor-bearing animals were administered intraperitoneally with vehicle or 10 mg/kg AACOCF3 30 min prior to irradiation with 3 Gy (Therapax DXT 300 X-ray machine; Pantak Inc.). Treatment was repeated for 5 consecutive days. Tumor size was monitored by external caliper measurements. For tumor growth delay studies using CDIBA, 10^6 LLC cells or 2 x 10^6 GL261 cells were implanted into the hind limbs of C57/BL6 mice. Tumor-bearing animals were administered intraperitoneally with vehicle or 0.5-1.0 mg/kg CDIBA once daily for 5 (LLC) or 7 (GL261) consecutive days. Tumor size was monitored by external caliper measurements. For tumor growth studies using the genetic knockout of $cPLA_2\alpha$, $cPLA_2\alpha^{-/-}$ mice were kindly provided by Dr. JV Bonventre (Renal Unit, Brigham Women's Hospital, Harvard Medical School, Boston, MA, USA). 10^6 LLC cells or 2 x 10^6 GL261 cells were implanted into the hind limbs of $cPLA_2\alpha^{+/+}$ and $cPLA_2\alpha^{-/-}$ C57/BL6 mice. Tumor volume was measured using Power Doppler Sonography.

Assessment of LPA from cell supernatants and plasma

For *in vitro* experiments, HUVEC and U87 or D54 cells were plated in 6-well co-culture plates. Confluent cultures were irradiated with 3 Gy and cell supernatants were collected 60 minutes following treatment. LPA was measured using a competitive ELISA assay according to the manufacturer's instructions (Echelon Biosciences Inc., Salt Lake City, UT). For *in vivo* experiments, 10^6 LLC cells or 2 x 10^6 GL261 cells were implanted into the hind limbs of C57/BL6 mice. Once tumors exceeded 4-6 mm in diameter, the mice were stratified into groups of 3-4 animals representing similar distributions of tumor sizes. Tumor-bearing animals were administered intraperitoneally with vehicle or 1.0 mg/kg CDIBA once daily for 5 consecutive days. Blood samples were collected from the tails of anesthetized mice prior to the initiation of treatment and one hour after the final treatment. Samples were immediately processed for plasma isolation and stored at -80°C. LPA concentration was analyzed according to the manufacturer's instructions.

shRNA silencing of cPLA2α

HUVECs were transiently transfected using the pGIPZ lentiviral plasmid vector (Open Biosystems, Huntsville, AL, USA). This bicistronic vector allows estimation of the level of transfection by the expression of shRNA of interest in the first cistron, while keeping a high level of expression from second cistron encoding GFP. The vector contained either nonsilencing shRNA or shRNA specific for human $cPLA_2\alpha$. Quality control of the vectors was performed by restriction enzyme digestion with Sal1. Once HUVECs reached 50% confluency, cells were transfected with 5 μg of shRNA plasmid DNA in low-serum OPTI-MEM. After 48 h of incubation, the medium was aspirated and cells were replenished with endothelial

growth medium. Cells were then examined microscopically for TurboGFP expression to estimate the level of transfection and then subjected to further treatment.

Western immunoblot analysis

After treatment, total cell lysates were harvested from HUVECs, MEFs, 3B11, LLC, or H460 cells at the indicated times. Total protein extraction was performed using M-PER kit (Pierce, Rockford, IL, USA). Protein concentration was quantified using BCA Reagent (Pierce). Protein extracts (40-80 μg) were subjected to western immunoblot analysis using antibodies for the detection of phospho-Akt$^{Thr308/Ser473}$, phospho-ERK1/2$^{Thr202/Tyr204}$, total Akt, cyclin B1 (all from Cell Signaling Technologies, Danvers, MA, USA), total ERK1/2, autotaxin and EDG-4 (all from Santa Cruz Biotechnology, Santa Cruz, CA), EDG-1 (Biomol International, Plymouth Meeting, PA), EDG-2 (Abgent, San Diego, CA), and EDG-3 (Antibody Solutions, Mountain View, CA). An antibody to actin (Sigma) was used to evaluate protein loading in each lane. Immunoblots were developed using the Western Lightning Chemiluminescence Plus detection system (PerkinElmer, Wellesley, MA, USA) according to the manufacturer's protocol.

PLA_2 activity

After treatment, HUVECs were harvested and assayed for PLA_2 activity using a PLA_2 activity kit (Cayman, Ann Arbor, MI, USA) according to manufacturer's instructions. Briefly, 1.5mM arachidonoyl thio-phosphotidylcholine (PLA_2 substrate) was incubated with 20 μL of lysed cells in 96-well plate for 1 h at room temperature. Reaction was stopped by addition of DTNB/EGTA, and optical density (OD) was

measured using Microplate reader at 405 nm. Average fold increase in PLA_2 activity was calculated as (OD of treated samples normalized to sample total protein)/(OD of control normalized to control total protein).

Clonogenic survival

HUVECs were plated on fibronectin-lined plates (BD Biosciences, Bedford, MA, USA) and were allowed to attach for 5 h. Cells were then treated with EtOH or various PLA_2 inhibitors followed by irradiation with 0, 2, 4, or 6 Gy. In separate experiments, 3B11, LLC, and H460 cells were plated and allowed to attach for 5 h. Cells were then treated with EtOH or 1 μmol/L $AACOCF_3$ for 30 min followed by irradiation with 0, 2, 4, or 6 Gy. Medium was changed after irradiation. After 7–14 days, plates were fixed with 70% EtOH and stained with 1% methylene blue. Colonies consisting of over 50 cells were counted with a dissection microscope. Average survival fraction was calculated as (number of colonies/number of cells plated)/(number of colonies for corresponding control/number of cells plated).

Morphologic analysis of cells stained with DAPI or PI

HUVECs were grown on slides, treated with EtOH or $cPLA_2$ inhibitors for 30 min and irradiated with 3 Gy. In shRNA approach, HUVECs were grown on slides, transfected with nonsilencing shRNA or $cPLA_2\alpha$ shRNA and irradiated with 3 Gy 48 h later. $MEF^{cPLA2\alpha\ +/+}$ and $MEF^{cPLA2\alpha\ -/-}$ were grown on slides and irradiated with 3 Gy. After 24, 48, 72, and 96 h post-irradiation, cells were fixed in 100% cold methanol. Cells were stained with 2.5 mg/ml 4',6-diamidino-2-phenylindole (DAPI) in phosphate-buffered saline (PBS) (Life Technologies) or with 1.0 mg/ml PI in PBS. During the shRNA approach, transfected HUVECs were fixed in 4%

paraformaldehyde to retain high level of GFP fluorescence and treated with 100 mg/ml RNase for 30 min at 37°C to prevent RNA staining by PI. Photographs were taken using an Olympus BX60 fluorescent microscope equipped with Retiga 2000R digital camera. Images were processed using AxioVision Software. Giant multinucleated cells (for HUVECs) and cells with nuclear condensation and fragmentation (for HUVECs and MEFs) were counted in multiple randomly selected fields. The average percentage of such cells over total cell number or average fold increase over control was calculated.

Flow cytometry analysis with annexin V-FITC and PI

Treated HUVECs were collected after 24, 48, 72, and 96 h. Annexin V-FITC apoptosis Detection Kit (BD Pharmingen, San Diego, CA, USA) was used for staining of the cells. Briefly, Annexin V-FITC (5 ng) and PI (50 ng) were added to 10^5 cells. Stained cells were analyzed by flow cytometry. For each treatment, the average fold increase of apoptotic cells over control was calculated.

Thin-layer chromatography for LPC detection

HUVECs were grown to 90% confluency in 100mm culture dishes, washed twice with PBS, and labeled for 90 min using ^{3}H-palmitic acid (10 μCi/ml in PBS, pH 7.5) (Perkin Elmer Wellesley, MA, USA). After labeling, cells were washed twice with PBS, treated with 3 Gy, and placed on ice 3 min after the beginning of irradiation. Lipids were extracted using a modified Bligh and Dyer method (Bligh and Dyer, 1959). Briefly, cells were scraped in 0.8 ml of cold acidified MeOH (0.1M HCl:methanol, 1:1, v/v), transferred into cold 1.5 ml tubes, and vortexed for 1 min with 0.4 ml cold chloroform. The extractions were centrifuged at 18 000 x g for 5 min

at 4°C, dried, and dissolved in 20 µl of chloroform. The samples were spotted onto 0.25mm Silica Gel 60Å TLC plate (Whatman Inc., Florham Park, NJ, USA) along with standards (PC, LPC, PA, LPA, and SM), resolved with chloroform:methanol:acetic acid:water (50:28:4:8 by volume) and stained with iodine vapor. The TLC plate was then dried and exposed to a Phosphoimager tritium screen (GE Healthcare, Piscataway, NJ, USA) for 90 h. The average amount of labeled LPC was quantitated using a Typhoon 9400 Variable mode Imager (GE Healthcare).

WST-1 assay for metabolic activity

HUVECs were plated into a 96-well plate at a density of 5 x 10^3 cells per well. The following day cells were treated with varying concentrations of different LPC species (16:0, 18:0, 18:1, or 20:0) dissolved in 70% EtOH. After 24 h of treatment, 10 µl of WST-1 reagent from Rapid Cell Proliferation Kit (EMD Biosciences) were added to each well, followed by 1 h incubation at 37°C. OD was measured using Microplate reader at 460 nm. Average cell survival was calculated as a percent of untreated.

MTS assay for metabolic activity

3B11 cells were plated in 96-well plates (5,000 cells per well) and allowed to attach for 24 hours. Cultures were treated with vehicle or 2 µM CDIBA for 24 or 72 hours in the absence or presence of 10 µM LPC, LPA, or AA. Metabolic activity was analyzed according to the manufacturer's instructions by the CellTiter 96® AQ_{ueous} Non-Radioactive Cell Proliferation Assay (Promega, Madison, WI).

BrdU incorporation assay for cellular proliferation

3B11 cells were plated in 96-well plates (5,000 cells per well) and allowed to attach for 24 hours. Cultures were treated with vehicle or 2 μM CDIBA for 24 or 72 hours in the absence or presence of 10 μM LPC, LPA, or AA. BrdU incorporation was measured by the 5-Bromo-2´-deoxy-uridine (BrdU) Labeling and Detection Kit III (Roche Applied Science, Indianapolis, IN).

Matrigel-based tubule formation assay

In order to analyze capillary-like formation, 24-well plates or 96-well plates were coated with Matrigel (300 μL or 75 μL per well, respectively; BD Biosciences) and incubated for 30 min at 37°C. HUVEC, MPMEC or 3B11 cells were plated over solidified Matrigel and allowed to attach for 30 min prior to treatment. Cells were treated with 1 μM $AACOCF_3$ or 1 μM MAFP 30 minutes prior to irradiation with 3 Gy. Once tubules began to form from the control cells, digital microphotographs of the wells were obtained. Four randomly selected high power fields (HPF) per sample were counted, and tubule formation was quantified as the average number of tubule branches per HPF. For radiation-independent angiogenesis studies, 3B11 or HUVEC were plated over solidified Matrigel and allowed to attach for 30 minutes prior to treatment. Cells were then treated with vehicle or 2 μM CDIBA for 6 hours (3B11) or 24 hours (HUVEC), and tubule formation was quantified.

Boyden chamber transwell invasion and migration assay

HUVEC, 3B11 or MPMEC (100,000 cells/well) were added to the top chamber of 24 well plates with 8 μm matrigel-coated inserts (Costar Corning, Corning, NY). Fresh medium (600 μl) was added to the bottom chamber, and cells

were incubated for 30 minutes to allow attachment. For radiosensitization studies, both chambers were then treated with vehicle or $cPLA_2$ inhibitors (1 μmol/L $AACOCF_3$ or 1 μmol/L MAFP) for 30 min prior to irradiation with 3 Gy. For co-culture experiments, HUVEC and A549 cells were plated on the bottom chamber and treated with 2 μM BrP-LPA for 30 minutes prior to irradiation with 3 Gy. For angiogenesis studies, chambers were treated with 2 μM CDIBA in the absence or presence of 10 μM LPC, LPA, or AA. Cells were incubated for 24 hours at 37°C in 5% CO_2. After 24 hours, all remaining cells on the upper surface of the transwell insert filter were removed with a cotton swab. The insert filters were rinsed in PBS, fixed in 100% methanol, and stained with DAPI (2.5 ng/μl). Migrated cells in 4-6 randomly selected HPFs from each sample were counted, and the average number of migrated cells per HPF was calculated.

Scratch assay for cell migration

HUVEC, A549, 3B11 or LLC cells were grown to 70–80% confluency, and four parallel wounds were created on each plate using a 10 μl pipette tip. HUVEC were treated with vehicle or $cPLA_2$ inhibitors (1 μmol/L $AACOCF_3$ or 1 μmol/L MAFP) for 30 minutes prior to irradiation with 3 Gy. 3B11 and LLC cells were treated with vehicle or the $cPLA_2$ inhibitor CDIBA (2 μM) for 24 hours. Cells were then stained with 1% methylene blue and six HPFs from each sample were counted. The average percentage of cell density in the wounded area for each treatment was calculated as (number of cells in wounded area)/(number of cells in unwounded area).

Ki67 immunofluorescence staining for assessment of proliferation

3B11, MPMEC, or LLC cells were grown to 60–70% confluency on slides. Cultures were treated with vehicle or 2 μM CDIBA (3B11 and LLC cells only) for 24 hours in the absence or presence of 10 μM LPC, LPA, or AA. Cells were then fixed in ice-cold methanol and permeabilized in 0.25% Triton X-100 for 10 minutes at room temperature. Following permeabilization, cells were incubated with rabbit anti-Ki67 antibody (1:100, Abcam Inc., Cambridge, MA) overnight at 4°C and with Alexa Fluor 488-conjugated goat anti-rabbit antibody (1:500, Invitrogen Molecular Probes, Carlsbad, CA) for one hour at room temperature before imaging. Counterstaining was performed using DAPI (2.5 ng/μl), and the number of positively-stained cells was counted using immunofluorescence microscopy (4 HPFs per sample).

Power doppler sonography analyses of tumor blood flow and tumor volume

Tumors were sonographically imaged with a VisualSonics VEVO 770 small animal high resolution ultrasound scanner equipped with a 40 MHz transducer and a mechanically scanned, single-element aperture (VisualSonics). The focal zone of the transducer was set at 6 mm from the scanning surface. The scanning plane was perpendicular to the long axis of the lower extremity along the entire length of the tumor. Three-dimensional images in Power Doppler mode were acquired by computer-controlled translation of the transducer over the whole length of the tumor by acquiring two-dimensional images every 100 Am. The following ultrasound scanner settings were used: Power Doppler transmission frequency-23 MHz, Power Gain 100%, wall filter 2.3 mm/s, scan speed 2.0 mm/s. Three-dimensional tumor volume was reconstructed using semiautomated segmentation of 10 to 12 parallel planes through the two-dimensional images using the VisualSonics image analysis

software. To determine blood flow, the average vascular index (%) was calculated as the ratio of color coded pixels (representing blood flow) to the total pixel volume of the tumor.

Histologic analysis of tumor vascularity

Tumors were resected, fixed in 10% formalin, and sectioned into 5 μm sections. Sections were incubated with 20 μg/mL Proteinase K for antigen retrieval and then hybridized overnight with rabbit antihuman von Willebrand Factor (vWF) antibody (1:100; DakoCytomation). Sections were subsequently incubated with Alexa Fluor 488-conjugated goat antirabbit antibody (1:500; Invitrogen Molecular Probes) for 1 h at room temperature before imaging. Positive staining was observed by immunofluorescent microscopy, and vessels were counted (6 randomly selected HPF per sample). Vascularity was determined as the average number of stained vessels per HPF.

TUNEL staining and immunofluorescence staining for phospho-Akt

Mice bearing LLC tumors received daily intraperitoneal injections of vehicle or 10 mg/kg $AACOCF_3$ 30 min prior to irradiation with 3 Gy. Treatment was continued for 5 consecutive days. Twenty-four hours after the final treatment, tumors were harvested, fixed in 10% formalin, and sectioned into 5 μm sections. Terminal deoxynucleotidyl transferase dUTP nick end labeling (TUNEL) staining was done with the DeadEnd Colorimetric TUNEL System (Promega) following the manufacturer's instructions. Positive staining was observed by light microscopy. To detect Akt phosphorylation, sections were incubated with 20 μg/mL Proteinase K for antigen retrieval and then hybridized overnight at 4°C with antibodies for phospho-

$Akt^{Thr308/Ser473}$ (1:100; Cell Signaling Technologies). Sections were subsequently incubated with Alexa Fluor 488- conjugated goat antirabbit antibody (1:500; Invitrogen Molecular Probes) for 1 h at room temperature. Counterstaining was done using DAPI (2.5 ng/μL), and positive staining was observed by immunofluorescence microscopy.

Immunofluorescence co-staining for vWF and alpha-smooth muscle actin (α-SMA) or desmin

Formalin-fixed LLC tumor sections were treated with 20 μg/ml Proteinase K followed by mouse Ig blocking reagent from the M.O.M. Immunodetection Kit (Vector Laboratories, Burlingame, CA) for one hour at room temperature. Sections were then incubated at 4°C overnight with anti-vWF and anti-α-SMA or anti-desmin (all 1:100, DakoCytomation, Carpinteria, CA). Slides were rinsed in PBS and sections were incubated with DAPI (1:1000), Alexa Fluor 594-conjugated goat anti-mouse antibody (1:200, Invitrogen Molecular Probes, Carlsbad, CA) and Alexa Fluor 488-conjugated goat anti-rabbit antibody (1:500; Invitrogen Molecular Probes) for one hour at room temperature. Positive staining was observed by immunofluorescence microscopy.

Tumor vascular window model and vascular length density analysis

The tumor window model experiment was described previously (Geng et al., 2001). Briefly, LLC tumor cells were injected into the dorsal skinfold of C57/BL6 mice. After approximately 2 weeks, sufficient vascular networks had developed within all of the mice. Mice were then treated with $AACOCF_3$, 3 Gy, or $AACOCF_3$ plus 3 Gy. Prior to treatment, the window frame was marked with coordinates, which were used to photograph the same microscopic field each day. Blood vessel

appearance was monitored at 24-h increments over a period of 120 h. Once the study was complete, color photographs were scanned into Photoshop and analyzed using ImagePro software. Within this software, vascular center lines were positioned along the entire length of the blood vessels. Vascular length density was then calculated by the software as total pixilation of blood vessel length per area of tissue.

Statistical analysis

For univariate analysis, the two sample student t test was applied. All experiments were performed in triplicate and differences between treatment groups were estimated using a 95% confidence interval. To estimate the number of mice required, we note that preliminary data suggested that the $cPLA_2$ inhibitors significantly suppressed tumor growth in irradiated tumors by 3-fold as compared to radiation or drug alone. Assuming a coefficient of variation of 50%, 6-7 tumors per treatment group were evaluated for sufficient precision and comparison of treatment response. Descriptive statistics were performed using SigmaPlot 8.0 data analysis software. Data are presented as group means ± SE. A calculated p-value less than 0.05 was considered statistically significant.

CHAPTER III

CYTOSOLIC PHOSPHOLIPASE A2 REGULATES THE VIABILITY OF IRRADIATED VASCULAR ENDOTHELIUM

Introduction

The immediate molecular events that trigger the biological response to ionizing radiation are initiated by the hydrolysis of water. The resulting hydroxyl radicals interact with cellular components such as DNA resulting in DNA strand breaks and subsequent activation of well described signal transduction pathways. In contrast, immediate signal transduction initiated at the cell membrane is less well characterized. For example, ceramide is generated in endothelial cells within minutes after exposure to 20 Gy that later results in apoptosis (Haimovitz-Friedman et al., 1994; Kolesnick and Fuks, 2003). However, endothelial cell viability is not affected by low doses of radiation (2-5 Gy) pointing to involvement of the activation of pro-survival PI3K/Akt signaling (Edwards et al., 2002; Geng et al., 2004; Tan et al., 2006; Tan and Hallahan, 2003).

There are multiple reports demonstrating increased viability of vascular endothelial cells in response to low doses of ionizing radiation due to activation of pro-survival signaling pathways (Maclachlan et al., 2005; Mikkelsen and Wardman, 2003; Tan et al., 2006; Tan and Hallahan, 2003; Valerie et al., 2007). Biologically active lipids and proteins, such as phospholipases, lipid kinases and phosphatases, that regulate the production of lipid second messengers, can initiate pro-survival signal transduction (Cabral, 2005; Farooqui and Horrocks, 2006). For example, phospholipase A2 (PLA_2) hydrolyzes phospholipids at the *sn-2*-acyl ester bond, generating free fatty acids and lysophospholipid second messengers (Chakraborti,

2003). The PLA_2 superfamily can be divided into 10 enzyme groups by gene sequences. Based on biological properties, the classification of PLA_2 can be simplified into 3 main types: the cytosolic ($cPLA_2$), the secretory ($sPLA_2$) and the intracellular Ca^{2+}-independent ($iPLA_2$) (Chakraborti, 2003). In mammalian cells, the *sn-2*-position of phospholipids is enriched with arachidonic acid, AA (Bonventre, 1999). On the other hand, the most abundant phospholipid in mammalian cell membranes is phosphatidylcholine. Therefore, in addition to the release of free AA, the activation of $cPLA_2$ increases production of lysophosphatidylcholine (LPC).

LPC functions as the second messenger in signal transduction pathways, that regulate a number of cellular responses (Chakraborti, 2003; Prokazova et al., 1998). Recent publications suggest an important role of LPC in endothelial cell activation leading to increased vascular proliferation, migration, expression of adhesion molecules and inflammation. LPC stimulated proliferation in endothelial cells by transactivating the vascular endothelial growth factor receptor 2 and activating Akt and ERK1/2 (Fujita et al., 2006). Increased levels of LPC are linked directly to cytokine and chemokine production in endothelial cells by activating MAPK and PI3K/Akt pathways, thus regulating the chemotaxis of particular leukocyte subpopulations during inflammation (Murugesan et al., 2003). LPC also displays biphasic regulation of inflammatory factors in endothelial cells, causing activation of NF-κB at low concentrations and its inhibition at higher concentrations (Sugiyama et al., 1998).

Pro-survival signal transduction activated by ionizing radiation within vascular endothelium includes phosphatidylinositol 3-kinase/Akt (PI3K/Akt) and mitogen-activated protein kinase (MAPK) pathways (Dent et al., 2003c; Edwards et al., 2002; Maclachlan et al., 2005; Tan et al., 2006; Valerie et al., 2007). These pathways

determine cellular response and sensitivity to radiation by ultimately controlling cell metabolism, proliferation and cell death (Dent et al., 2003b; Valerie et al., 2007). In the present study, we identified a sequence of molecular events in irradiated vascular endothelial cells, constituting an immediate pro-survival signaling pathway activated by ionizing radiation. This pathway involves activation of $cPLA_2$ followed by the increased production of LPC and phosphorylation of Akt and ERK1/2. This pathway can contribute to endothelial cell viability.

Results

Temporal relationship of Akt and ERK1/2 phosphorylation and activation of cytosolic PLA_2 following 3 Gy

We have previously reported radiation-induced phosphorylation of Akt in endothelial cells (Tan et al., 2006; Tan and Hallahan, 2003). Comparison of treated cells with a time-matched sham-irradiated control demonstrated that maximal phosphorylation of Akt, as well as ERK1/2, occurred at 3 minutes after irradiation with 3 Gy (**Figures 2A**, **B**). Increased Akt phosphorylation at Thr^{308}/Ser^{473} was first detected at 2 minutes after exposure to 3 Gy (1.8-fold increase over sham-irradiated control, **Figure 2B**), reached maximum after 3 minutes (2.4-fold increase) and remained elevated at 10 minutes (1.3-fold increase). ERK1/2 phosphorylation at Thr^{202}/Tyr^{204} in response to treatment with 3 Gy was transient, first noticed as early as 2 minutes after the beginning of irradiation (1.3-fold increase), reaching maximum at 3 minutes (1.73-fold increase) and returning to basal level at 10 minutes (**Figure 2B**).

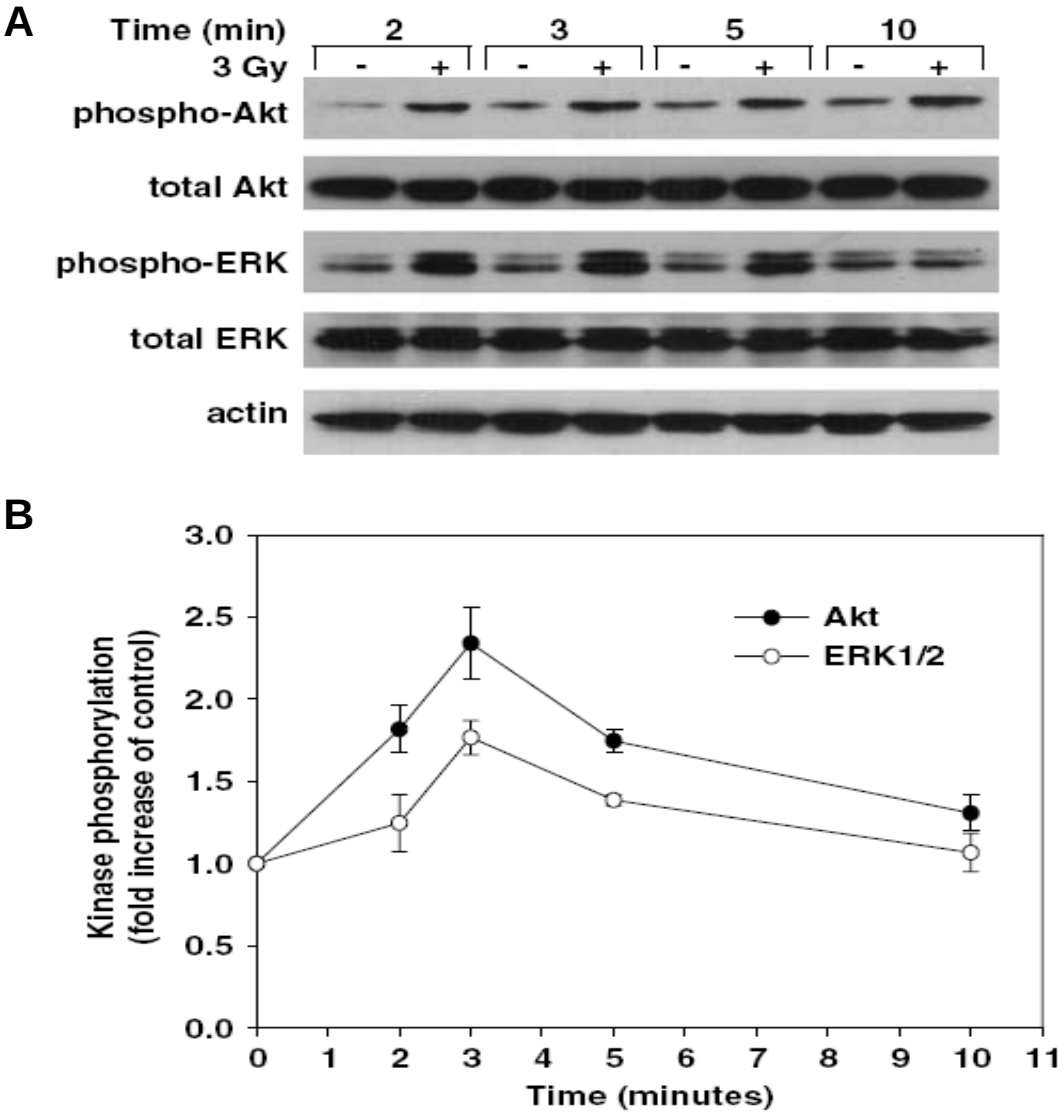

Figure 2. Irradiation with 3 Gy results in immediate phosphorylation of extracellular signal-regulated kinase (ERK)1/2 and Akt in irradiated human humbilical vein endothelial cells (HUVECs). HUVECs were treated with 3 Gy and lysed 2–30 min after the beginning of irradiation. (A) Western blot analysis with phosphospecific antibodies to $Akt^{Thr308/Ser473}$ or $ERK1/2^{Thr202/Tyr204}$, total Akt or ERK1/2, and actin is shown. (B) The densitometry of Akt and ERK1/2 phosphorylation is shown.

Total cellular phospholipase A_2 was activated during a similar time course (**Figure 3A**). The maximal activation of PLA_2 occurred 3 minutes after irradiation (**Figure 3A**; 3.36-fold increase over sham-irradiated control), which coincided with the peak phosphorylation of ERK1/2 and Akt (**Figures 2A, B**). To determine which of the subtypes of the PLA_2 family is activated by 3 Gy, we treated HUVEC with specific inhibitors of $cPLA_2$ (1 μM $AACOCF_3$ or 1 μM MAFP), $sPLA_2$ (100 nM $sPLA_2$-IIA inhibitor I) or $iPLA_2$ (1 μM $PACOCF_3$) for 30 minutes prior to exposure to 3 Gy. The concentrations of inhibitors that were used in experiments were chosen to assure the specific effects for the subtypes of the PLA_2 family. $AACOCF_3$ is a potent and selective slow-binding inhibitor of cytosolic PLA_2 (IC_{50}=2-10 μM for various cells); MAFP is an irreversible inhibitor of both calcium-dependent and calcium-independent cytosolic PLA_2 (IC_{50}=~ 2 and 5 μM for $cPLA_2$ and $iPLA_2$ correspondingly); $sPLA_2$-IIA inhibitor I was shown to effectively block $sPLA_2$-IIA-induced PGE_2 production at 100 nM in human rheumatoid synoviocytes; $PACOCF_3$ is novel Ca^{2+}-independent PLA_2 inhibitor with IC_{50}=3.8 μM. Cells were harvested 3 minutes after the beginning of irradiation. In HUVEC pretreated with inhibitors of $cPLA_2$, radiation-induced activation of PLA_2 was completely abrogated (**Figure 3B**). In comparison, pretreatment of cells with inhibitors of $sPLA_2$ or $iPLA_2$ showed less than 20% decrease in PLA_2 activation (**Figure 3B**). These data suggest that the major PLA_2 subtype activated by low doses of ionizing radiation is the cytosolic isoform, $cPLA_2$. To determine whether $cPLA_2$ participates in radiation-induced phosphorylation of ERK1/2 and Akt, HUVEC were pretreated with the inhibitors for $cPLA_2$, $sPLA_2$ or $iPLA_2$, irradiated with 3 Gy and lysed at 3 minutes after irradiation. Western blot analysis showed that inhibitors of $cPLA_2$, but not the inhibitors of $sPLA_2$ or $iPLA_2$, markedly decreased radiation-induced activation of Akt and ERK1/2,

suggesting that $cPLA_2$ contributes to the radiation-induced activation of these kinases (**Figure 3C**).

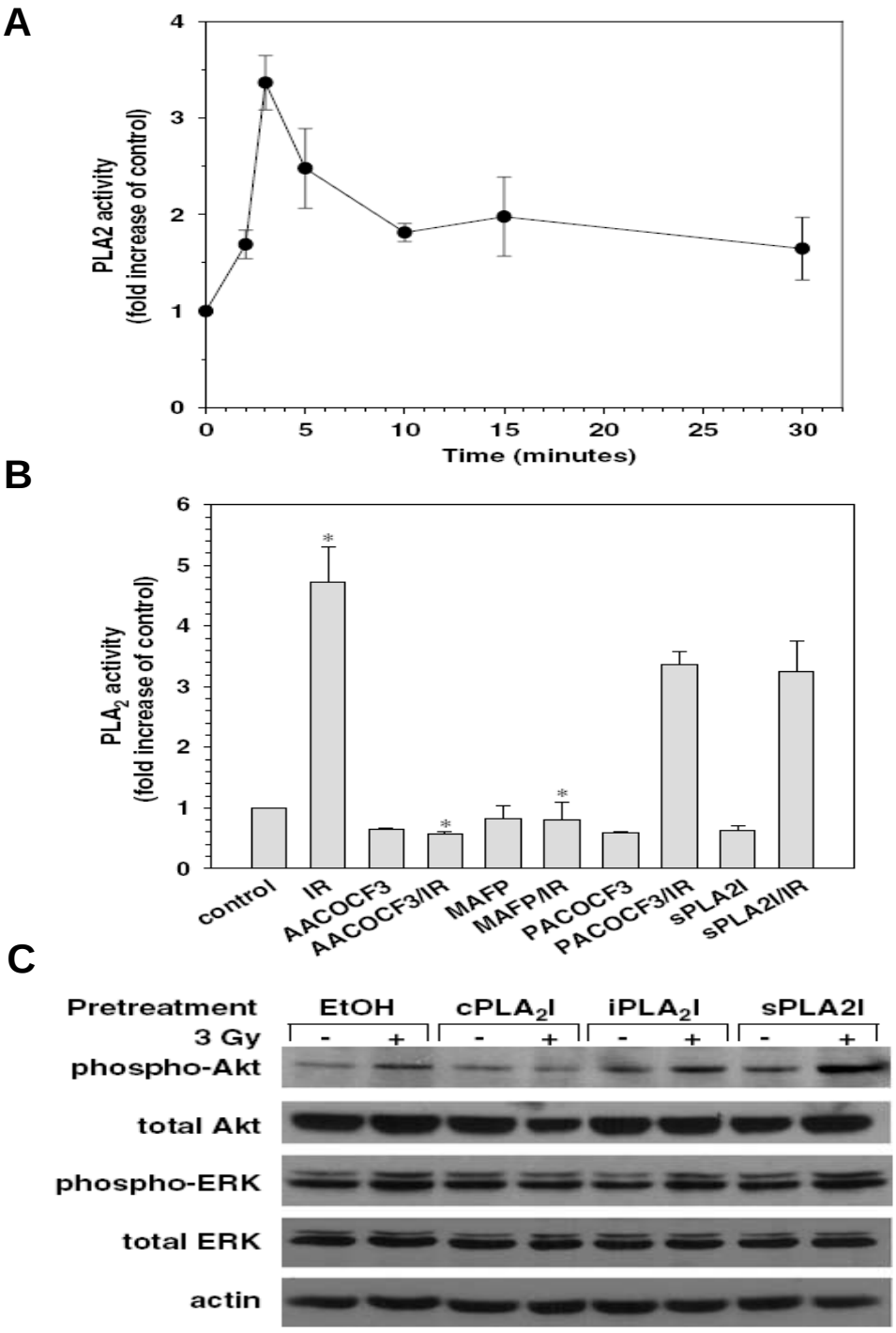

Figure 3. Cytosolic phospholipase A2 ($cPLA_2$) is required for radiation-induced ERK1/2 and Akt phosphorylation in irradiated HUVEC. (**A**) The enzymatic activity of PLA_2 is shown. (**B, C**) HUVEC were treated with 3 Gy or in combination with PLA_2 inhibitors (1 μM $AACOCF_3$; 1 μM MAFP, methyl arachidonyl fluorophosphonate, $cPLA_2$ inhibitors; 1 μM $PACOCF_3$, $iPLA_2$ inhibitor; and 100 nM $sPLA_2I$) which were added 30 minutes before irradiation. Cells were lysed 3 minutes after the beginning of irradiation. (**B**) The enzymatic activity of PLA_2 is shown with SEM from three experiments; ∗, $P < 0.05$. (**C**) Shown is the Western blot for phospho-Akt, phospho-ERK1/2, total Akt or ERK1/2, and actin.

To verify the role of $cPLA_2$, we studied radiation-induced phosphorylation of Akt and ERK1/2 in mouse embryonic fibroblasts (MEF) from $cPLA_2\alpha^{+/+}$ and $cPLA_2\alpha^{-/-}$ mice (Bonventre, 1999), as well as HUVEC that were transiently transfected with non-silencing shRNA or shRNA for the predominant isoform of this enzyme, $cPLA_2\alpha$. Transfection of HUVEC with $cPLA_2\alpha$-shRNA lead to a ~70% decrease in $cPLA_2\alpha$ protein level as compared to non-silencing-shRNA (**Figure 4A**). Irradiation of HUVEC transfected with non-silencing-shRNA resulted in a time course of Akt and ERK1/2 phosphorylation similar to that observed in irradiated non-transfected HUVEC (**Figures 4B** and **2A**). A similar trend, but with less pronounced activation, was observed in irradiated $MEF^{cPLA2\alpha+/+}$ (**Figure 4C**). This decreased effect of radiation could be due to a compensatory mechanism that allows other isoforms of the enzyme to assume the functions of the deficient family member. Radiation-induced phosphorylation of Akt and ERK1/2 was completely abrogated in HUVEC transfected with $cPLA_2\alpha$-shRNA (**Figure 4B**) as well as in $MEF^{cPLA2\alpha-/-}$ (**Figure 4C**) resembling the effect of $cPLA_2\alpha$ inhibitors (**Figure 3C**). These genetic knockdown and knockout models support the regulatory role of $cPLA_2$ and implicate involvement of its α-isoform in the radiation-induced activation of pro-survival kinases Akt and ERK1/2.

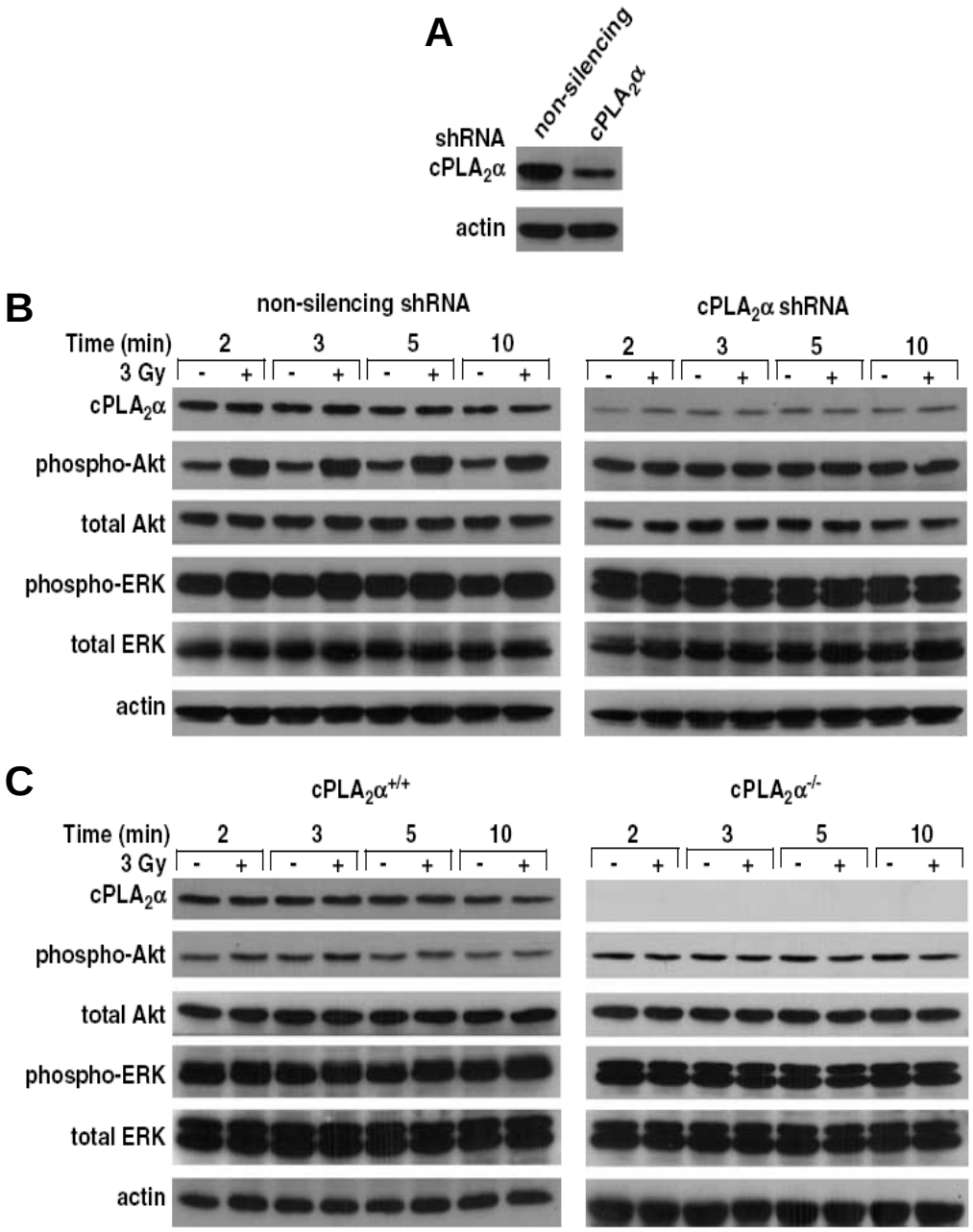

Figure 4. Knockout or knockdown of cPLA$_2\alpha$ prevents radiation-induced ERK1/2 and Akt phosphorylation in irradiated cells. (**A, B**) HUVEC were transiently transfected with non-silencing shRNA or shRNA for cPLA$_2\alpha$, treated with 3 Gy and lysed 2-10 minutes after the beginning of irradiation. Shown is the Western blot analysis for cPLA$_2\alpha$, phospho-Akt, phospho-ERK1/2, total Akt or ERK1/2, and actin. (**C**) Embryonic fibroblasts from mice with wild type cPLA$_2\alpha$ (cPLA$_2\alpha^{+/+}$) and form cPLA$_2\alpha$ KO mice (cPLA$_2\alpha^{-/-}$) were treated with 3 Gy and lysed 2-10 minutes after beginning irradiation. Shown is the Western blot for cPLA$_2\alpha$, phospho-Akt, phospho-ERK1/2, total Akt or ERK1/2, and actin.

Radiation-induced LPC production and effects of exogenously added LPC species

Since the most abundant phospholipid in the mammalian cell membrane is phosphatidylcholine, radiation-induced activation of $cPLA_2$ could lead to the increased production of LPC. To determine whether 3 Gy of radiation induces LPC production, we labeled HUVEC with ^{3}H-palmitic acid for 90 minutes and then treated with 3 Gy. TLC of extracted total lipids from the irradiated HUVEC revealed a statistically significant increase in LPC production of 1.6-fold as compared to untreated cells (**Figure 5A, B**). To determine whether this increase in LPC is involved in radiation-induced signal transduction, we compared HUVEC response to ionizing radiation to the response triggered by various exogenously added LPC species. Four different LPC species (up to 20 μM) led to a slight increase in cell survival (up to 20%, **Figure 5C**). Following this observation, we studied the effect of LPC on the activation of pro-survival pathways. Four LPC species (10 μM) added to HUVEC resulted in ERK1/2 and Akt phosphorylation with the maximum phosphorylation at 5 minutes (**Figure 5D, E**). This maximal phosphorylation time point correlates with the time course of radiation-induced activation of ERK1/2 and Akt (**Figure 2A, B**).

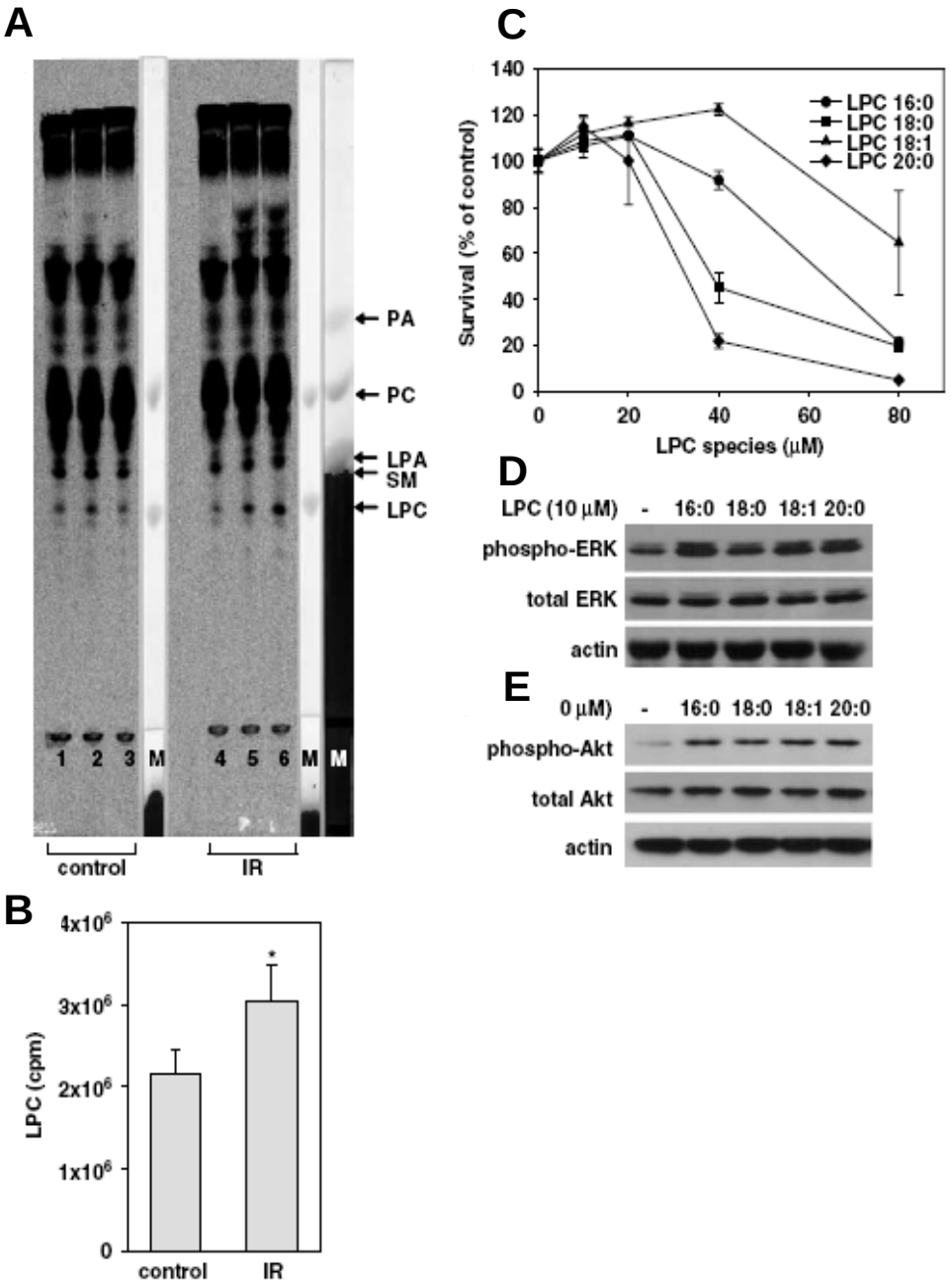

Figure 5. Radiation induces increased LPC production that leads to phosphorylation of ERK1/2 and Akt. (**A, B**) HUVEC were labeled with ^{3}H-palmitic acid for 90 minutes and irradiated with 3 Gy. Total cellular phospholipids were extracted 3 minutes after irradiation. (**A**) Shown is TLC of extracted and standard lipids. (**B**) Shown is a bar graph of the average LPC production for each treatment; ∗, $P < 0.05$M. (**C**) HUVEC were treated with various LPC species (up to 80 μM). Shown are viability curves 24 h after treatment with average percent of survival. (**D, E**) HUVEC were treated with 10 μM of each indicated LPC species. Cells were lysed 5 minutes later and subjected to Western blot analysis for phospho- and total ERK1/2 (**C**), phospho- and total Akt (**D**), and actin.

Involvement of cPLA$_2$ in radiation-induced cell death

To determine the role of cPLA$_2$ in the viability of irradiated endothelial cells, we used specific cPLA$_2$ inhibitors in a number of cell survival assays. Clonogenic survival analysis showed that each inhibitor produced a statistically significant decrease in the viability of HUVEC as compared to irradiation alone (**Figure 6A**). This effect was specific for cPLA$_2$ inhibitors and was not observed when inhibitors for Ca^{2+}-independent or secretory PLA$_2$ were used (**Figure 6B**). To determine the molecular mechanisms of this enhanced cell death, we first analyzed the effect of cPLA$_2$ inhibition on cell cycle regulation in irradiated endothelial cells. As expected (Hwang and Muschel, 1998), radiation alone caused a significant increase in the percentage of cells in G1/G0 phase which was concurrent with a decrease in S-phase at 24-48 hours (data not shown). Similar results were observed in irradiated cells pretreated with cPLA$_2$ inhibitors (data not shown).

We next studied levels of cyclin B1, which regulates the activity of Cdk1 and transition through the cell cycle (Castedo et al., 2002; Kramer et al., 2004). After 24-48 hours of treatment, cyclin B1 was dramatically increased in the cells treated with cPLA$_2$ inhibitors and radiation, while cells treated with radiation alone showed a significant delay in cyclin B1 expression (**Figure 6E**). Since we did not detect any significant differences in cell cycle between irradiated cells and cells treated with cPLA$_2$ inhibitors and radiation, the observed cyclin B1 accumulation was cell cycle-independent which can be associated with mitotic catastrophe (Castedo et al., 2004; Castedo et al., 2002; Ianzini et al., 2006).

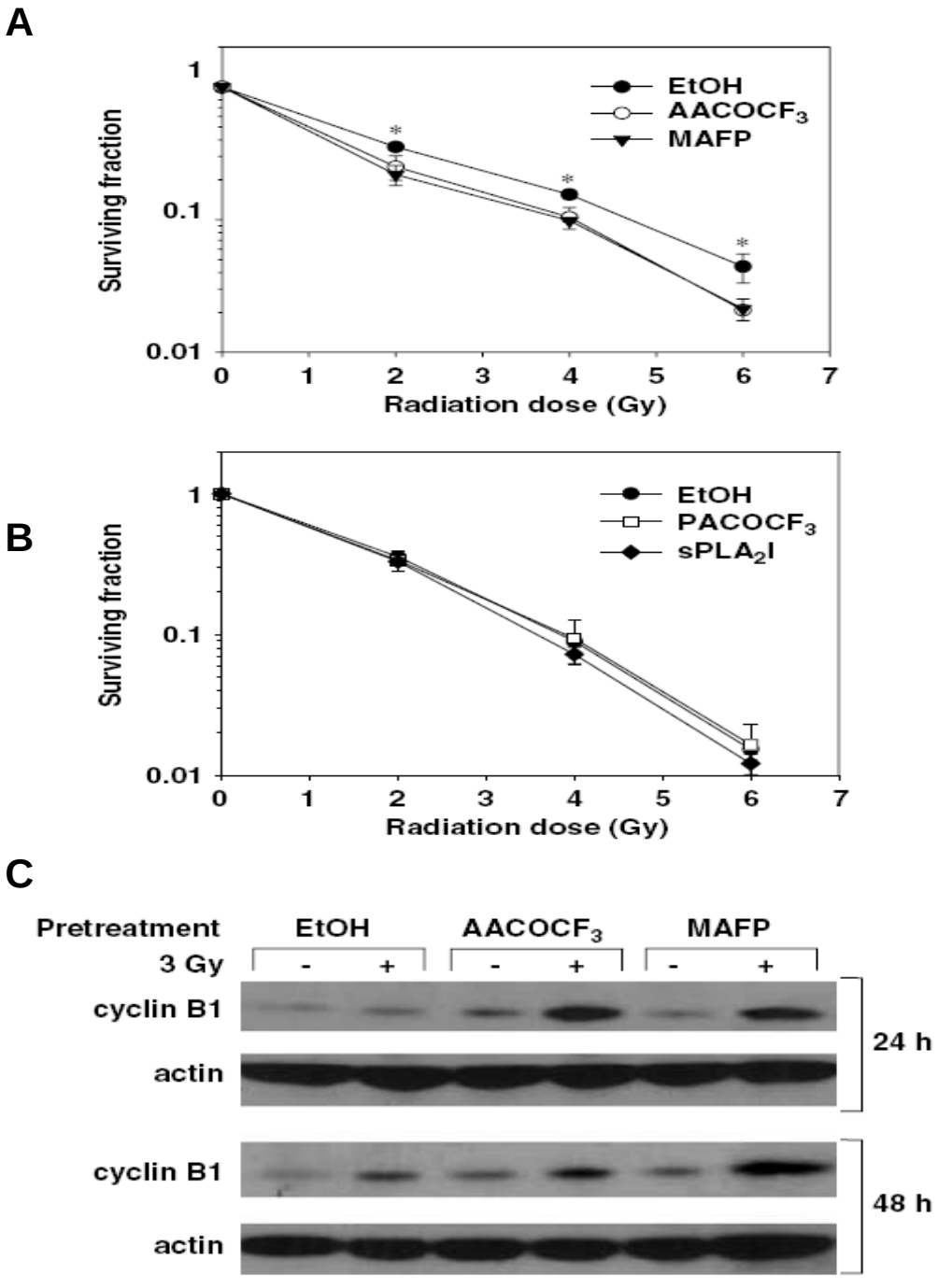

Figure 6. Inhibition of $cPLA_2$ decreases clonogenic survival of irradiated HUVEC and leads to cyclin B1 accumulation within 24-48 hours of irradiation. (**A, B**) HUVEC were plated on fibronectin coated plates. Inhibitors for $cPLA_2$ (**A**) or $iPLA_2$ and $sPLA_2$ (**B**) were added 30 minutes before irradiation. Two weeks later, colonies over 50 cells were counted and normalized for plating efficiency. Shown are average surviving fractions and SEM from three experiments; ∗, $P < 0.05$. (**C**) HUVEC were treated with EtOH (solvent control) or $cPLA_2$ inhibitors for 30 minutes, irradiated with 3 Gy and lysed after 24 or 48 hours. Shown is the Western blot analysis using anti-cyclin B1 and actin antibodies.

Thus, we determined the effect of $cPLA_2$ inhibition on the morphology of irradiated endothelial cells after 24-96 hours of treatment. At 24-48 hours after combined treatment, we observed a 6-fold increase in multinucleated giant cells as compared to control cells (**Figure 7A, B**). This effect was also detected in cells treated with radiation alone, but it was delayed and significantly less pronounced (**Figure 7B**). The formation of multinucleated giant cells concurrent with cell cycle-independent accumulation of cyclin B1 implicates mitotic catastrophe occurring during the inhibition of $cPLA_2$-dependent pro-survival signaling in irradiated endothelial cells.

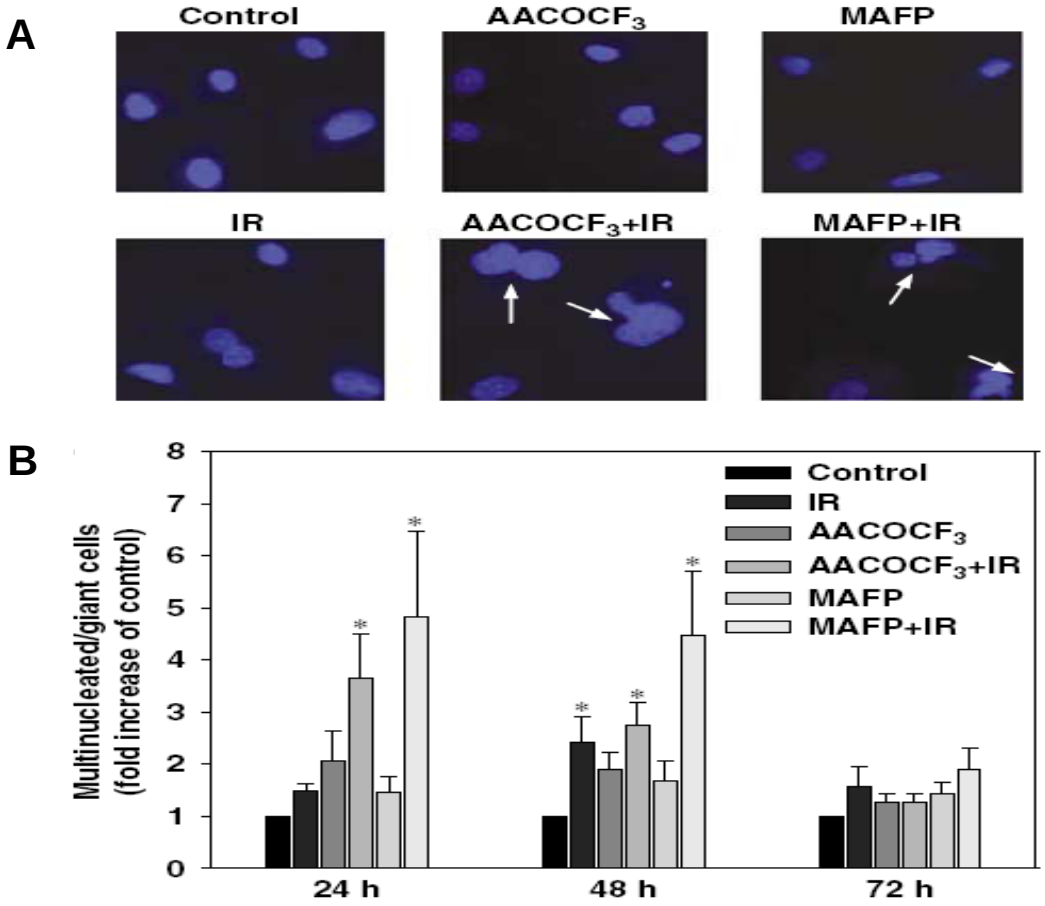

Figure 7. Inhibition of $cPLA_2$ leads to mitotic catastrophe within 24-48 hours of irradiation. (**A, B**) HUVEC were treated with EtOH or $cPLA_2$ inhibitors for 30 minutes, irradiated with 3 Gy and fixed 24, 48 or 72 hrs later. (**A**) Shown are DAPI-stained cells 24 hrs after treatment. Arrows indicate multinucleated/giant cells. (**B**) Cells were counted in 6 HPF. Shown is a bar graph of the average fold-increase in multinucleated/giant cells for each treatment compared to control cells with SEM from four experiments; ∗, $P < 0.05$.

In most cases, mitotic catastrophe evolves to cell death through apoptosis (Castedo et al., 2004; Castedo et al., 2002). To determine whether apoptosis occurred in irradiated HUVEC pretreated with $cPLA_2$ inhibitors, we studied Annexin V and propidium iodide staining as well as nuclear morphology using PI staining. In both assays, we did not detect an increase in programmed cell death at 24-48 hours after treatment (**Figure 8A-C**). However, when HUVEC were pretreated with $cPLA_2$ inhibitors prior to irradiation, the number of Annexin V-positive cells increased by 2-3-fold at 72 hours and by 7-11-fold at 96 hours, as compared to control cells (**Figure 8A, B**). Moreover, PI-staining showed a 30-40% increase in apoptotic nuclei at 72 hours after treatment (**Figure 8C**).

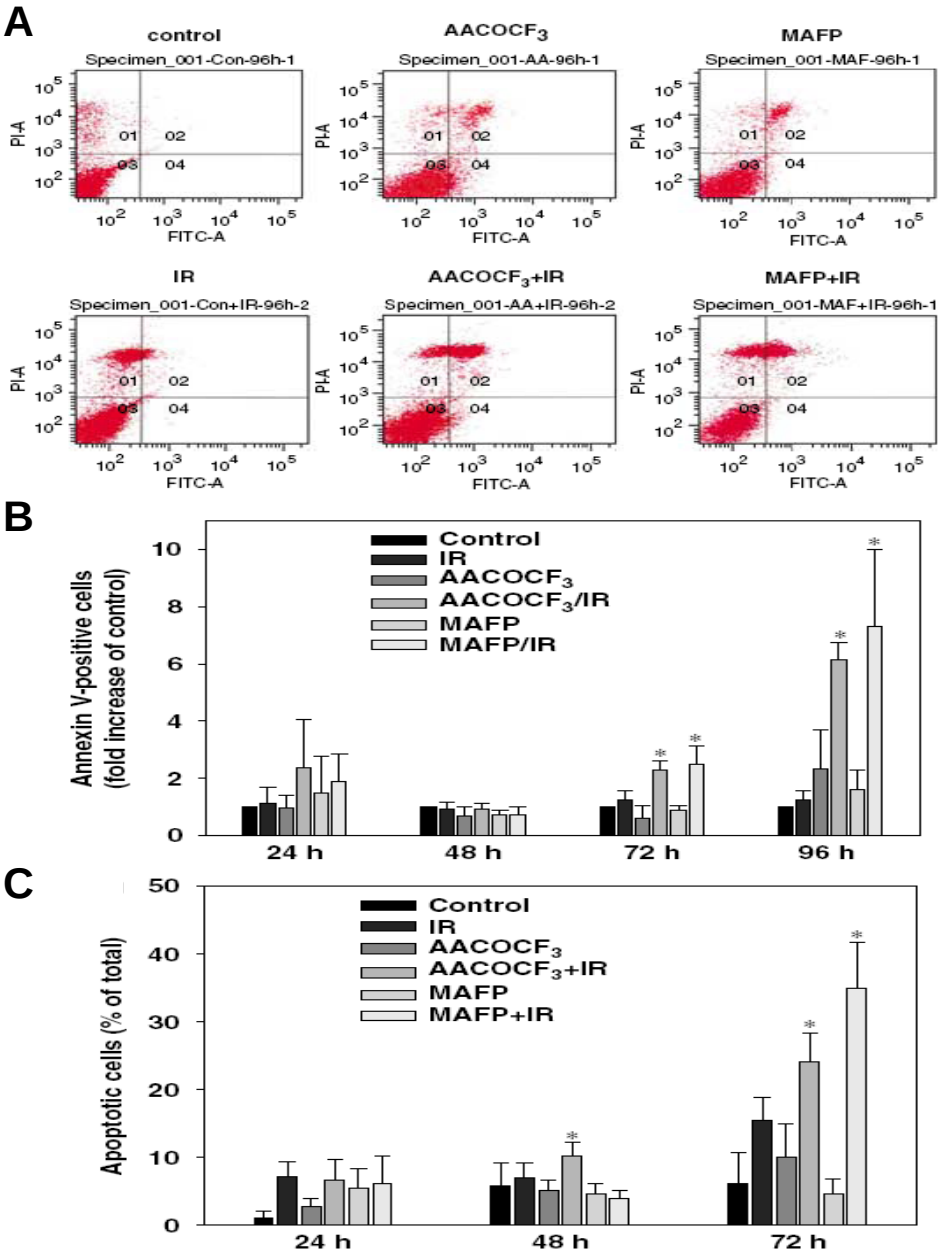

Figure 8. cPLA$_2$ inhibition leads to delayed programmed cell death 72-96 hours after irradiation.(**A, B**) HUVEC were treated with EtOH or cPLA$_2$ inhibitors for 30 minutes, irradiated with 3 Gy, collected after 24, 48, 72 and 96 hours, stained with Annexin V-FITC and PI and analyzed by flow cytometry. Shown are (**A**) representative diagrams of the distribution of stained cells and (**B**) a bar graph of the average fold increase in the percent apoptotic cells in each treatment normalized to control cells with SEM of four experiments; ∗, $P < 0.05$. (**C**) HUVEC were grown on slides, treated with EtOH or cPLA$_2$ inhibitors for 30 minutes, irradiated with 3 Gy, fixed 24, 48 or 72 hours later and stained with PI. Cells with chromatin condensation and nuclear fragmentation were counted in multiple randomly selected fields. Shown is a bar graph of the average percent of apoptotic cells for each treatment with SEM from four experiments; ∗, $P < 0.05$.

To verify the role of $cPLA_2$ in radiation-induced cell viability, we studied mitotic catastrophe and apoptosis in irradiated HUVEC transfected with non-silencing shRNA or $cPLA_2\alpha$ shRNA as well as in irradiated $MEF^{cPLA2\alpha+/+}$ and $MEF^{cPLA2\alpha-/-}$. Trends similar to the effects of $cPLA_2$ inhibitors in irradiated HUVEC were observed in both genetic models (**Figures 9** and **10**). In HUVEC transfected with $cPLA_2\alpha$ shRNA, the mitotic catastrophe at 48 h after irradiation was significantly increased as compared to sham-irradiated cells (60% *vs*. 40%, **Figure 9A, B**). This difference was sustained up to 96 h after radiation, while no statistically significant changes in mitotic catastrophe were observed in irradiated and sham-irradiated HUVEC transfected with non-silencing shRNA over the course of the study (**Figure 9B**). In apoptotic experiments, 24, 48 or 72 hours after irradiation, no significant change was observed in either cell type (**Figure 9C**). However, 96 hours after treatment, irradiated HUVEC transfected with $cPLA_2\alpha$ shRNA but not with non-silencing shRNA demonstrated a modest but statistically significant increase in apoptosis, as compared to sham-irradiated cells (60% vs. 45%, **Figure 9C**). In irradiated $MEF^{cPLA2\alpha+/+}$ and $MEF^{cPLA2\alpha-/-}$, similar levels of multinucleated/giant cells accumulation were observed at 24 and 48 h after treatment as compared to sham-irradiated cells (60% *vs*. 30%, **Figure 10A**). At 72 h, this difference was sustained in irradiated $MEF^{cPLA2\alpha+/+}$, but not in $MEF^{cPLA2\alpha-/-}$ (**Figure 10A**). In the apoptotic study, 24 or 48 hours after irradiation, no significant change was observed in either cell type (**Figure 10B**). However, 72-96 hours after treatment, irradiated $MEF^{cPLA2\alpha-/-}$ demonstrated an increase in apoptosis up to 4-fold, as compared to sham-irradiated cells (**Figure 10B**, 80% vs. 20%). In contrast, we observed no statistically significant increase in apoptosis in irradiated $MEF^{cPLA2\alpha+/+}$ vs. control cells (**Figure 10B**).

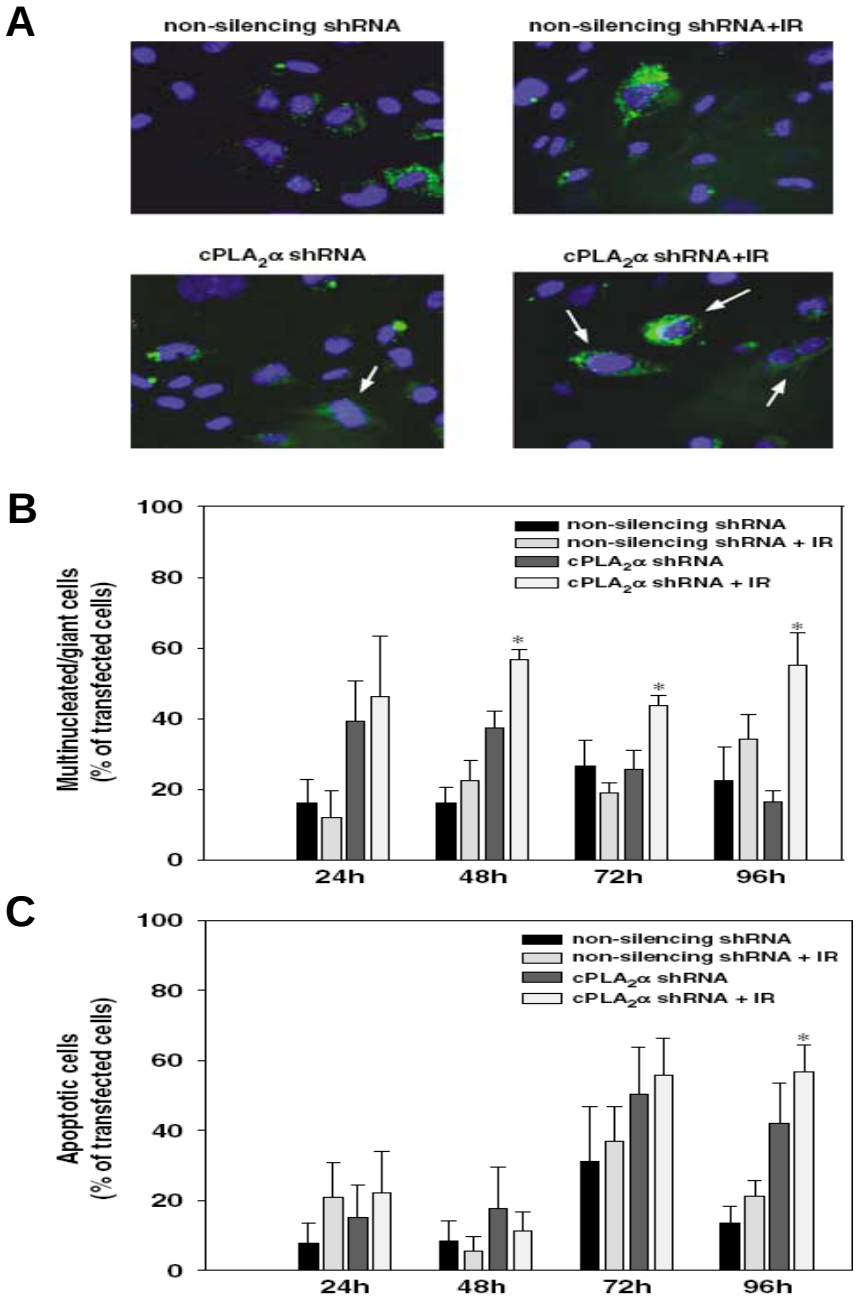

Figure 9. Radiation leads to increase in multinucleated/giant and apoptotic cells following knockdown of cPLA$_2\alpha$. (**A-C**) HUVEC transfected with non-silencing shRNA or cPLA$_2\alpha$ shRNA were irradiated with 3 Gy and fixed 24, 48, 72 or 96 hours later. Cells were stained with DAPI (**A, B**) or PI (**C**). (**A**) Shown are microscopic photographs of DAPI-stained HUVEC 24 hours after treatment. GFP fluorescence (green) indicates transfected cells. Arrows indicate multinucleated/giant cells. (**B**) Multinucleated and giant cells were counted in 6 randomly selected fields. Shown is a bar graph of the average percent of multinucleated giant cells with SEM from triplicates; ∗, $P < 0.05$. (**C**) Cells with chromatin condensation and nuclear fragmentation were counted in 6 randomly selected fields. Shown is a bar graph of the average percentage of apoptotic cells with SEM from triplicates;∗, $P < 0.05$.

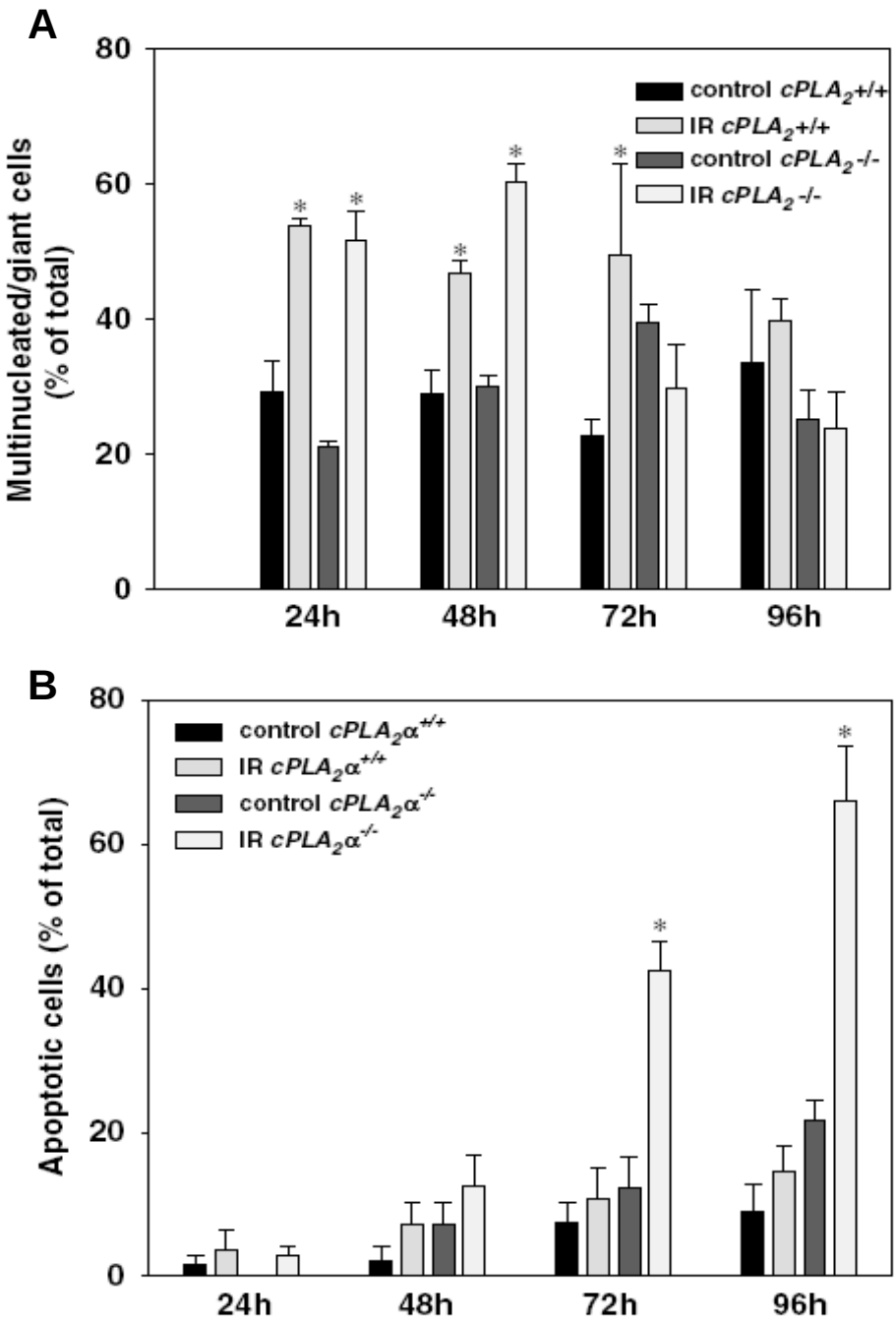

Figure 10. Radiation leads to increase in multinucleated/giant and apoptotic cells following knockout of cPLA$_2\alpha$. Mouse embryonic fibroblasts (*cPLA$_2\alpha^{+/+}$* or *cPLA$_2\alpha^{-/-}$*) were irradiated with 3 Gy and fixed 24, 48, 72 or 96 hours later. Cells were stained with DAPI (**A**) or PI (**B**). (**A**) Multinucleated and giant cells were counted in 6 randomly selected fields. Shown is a bar graph of the average percent of multinucleated giant cells with SEM from triplicates; ∗, $P < 0.05$. (**B**) Cells with chromatin condensation and nuclear fragmentation were counted in 6 randomly selected fields. Shown is a bar graph of the average percentage of apoptotic cells with SEM from triplicates; ∗, $P < 0.05$.

Effects of $cPLA_2$ on endothelial functions in irradiated HUVEC

We investigated the role of $cPLA_2$ in HUVEC migration by using two approaches: endothelial cell migration through a filter and endothelial cell gash closure (**Figure 11**). In both assays, radiation alone or inhibition of $cPLA_2$ with $AACOCF_3$ alone resulted in a 15% decrease in HUVEC migration, which was not statistically significant (**Figure 11A, C**). Inhibition of $cPLA_2$ with MAFP alone demonstrated a greater decrease in gash closure than in migration through the filter (**Figure 11A, C**, 50% vs. 20%), possibly suggesting different mechanisms of $cPLA_2$ inhibition involved in each type of migration. However, inhibition of $cPLA_2$ with either $AACOCF_3$ or MAFP followed by irradiation maximally abolished HUVEC migration in both assays leaving only 40% of cells capable of migration (**Figure 11**).

We also found that inhibition of $cPLA_2$ activity affected endothelial tubule formation in irradiated HUVEC. Untreated cells attached to matrigel when plated and formed capillary–like structures within 24 hours following irradiation. Irradiated cells or cells treated with $cPLA_2$ inhibitors alone did not show a significant difference in the number of capillary-like tubules as compared to that of untreated cells (**Figure 12**). However, irradiation combined with $cPLA_2$ inhibition caused a pronounced decrease of 3-fold (30% of control) in the number of formed tubules (**Figure 12**).

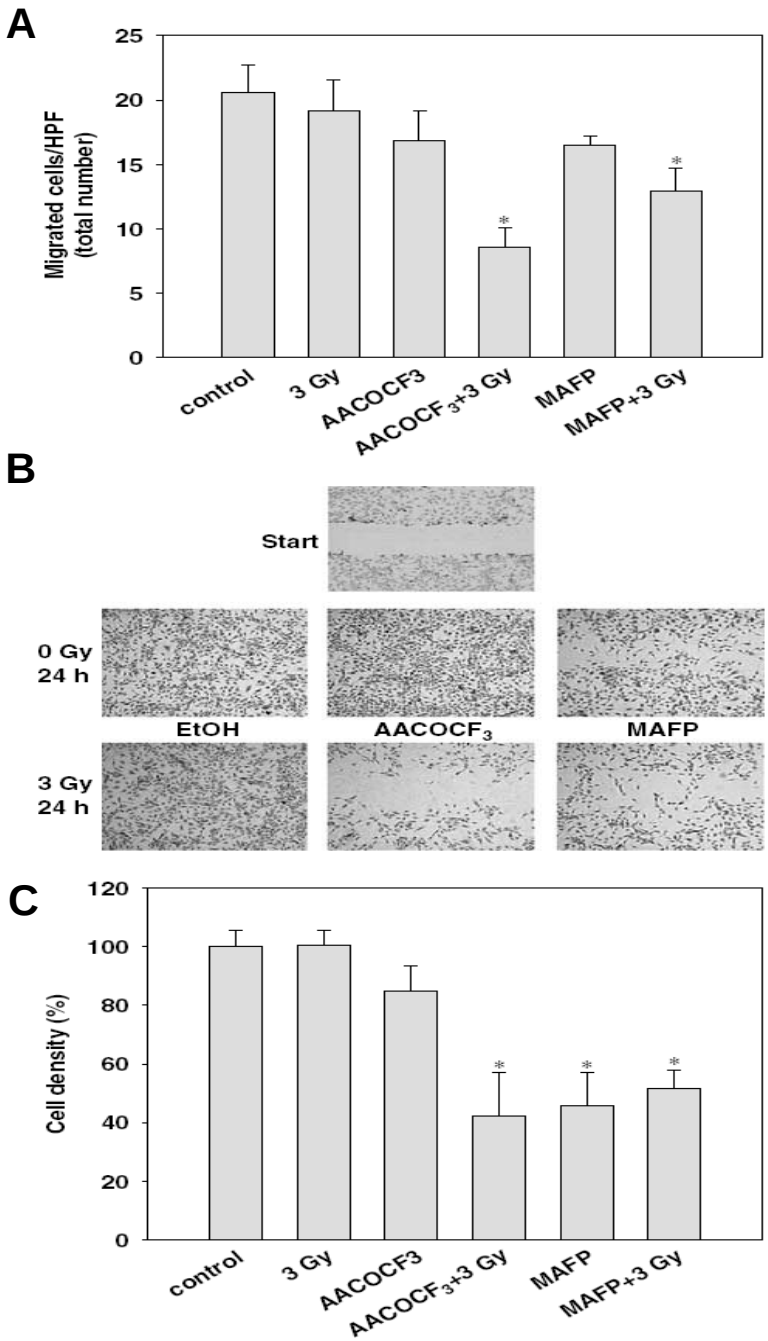

Figure 11. $cPLA_2$ inhibition decreases migration in irradiated HUVEC. (**A**) HUVEC were added to the top chamber of 6 well plates with 8.0 micron inserts. Both chambers were treated with EtOH or $cPLA_2$ inhibitors for 30 minutes and irradiated with 3 Gy. 24 hrs later, migrated cells were stained with DAPI and counted (5 HPF per sample). Shown is a bar graph for the total number of migrated cells per HPF; ∗, $P < 0.05$). (**B, C**) HUVEC were grown to 70-80% confluency. Four parallel wounds were created on each plate using a 200 μL pipette tip, and cells were treated with EtOH or $cPLA_2$ inhibitors for 30 minutes and irradiated with 3 Gy. 24 hrs later, cells were stained with 1% methylene blue and counted. Shown are (**B**) micrographs of stained cells and (**C**) a bar graph of the corresponding average percentage of migrated cells with SEM from six experiments; ∗, $P < 0.05$.

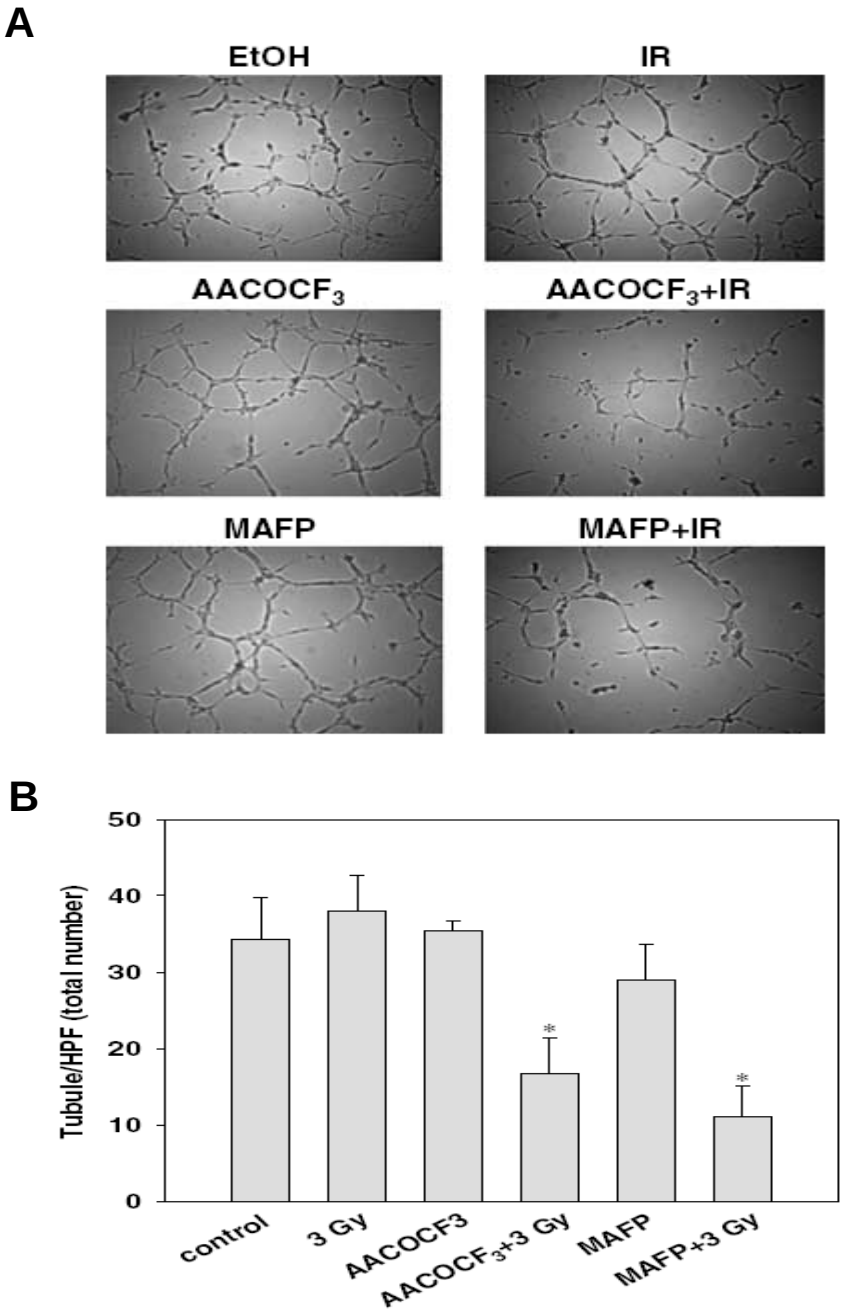

Figure 12. $cPLA_2$ inhibition decreases migration and tubule formation in irradiated HUVEC. (**A, B**) Capillary tubule formation assay. HUVEC were cultured onto Matrigel for 30 minutes, treated with EtOH or $cPLA_2$ inhibitors for 30 minutes and irradiated with 3 Gy. Tubules were counted under microscopy 24 hours later (5 HPF per sample). Shown are (**A**) representative micrographs of capillary tubule formation and (**B**) total number of formed tubules per HPF in the bar graph with SEM from six experiments; ∗, $P < 0.05$.

Discussion

Many common and life threatening human diseases, including atherosclerosis, diabetes, cancer and aging, have free radical reactions as an underlying mechanism of injury. Free radicals and other reactive oxygen and nitrogen species (ROS/RNS) are generated endogenously (Valko et al., 2007). Overproduction of ROS results in oxidative stress, a deleterious process that can be an important mediator of damage to cell structures and biological molecules. In contrast, beneficial effects of ROS occur at low/moderate concentrations and involve physiological roles in cellular responses, such as in the activation of signaling pathways (Mikkelsen and Wardman, 2003; Valerie et al., 2007; Valko et al., 2007). ROS/RNS-dependent damage to vascular endothelium involving radiation-induced environmental stress and radiotherapy is widely studied (Pelevina et al., 2006; Rodel et al., 2007). However, the molecular mechanism by which vascular endothelial cells respond to low doses of ionizing radiation has yet to be elucidated.

Our previous studies have shown that ionizing radiation triggers pro-survival signaling pathways that are specific and responsible for the inherent radioresistance of vascular endothelium. (Edwards et al., 2002; Geng et al., 2001; Tan et al., 2006; Tan and Hallahan, 2003). The details regarding the immediate events responsible for activation of these pathways are not entirely known, however. Here we demonstrated that 3 Gy of ionizing radiation induced phosphorylation of two pro-survival kinases Akt and ERK1/2 at 2 minutes, with maximum phosphorylation occurring 3 minutes after exposure. Rapid and transient activation of these kinases could involve the interaction of radiation-triggered ROS with membrane lipids, signaling proteins or DNA (Kolesnick and Fuks, 2003; Kufe and Weichselbaum, 2003; Truman et al., 2005). We were specifically interested in lipid-derived second messengers that are

immediately mobilized following irradiation. One such signaling pathway involves phospholipase A2. In irradiated HUVEC, we detected immediate activation of cytosolic PLA_2. Moreover, radiation-induced phosphorylation of Akt and ERK1/2 was dependent upon and occurred immediately after activation of $cPLA_2$. Similar results were obtained using irradiated HUVEC transfected with shRNA for $cPLA_2\alpha$ as compared to non-silencing shRNA and mouse embryonic fibroblasts from $cPLA_2\alpha^{+/+}$ and $cPLA_2\alpha^{-/-}$ mice. Such findings indicate a regulatory role of $cPLA_2$ in the activation of radiation-induced Akt and ERK1/2 phosphorylation and suggest that the α-isoform of the $cPLA_2$ family is a principal enzyme responsible for this regulation.

Activation of $cPLA_2$ leads to the increased production of lysophospholipids, such as LPC (Chakraborti, 2003; Hirabayashi et al., 2004; Prokazova et al., 1998). This biologically active lipid functions as the second messenger in signal transduction pathways, that regulate vascular proliferation, migration, expression of adhesion molecules and inflammation (Fujita et al., 2006; Murugesan et al., 2003; Prokazova et al., 1998). In our study of irradiated HUVEC, LPC production was increased 1.6-fold as compared to untreated cells. To test whether this is involved in the transduction of radiation signaling, we compared the responses of irradiated HUVEC to the responses caused by exogenously added LPC. Cellular survival and proliferation in response to LPC treatment are dependent on LPC concentration (Prokazova et al., 1998). Concentrations as great as 25 μM of LPC have been reported to increase proliferation of HUVEC (Fujita et al., 2006), while higher concentrations promoted cell death (Tsutsumi et al., 2006). In our study, 10 μM of four different exogenous LPC species did not cause a statistically significant change in cell proliferation. In addition, 10 μM of various LPC species resulted in ERK1/2 and Akt phosphorylation similar to those

observed in irradiated cells. This suggests that PLA_2-dependent production of LPC could be the mediator of endothelial radioresistance. Similarly, Fujita and coworkers (Fujita et al., 2006), have shown that 20 μM LPC activated the same pro-survival kinases leading to increased HUVEC proliferation. We also have shown that inhibition of $cPLA_2$ significantly enhanced radiation-induced cell death in endothelial cells. We characterized the mechanisms of this cell death and detected an increased number of multinucleated and giant cells and cell cycle-independent accumulation of cyclin B1 within 24-48 hours of irradiation. These features are characteristic of mitotic catastrophe (Ricci and Zong, 2006). Later, mitotic catastrophe led to a delayed programmed cell death which was detected at 72-96 hours after treatment. In addition to the regulation of endothelial cell viability, we demonstrated that $cPLA_2$ inhibition affected endothelial cell function, resulting in attenuated migration and tubule formation in irradiated HUVEC.

The role of $cPLA_2$ in pro-survival signaling, viability and radioresistance of irradiated cells was also confirmed using genetic knockdown and knockout models. However, while the shRNA approach using HUVEC resulted in effects very similar to those observed in irradiated HUVEC pretreated with chemical inhibitors of $cPLA_2$, the effects in $cPLA_2$ KO MEF were less pronounced. A possible explanation for the observed difference in the genetic knockout model is that, in the absence of one isoform, other isoforms of the enzyme could provide a compensatory mechanism by assuming the functions of the deficient isoform.

There are great differences in human organ and tissue sensitivity for radiation-induced damage (Pierce et al., 1996; Upton, 1990). Low doses of ionizing radiation (2-3 Gy) do not affect the viability of vascular endothelial cells. Moreover, there are studies demonstrating that active $cPLA_2$ and its product LPC are necessary for

viability and proliferation of endothelial cells (Fujita et al., 2006; Herbert et al., 2005). We determined immediate radiation-dependent activation of a pro-survival signaling pathway that regulates viability and function of vascular endothelium. Our studies indicate a sequence of molecular events in irradiated endothelial cells, constituting an immediate signaling pathway activated by ionizing radiation (**Figure 13**). Activation of $cPLA_2$ resulted in production of LPC and subsequent phosphorylation of Akt and ERK1/2. Inhibition of this pathway at different levels (Geng et al., 2001; Geng et al., 2004; Tan et al., 2006; Tan and Hallahan, 2003) enhanced radiation-induced cell death characterized by mitotic catastrophe followed by a delayed programmed cell death. We propose that $cPLA_2$ signaling mediates the radiation-dependent pro-survival response in vascular endothelial cells and, therefore, could represent one key regulator of inherent endothelial radioresistance. These data establish a biological basis for the development of radiation mitigators and protectors.

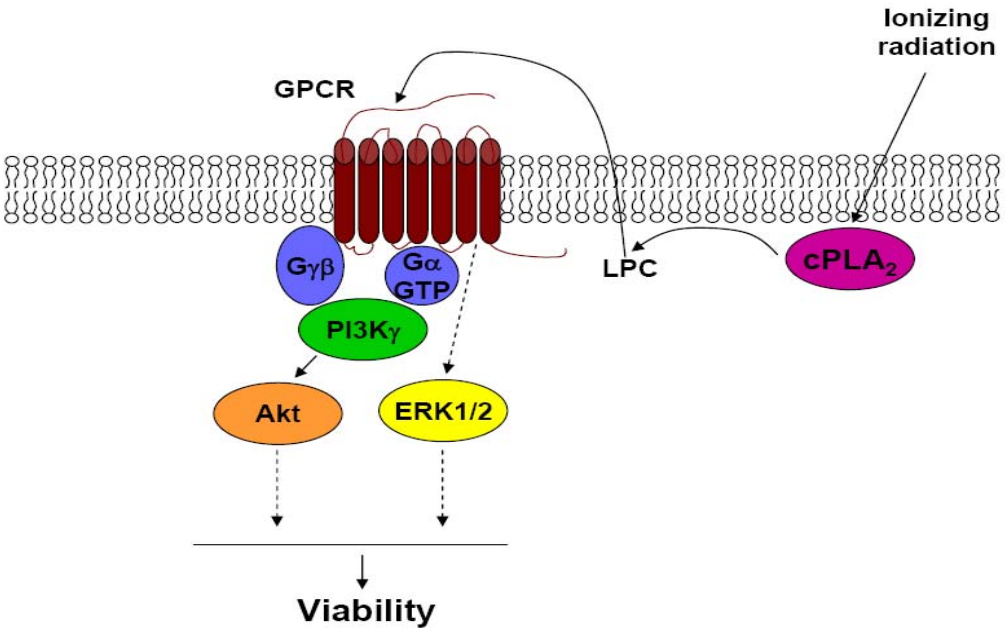

Figure 13. Proposed sequence of events in irradiated HUVEC. Ionizing radiation triggers the activation of $cPLA_2$ followed by increased production of LPC, activation of GPCRs, and phosphorylation of Akt and ERK1/2 leading to increased cellular viability.

This work was published as:
Yazlovitskaya EM, **Linkous AG**, Thotala DK, Cuneo KC, Hallahan DE. Cytosolic Phospholipase A2 Regulates Viability of Irradiated Vascular Endothelium. *Cell Death and Differentiation* 2008; 15:1641-53.

CHAPTER IV

CYTOSOLIC PHOSPHOLIPASE A2 IS A NOVEL MOLECULAR TARGET FOR TUMOR SENSITIZATION TO RADIATION THERAPY

Introduction

Despite advances in therapeutic regimens, local failure in lung cancer continues to be a problem for radiation therapy (Clamon et al., 1999; Lee et al., 1999; Wagner, 2000). Currently, the most common approach to improve the outcome of radiotherapy is to combine radiation with chemotherapeutic agents (Dietz et al., 2008; Forastiere et al., 2006; Iranzo et al., 2008; McGinn et al., 1996; Stratford, 1992). However, many of the platinum-based chemotherapeutic agents used as standard treatment for lung cancer exhibit toxicity within normal tissues (Arany and Safirstein, 2003; Berns and Ford, 1997; Goldstein and Mayor, 1983; Mackall, 2000; Wang et al., 2004). Therefore, the development of non-toxic, yet effective molecular-targeted radiosensitizers is essential for improvement of the therapeutic ratio.

Understanding the tumor microenvironment response to radiation therapy is important for the development of efficient radiosensitizing agents (Levy et al., 1995b; Shweiki et al., 1995; Wachsberger et al., 2003). The work described in Chapter III demonstrated that the effectiveness of radiotherapy is limited by the response of the tumor vasculature (Wachsberger et al., 2003; Yazlovitskaya et al., 2008). Several studies have demonstrated that clinically relevant doses of ionizing radiation (2-5 Gy) elicit the activation of both Akt and ERK1/2 pro-survival signaling pathways in tumor endothelium (Dent et al., 2003a; Yazlovitskaya et al., 2008; Zhan and Han, 2004; Zingg et al., 2004). The result of such activation is increased radioresistance within the tumor blood vessels. Since ablation of the tumor vasculature enhances the

treatment of cancer (Folkman, 1971; Strijbos et al., 2008), radiosensitizers that target these survival pathways could significantly improve lung tumor response. Upon irradiation, signal transduction is generated during the interaction of ionizing radiation with cellular membranes (Haimovitz-Friedman et al., 1994; Valerie et al., 2007). Our recent study demonstrated that the radiation-induced activation of $cPLA_2$ in vascular endothelial cells resulted in the increased production of lysophosphatidylcholine (LPC), a lipid-derived second messenger which triggered Akt and ERK1/2 phosphorylation (Yazlovitskaya et al., 2008). LPC activates a wide range of cell types within the vascular system and can regulate a variety of biological functions including cellular migration, cytokine synthesis, and endothelial growth factor expression (Fujita et al., 2006; Marathe et al., 2001). According to our data and others, LPC could induce signal transduction through a variety of receptors, and the result of this signaling cascade is increased proliferation and survival of endothelial cells (Fujita et al., 2006; Yazlovitskaya et al., 2008). Such data suggests that $cPLA_2$ may play a critical role in the tumor vascular response to ionizing radiation and could be used as a molecular target for tumor radiosensitization.

In previous studies, much of the data was generated using normal vascular endothelial cells. However, the genes expressed by tumor endothelial cells differ significantly from the genes expressed by HUVEC and HMVEC. In order to analyze the efficacy of $cPLA_2$ inhibitors as radiosensitizers *in vitro*, we selected endothelial cells that are considered to be more clinically relevant to malignant disease (Walter-Yohrling et al., 2004). To test the hypothesis that $cPLA_2$ inhibition promotes the radiosensitization of tumor blood vessels, we used the 3B11 murine vascular endothelial cell line as well as murine pulmonary microvascular endothelial cells (MPMEC) isolated directly from mouse lung tissue.

To inhibit $cPLA_2$, we used Arachidonyltrifluoromethyl Ketone ($AACOCF_3$). This potent $cPLA_2$ inhibitor is a cell-permeable trifluoromethyl ketone analog of arachidonic acid (Farooqui et al., 2006). NMR studies have demonstrated that the carbon chain of $AACOCF_3$ binds in a hydrophobic pocket of $cPLA_2$ and the carbonyl group of $AACOCF_3$ forms a covalent bond with serine 228 in the enzyme active site (Farooqui et al., 2006; Street et al., 1993; Trimble et al., 1993). This $cPLA_2$ inhibitor has been used extensively to study the role of $cPLA_2$ in platelet aggregation and inflammation-associated apoptosis (Calzada et al., 2001; Duan et al., 2001; Fabisiak et al., 1998; Kirschnek and Gulbins, 2006). In the present study, however, we utilized $AACOCF_3$ to elucidate the role of $cPLA_2$ in the tumor vasculature response to ionizing radiation. We found that when combined with radiation, the inhibition of $cPLA_2$ with $AACOCF_3$ disrupts the biological functions of the tumor vasculature, enhances destruction of tumor blood vessels and suppresses tumor growth. Thus, $cPLA_2$ contributes to vascular endothelial cell radioresistance and presents a potential molecular target for tumor sensitization to radiotherapy.

Results

Inhibition of $cPLA_2$ with $AACOCF_3$ enhances cell death and prevents activation of pro-survival signaling in irradiated vascular endothelial cells

To determine whether treatment with $AACOCF_3$ affects cellular viability in irradiated tumor cells as well as vascular endothelial cells, we performed clonogenic survival assays for 3B11, LLC, and H460 cell lines. The studies showed that treatment with $AACOCF_3$ enhances radiation-induced cell death among 3B11 vascular endothelial cells (**Figures 14** and **15**). The most pronounced statistically significant increase in radiosensitization was observed at 2 Gy. At this dose, 3B11 cells exhibited a 30% decrease in survival in comparison to irradiated cells treated

with vehicle alone (**Figure 14**). Treatment with $AACOCF_3$ did not result in radiosensitization of LLC or H460 (**Figures 14** and **15**).

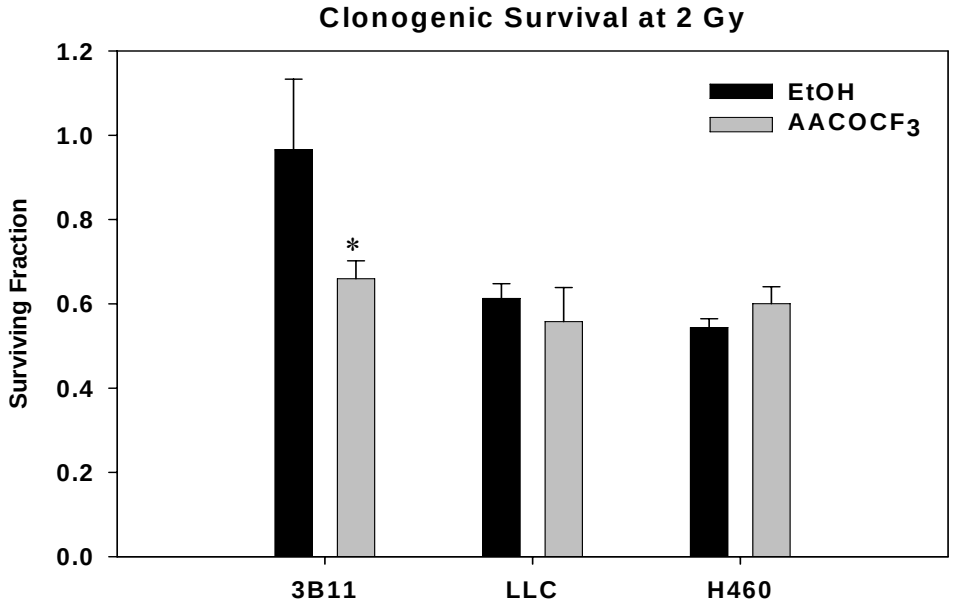

Figure 14. Inhibition of $cPLA_2$ with $AACOCF_3$ enhances cell death at 2 Gy in irradiated vascular endothelial cells. 3B11, LLC, and H460 cells were plated and treated with 1 μM $AACOCF_3$ for 30 min prior to irradiation. After 1 week, colonies consisting of ≥ 50 cells were counted and normalized for plating efficiency. Shown is a bar graph of percent survival after exposure to 2 Gy; *, $P < 0.05$.

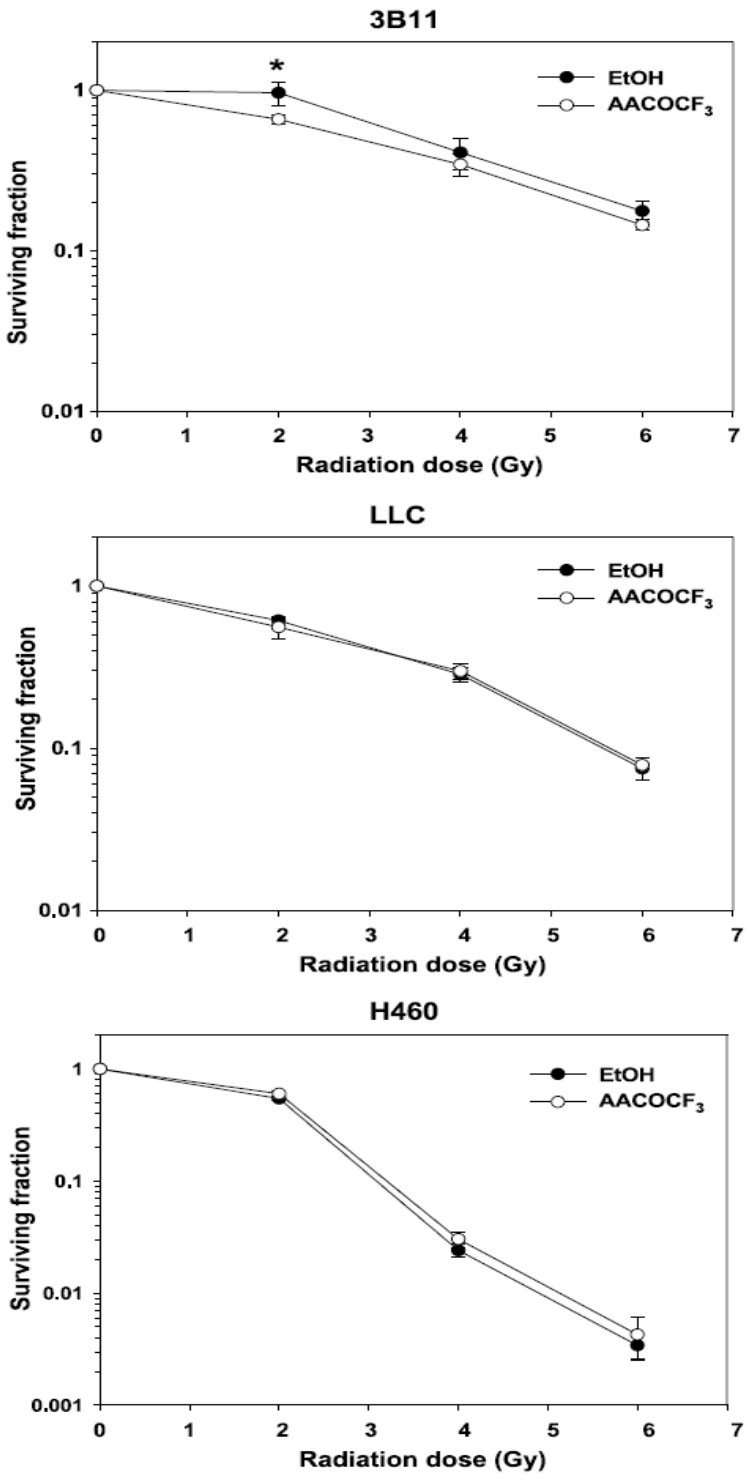

Figure 15. Inhibition of $cPLA_2$ with $AACOCF_3$ enhances radiation-induced cell death in vascular endothelial cells. Clonogenic Survival. 3B11, LLC, and H460 cells were plated and treated with 1 μM $AACOCF_3$ for 30 min prior to irradiation. After 1 week, colonies consisting of ≥ 50 cells were counted and normalized for plating efficiency. Shown are average surviving fractions and SEM from three experiments; * $P < 0.05$.

Our previous studies have demonstrated that in irradiated HUVEC, activation of $cPLA_2$ regulates ERK1/2 phosphorylation, one of the radiation-induced pro-survival kinases (Yazlovitskaya et al., 2008), To investigate whether the effects of $AACOCF_3$ on 3B11 cell viability are due to the similar changes in radiation-induced pro-survival signaling, we performed western immunoblot analysis for ERK1/2 phosphorylation using total cell lysates of all three tested cell lines (**Figure 16**). At 3 minutes post-irradiation, $AACOCF_3$ prevented the radiation-induced phosphorylation of ERK1/2 in vascular endothelial cells, but not in LLC or H460 tumor cells (**Figure 16**). This suggests that in response to radiation, differential radiation-induced $cPLA_2$-dependent activation of ERK1/2 is a key regulator of cell survival of vascular endothelial cells versus tumor cells.

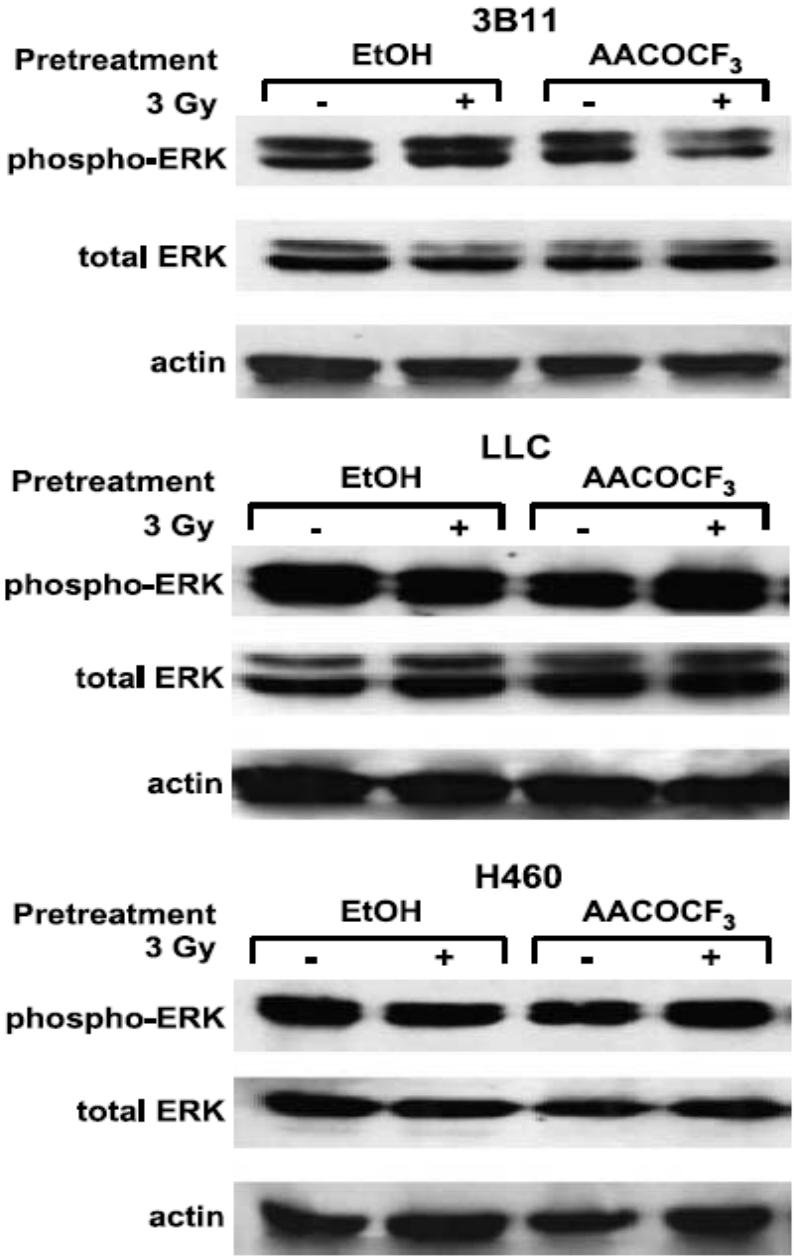

Figure 16. Inhibition of $cPLA_2$ with $AACOCF_3$ prevents activation of pro-survival signaling in irradiated vascular endothelial cells. ERK phosphorylation. 3B11, LLC, and H460 cells were treated with 1 μM $AACOCF_3$ for 30 min prior to irradiation with 3 Gy and lysed 3 min after the beginning of irradiation. Shown are the Western blot analyses with specific antibodies to phospho-ERK1/2, total ERK1/2, and actin.

Inhibition of cPLA$_2$ attenuates tubule formation in irradiated vascular endothelial cells

To determine whether cPLA$_2$ inhibition alters the ability of vascular endothelial cells to form capillary-like structures, 3B11 or MPMEC were treated with vehicle or 1 μM AACOCF$_3$ for 30 minutes prior to irradiation. Tubule formation was analyzed in Matrigel-coated 24-well plates. When 3B11 cells were treated with either AACOCF$_3$ or radiation alone, only a slight decrease in tubule formation was observed as compared to control cells (**Figure 17A**, 47 vs. 53 and 40 vs. 53, respectively). However, a combined treatment of AACOCF$_3$ followed by irradiation significantly decreased tubule formation as compared to control cells (**Figure 17A**, 29 vs. 53). A similar response was observed in MPMEC, in which treatment with AACOCF$_3$ prior to irradiation reduced the average number of tubules formed per HPF by 50% when compared to control cells (**Figure 17B**).

Inhibition of cPLA$_2$ results in decreased migration in irradiated vascular endothelial cells

To determine whether cPLA$_2$ inhibition affects the migratory ability of vascular endothelial cells, 3B11 or MPMEC were treated with vehicle or 1 μM AACOCF$_3$ for 30 minutes prior to irradiation. Migration was assessed by a transwell filter migration assay. In the 3B11 cell line, no significant reduction in migration was observed in cells treated with either radiation or AACOCF$_3$ alone (**Figure 18A**). In contrast, treatment with AACOCF$_3$ prior to irradiation reduced migration by 39% in comparison to cells treated with vehicle alone (**Figure 18A**, 62 vs. 112). MPMEC produced comparable results in which treatment with AACOCF$_3$ prior to irradiation significantly attenuated the number of migrated cells per HPF (**Figure 18B**, 11 vs. 63).

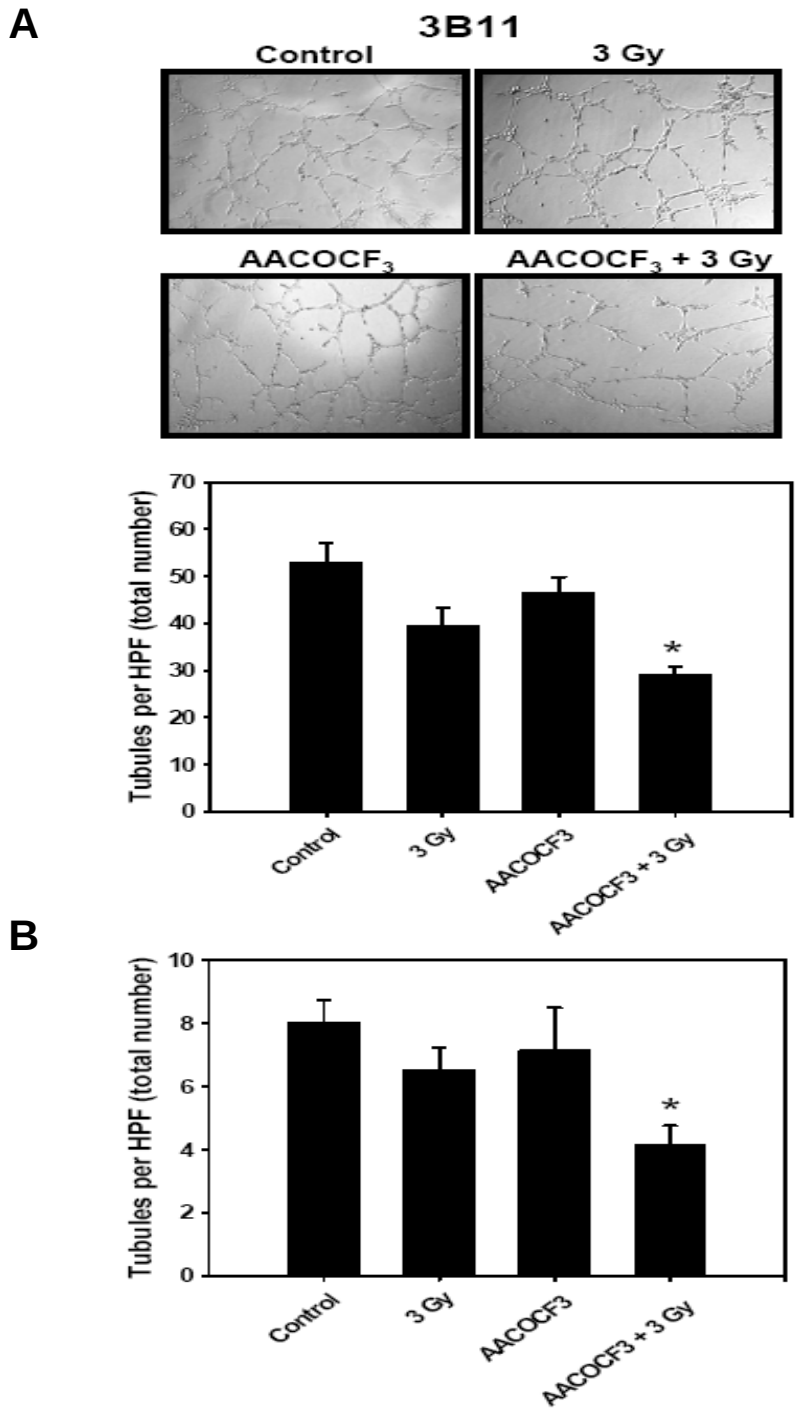

Figure 17. cPLA$_2$ inhibitor AACOCF$_3$ attenuates tubule formation in irradiated vascular endothelial cells. 3B11 cells (A) or primary MPMEC (B) were cultured onto Matrigel in the absence (control) or presence of 1 μM AACOCF$_3$ for 30 minutes and then irradiated with 3 Gy. (A) Representative micrographs of capillary tubule formation taken 5 hours after treatment are shown. Tubule formation was quantified as the number of tubule branches per high power field (4 HPF per sample). Shown are bar graphs of the average tubule formation for 3B11 (A) and MPMEC (B) with SEM from three independent experiments; *, $P < 0.05$.

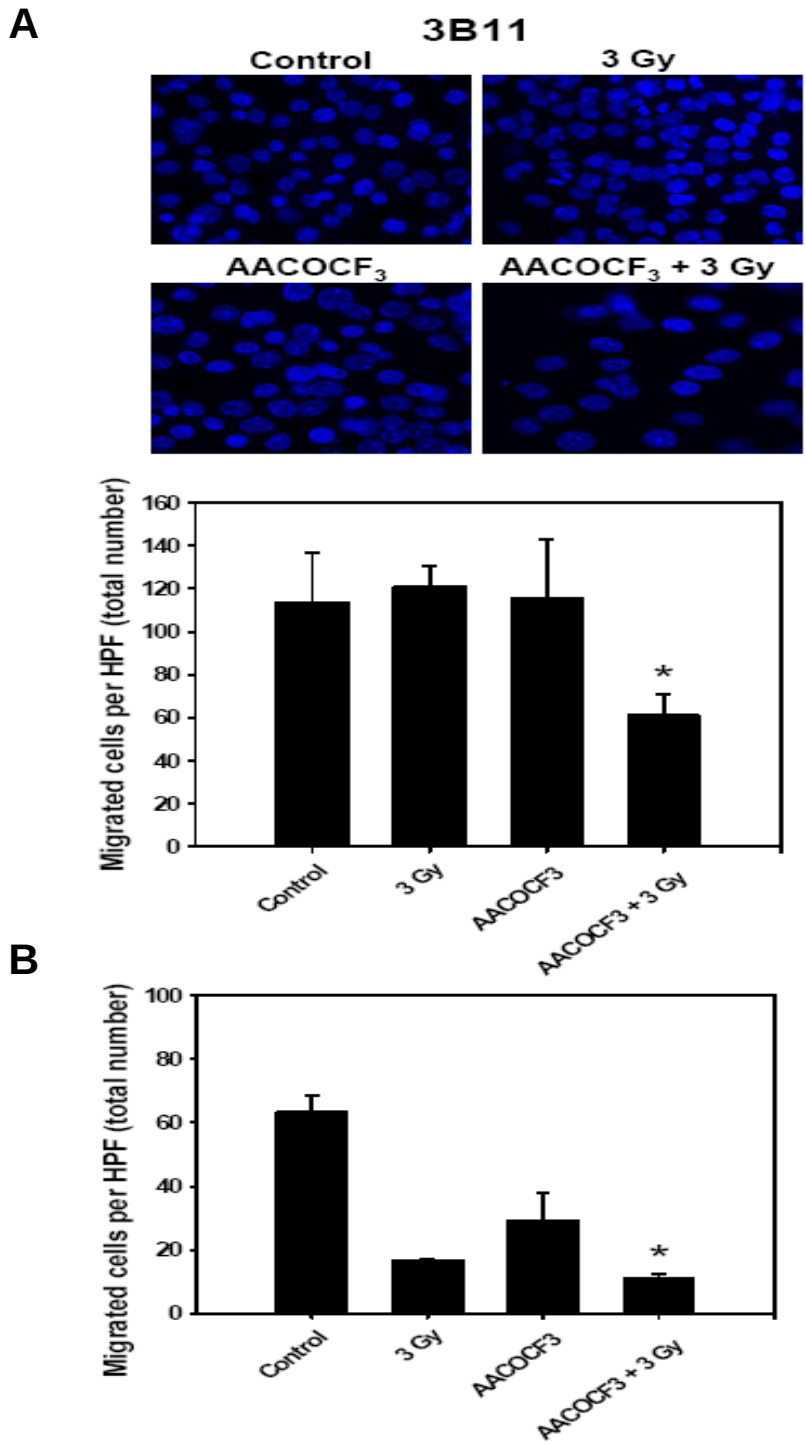

Figure 18. Inhibition of $cPLA_2$ with $AACOCF_3$ attenuates migration in irradiated vascular endothelial cells. 3B11 cells (**A**) or primary MPMEC (**B**) were added to the top chamber of 24 well plates with 8 μm Matrigel-coated inserts. Both chambers were treated with vehicle or 1 μM $AACOCF_3$ for 30 minutes prior to irradiation with 3 Gy. After 24 hours, migrated cells were stained with DAPI and counted (6 HPF per sample). Shown are representative micrographs of migrated 3B11 taken 24 hours after treatment (**A**) and bar graphs of the average number of migrated cells per HPF for 3B11 (**A**) and MPMEC (**B**) with SEM from three independent experiments; *, $P < 0.05$.

Inhibition of cPLA$_2$ represses tumor growth in irradiated mouse models

To determine the efficacy of cPLA$_2$ inhibition *in vivo*, both syngeneic and heterogeneic mouse lung tumor models were used. Mouse LLC or human H460 tumor cells were injected subcutaneously into the right hindlimbs of 6-week old male C57/BL6 or nude mice, respectively. Tumor-bearing mice received daily intraperitoneal injections of vehicle or 10 mg/kg AACOCF$_3$ 30 minutes prior to irradiation. Treatment was repeated for 5 consecutive days and tumor volume was determined by external caliper measurements. In the LLC model, treatment with either radiation or drug alone failed to produce a significant delay in tumor growth (**Figure 19A, B**, 2.6 days vs. 1.8 days, respectively.) Mice treated with a combined treatment of AACOCF$_3$ and radiation, however, produced a statistically significant tumor growth delay of 12.2 days (**Figure 19A, B,** $P < 0.05$). In the H460 tumor mouse model, inhibition of tumor growth was not observed in mice treated with AACOCF$_3$ alone (**Figure 19C**). Treatment with radiation resulted in a tumor growth delay of 5.5 days, but maximum tumor growth inhibition of 12.3 days was observed in mice treated with AACOCF$_3$ plus radiation (**Figure 19C**). **Fig.19D** illustrates the differences in H460 tumor volumes among treatment groups 13 days post-injection. Although radiation resulted in decreased tumor size compared to untreated mice (**Figure 19D**, 950 mm^3 vs. 1447 mm^3), a combined treatment of AACOCF$_3$ and radiation enhanced tumor growth suppression by an additional 40% (**Figure 19D**, 567 mm^3).

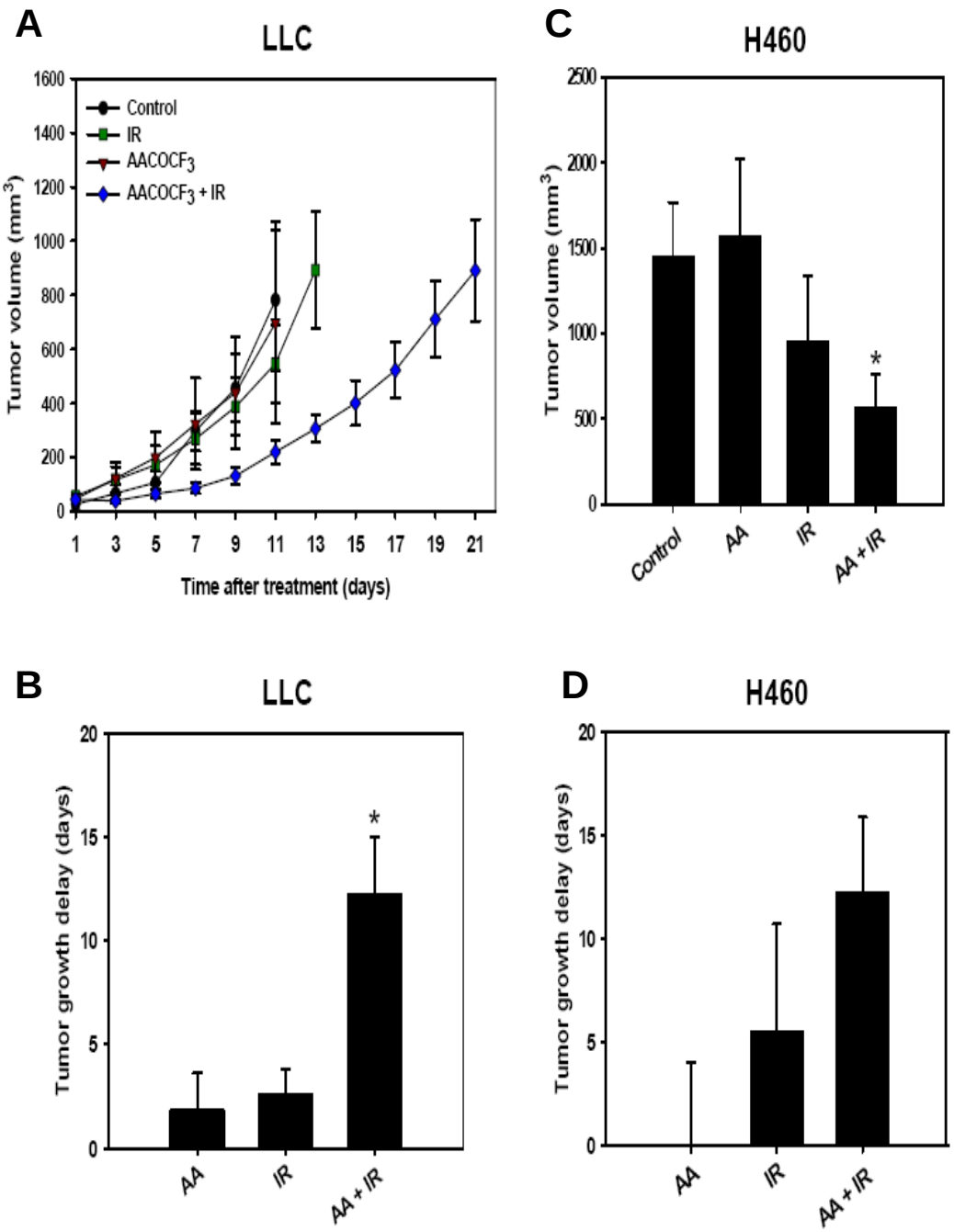

Figure 19. Inhibition of $cPLA_2$ with $AACOCF_3$ decreases tumor size in irradiated mouse models. Using heterotopic tumor models of LLC (**A, B**) or H460 (**C, D**), mice were treated i.p. with vehicle (control) or 10 mg/kg $AACOCF_3$ and tumors were irradiated 30 minutes later with 3 Gy. Treatment was repeated for 5 consecutive days. Tumor volumes were calculated using external caliper measurements. (**A**) Shown are mean LLC tumor volumes in each of the treatment groups. (**B**) LLC; Shown is a bar graph of the average number of days taken to reach 700 mm^3 in comparison to control with SEM from groups of 4 to 6 mice; *, $P = 0.02$. (**C**) H460; Shown is a bar graph of the average tumor volumes 13 days post-injection with SEM from groups of 4 to 6 mice; *, $P = 0.05$. (**D**) H460; Shown is a bar graph of the average number of days taken to reach 1400 mm^3 in comparison to control with SEM from groups of 4 to 6 mice.

$cPLA_2$ inhibition attenuates tumor blood flow and decreases vascularity in irradiated tumors

To determine if the $cPLA_2$ inhibitor $AACOCF_3$ impedes tumor blood flow, mice bearing LLC tumors were treated once daily for 5 consecutive days with either vehicle or 10 mg/kg $AACOCF_3$ for 30 minutes followed by irradiation with 3 Gy. Tumor blood flow was analyzed by three-dimensional Power Doppler Sonography. As shown in Fig. 20A, B, the average Vascular Indices were 12% and 15% for untreated and irradiated tumors, respectively. Treatment with $AACOCF_3$ resulted in a 1.6-fold decrease in tumor Vascular Index as compared to untreated mice (**Figure 20B**, 7.5% vs. 12%). This decrease in tumor vasculature was further potentiated in mice that received a combined treatment of $AACOCF_3$ and radiation (**Figure 20B**, 2-fold, 6% vs. 12%).

To investigate whether inhibition of $cPLA_2$ using $AACOCF_3$ affects tumor vascularity, tumor-bearing mice were treated with daily intraperitoneal injections of vehicle or 10 mg/kg $AACOCF_3$ 30 minutes prior to irradiation with 3 Gy. Treatment was continued for 5 consecutive days. Twenty-four hours after the final treatment, tumors were resected, fixed, and sectioned into 5 μm sections. Sections were then stained with anti-vWF antibody. Staining was assessed by immunofluorescent microscopy. **Fig. 20C, D**, illustrates the effects of $cPLA_2$ inhibition on vascularity within irradiated tumors. Radiation alone produced a slight reduction in vascularity in comparison to untreated mice (**Figure 20D**, 6% vs. 10%). In addition, treatment with $AACOCF_3$ resulted in a significant decrease in total blood vessel number (**Figure 20D**, 4%). The most pronounced reduction in overall vascularity, however, was observed in mice treated with $AACOCF_3$ followed by radiation (**Figure 20D**, 2%).

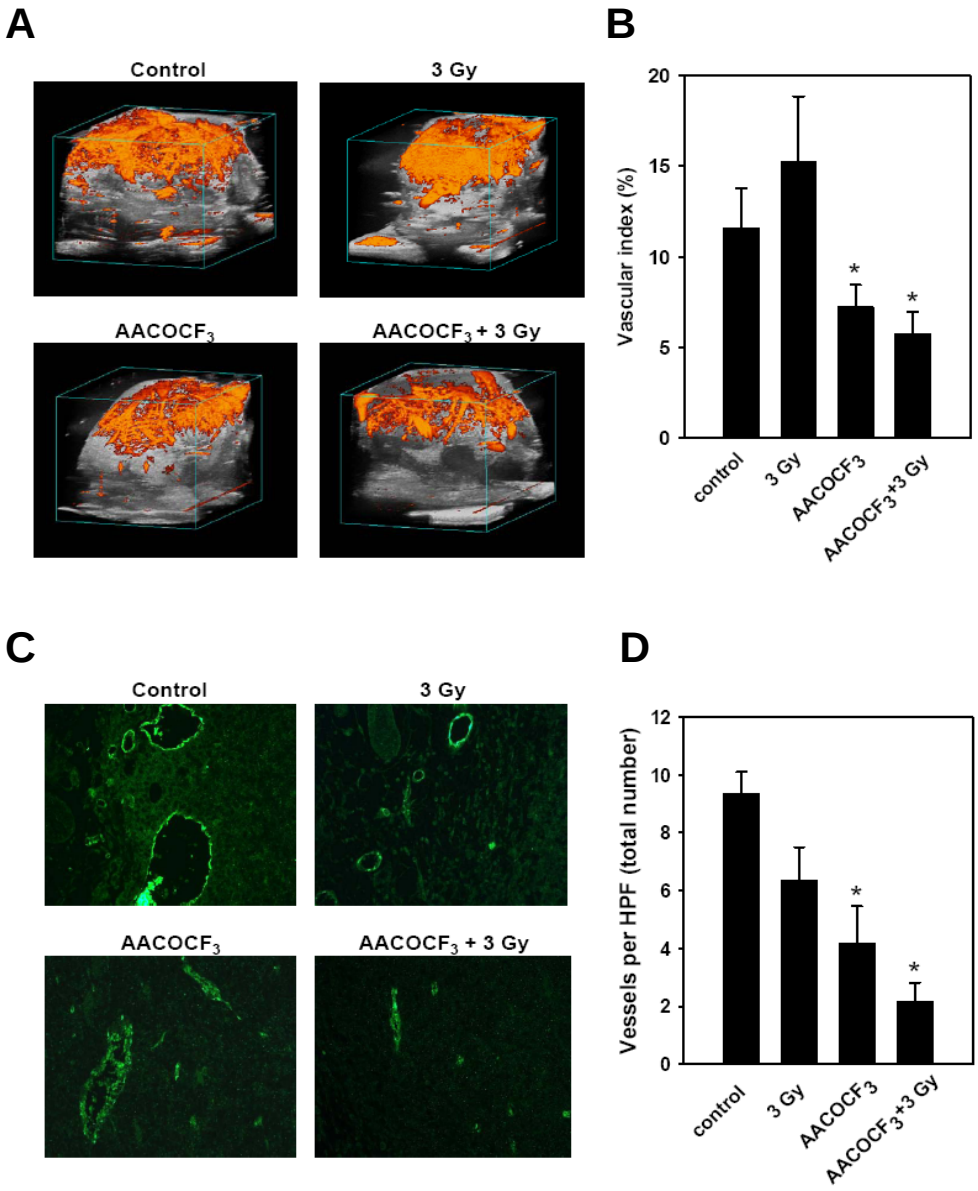

Figure 20. cPLA$_2$ inhibitor AACOCF$_3$ attenuates blood flow and vascularity in irradiated tumors. C57/BL6 mice with LLC tumors received i.p. injections of vehicle or 10 mg/kg AACOCF$_3$ 30 minutes prior to irradiation with 3 Gy. Treatment was repeated for 5 consecutive days. Twenty-four hours after the final treatment, tumor blood flow was analyzed by three-dimensional Power Doppler sonography (**A, B**) or tumors were harvested, fixed in 10% formalin, sectioned into 5 μm sections and stained with anti-vWF antibody (**C, D**). (**A**) Shown are representative images of tumor blood flow. (**B**) Shown is a bar graph of the average Percent Vascular Index with SEM from groups of 3 to 5 animals; *, $P < 0.05$. (**C**) Shown are representative micrographs of vWF-stained vessels. (**D**) Shown is the bar graph of the average number of stained vessels per HPF with SEM from groups of 3 to 5 mice; *, $P < 0.05$.

Treatment with $AACOCF_3$ results in apoptosis and inhibition of Akt phosphorylation within irradiated tumors

To determine the effects of $AACOCF_3$ on cellular viability *in vivo*, we performed TUNEL staining on LLC tumor sections from treated mice and analyzed the sections for the presence of apoptosis (**Figure 21A**). In tumor sections from untreated mice or mice treated with radiation alone, we did not find TUNEL-positive cells. Mice treated with the inhibitor alone exhibited TUNEL-positive staining within a small population of cells. The most pronounced effect was detected in tumors from mice treated with a combination of $AACOCF_3$ and irradiation. Within these tumors, we observed a significant increase in apoptosis (**Figure 21A**, black arrows).

To determine whether $AACOCF_3$ affects radiation-induced pro-survival signaling within irradiated tumors, we performed immunofluorescence staining for phospho-Akt on tumor sections from LLC-bearing mice (**Figure 21B**). In tumors from untreated mice or mice treated with 3 Gy, we observed increased levels of Akt phosphorylation. In comparison, treatment with drug alone resulted in decreased phospho-Akt levels throughout the entire tumor. Inhibition of Akt phosphorylation was further potentiated in tumors from mice that received a combined treatment of 10 mg/kg $AACOCF_3$ followed by irradiation with 3 Gy.

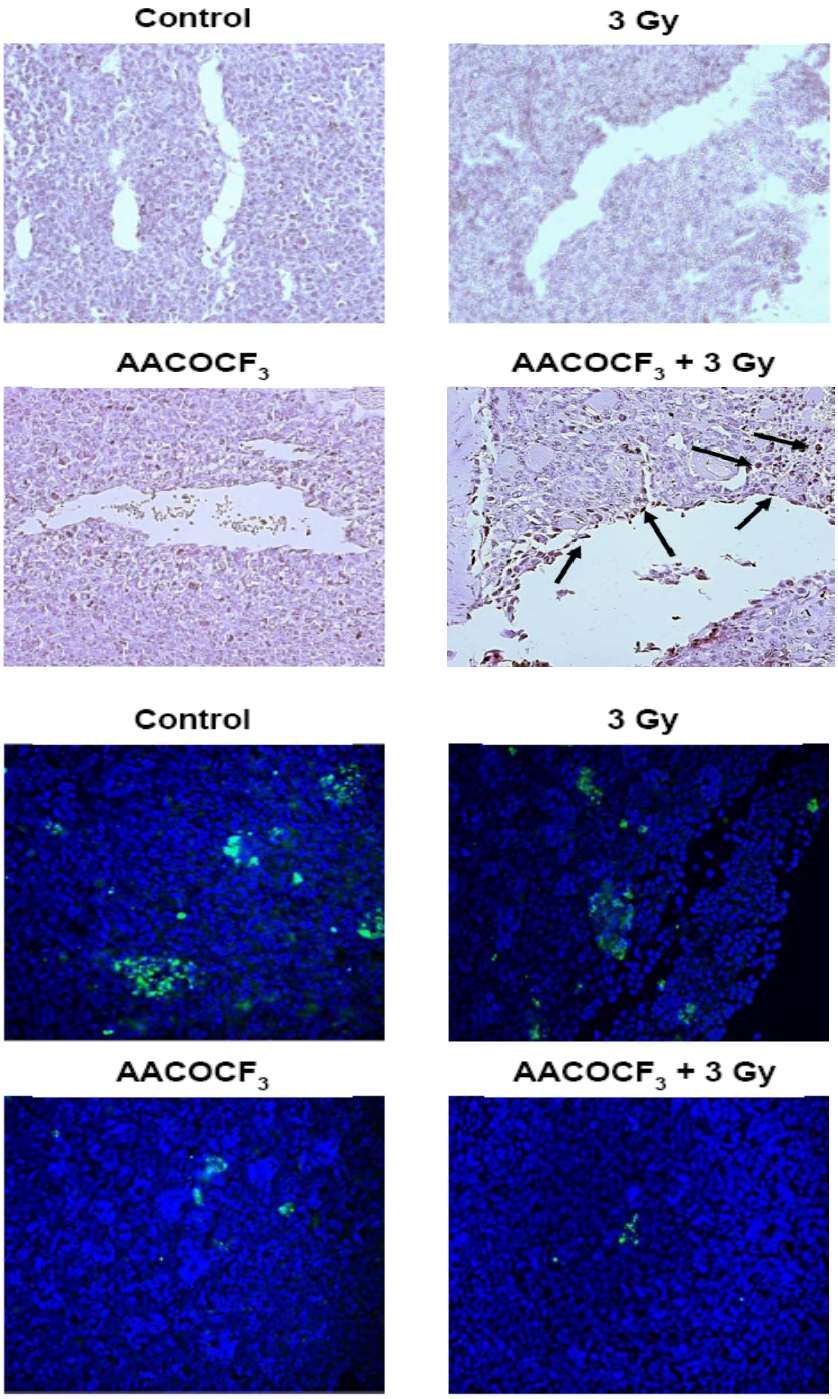

Figure 21. Treatment with $AACOCF_3$ results in increased apoptosis and decreased Akt phosphorylation within irradiated tumor models. (**A**) TUNEL staining and hematoxylin counterstaining were performed on 5 μm sections from LLC tumors. Shown are representative micrographs of tumors with blood vessels from treated mice. Black arrows indicate TUNEL-positive endothelial cells; red arrows indicate TUNEL-positive tumor cells. (**B**) Phospho-Akt immunofluorescence staining (green) and DAPI counterstaining (blue) were performed on LLC tumor sections from treated mice. Shown are representative micrographs of positive staining for Akt phosphorylation in LLC tumors

Tumor vascular window model and vascular length density analysis

To investigate the effects of $cPLA_2$ inhibition on tumor vasculature radiosensitivity, we used a dorsal skinfold window model. LLC cells were implanted into the dorsal skinfold window in C57/BL6 mice, and a sufficient vascular network was allowed to develop. Vascular windows were then treated with the $cPLA_2$ inhibitor $AACOCF_3$ 30 minutes prior to irradiation with 3 Gy. At 72 hours post treatment, the average Percent Vascular Length Densities were 71% and 42% for mice treated with drug alone or irradiation, respectively (**Figure 22**). A combined treatment of $AACOCF_3$ and radiation, however, resulted in statistically significant destruction of tumor blood vessels (**Figure 22**, 26%). These radiosensitization effects persisted at 96 hours post treatment, in which vascular length density was further reduced by $AACOCF_3$ followed by irradiation (**Figure 22B**, 13%).

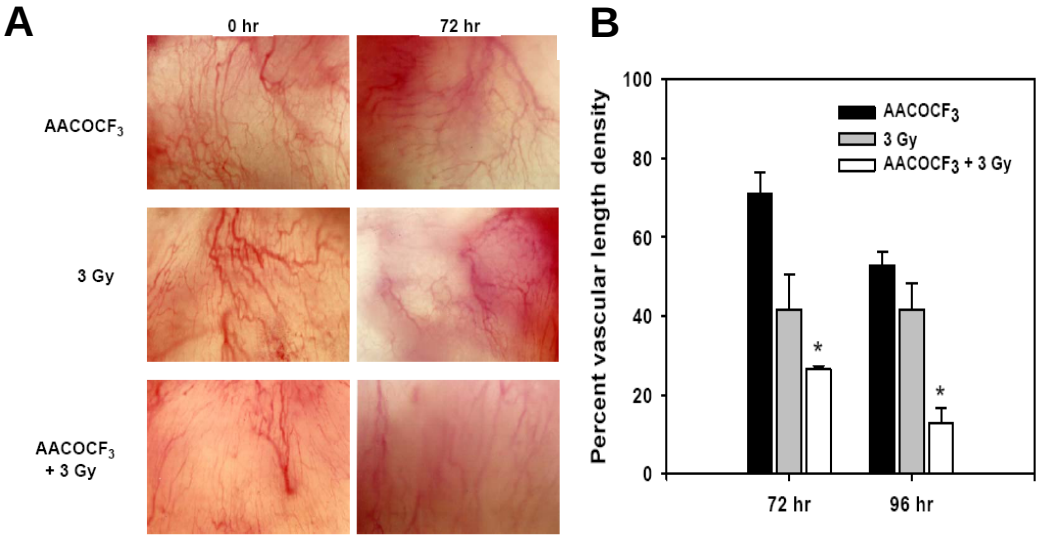

Figure 22. Tumor vascular window model and vascular length density analysis. LLC cells were implanted into the dorsal skinfold window in C57/BL6 mice. Following vascular network development, mice were treated with $AACOCF_3$ 30 minutes prior to irradiation with 3 Gy. Color photographs were taken daily to monitor blood vessel appearance. (**A**) Shown are representative micrographs of LLC tumor vascular window models at 0 hr and 72 hr after treatment. (**B**) Changes in the quantity of blood vessels over time were compared with that observed at 0 h. Shown is a bar graph of the percent vascular length density 72 and 96 hours after treatment of implanted tumors with SEM from groups of 3 to 5 mice; *, $P < 0.05$.

Discussion

In the tumor vascular endothelium, clinically relevant low doses of radiation trigger the activation of pro-survival signaling pathways. This results in enhanced radioresistance of tumor vasculature which can significantly diminish overall cancer treatment success rates. Thus, pharmacologic agents and therapeutic strategies that confer radiosensitivity to tumor blood vessels could improve tumor control. Cytosolic phospholipase A2 ($cPLA_2$) is a key component in the response of vascular endothelial cells to ionizing radiation. Radiation-induced activation of $cPLA_2$ leads to the downstream phosphorylation of the pro-survival targets Akt and ERK1/2 (Yazlovitskaya et al., 2008). In our present study, we provide evidence that chemical inhibition of $cPLA_2$ with $AACOCF_3$ can increase the radiation-induced destruction of tumor blood vessels and may significantly improve the response of radioresistant lung tumors to radiation therapy.

Using a syngeneic lung tumor model of Lewis Lung Carcinoma, we demonstrated that a combined treatment of $AACOCF_3$ and radiation inhibited tumor growth by 75% as compared to untreated tumors. To further verify the role of $cPLA_2$ in tumor growth progression, we used a xenograft lung tumor model of H460 cells. Treatment with $AACOCF_3$ plus radiation resulted in tumor growth suppression similar to that of the LLC tumor model. However, since H460 cells are more radiosensitive than LLC, the increase in radiosensitization from the combined treatment was not as pronounced. Therefore, these findings suggest that $cPLA_2$ is a relevant molecular target for lung tumors that are highly resistant to radiation therapy.

Another strategy to evaluate the efficacy of $cPLA_2$ inhibition *in vivo* is to quantitatively measure the effects on tumor blood flow (Goertz et al., 2002). In the current study, we used Power Doppler Sonography to provide a non-invasive

assessment of the efficacy of this antivascular therapy. This strategy is supported by prior studies of inhibition of molecular targets in the vascular endothelium (Edwards et al., 2002; Tan and Hallahan, 2003). We showed that $cPLA_2$ inhibition with $AACOCF_3$ reduced tumor blood flow in irradiated tumors. Thus, these data support the hypothesis that $cPLA_2$ inhibition combined with radiation leads to a disruption of tumor blood vessel function. To assess whether the overall tumor blood vessel number was affected by $cPLA_2$ inhibition, we used von Willebrand Factor (vWF) as a marker for vascularity. vWF is a glycoprotein that mediates platelet adhesion to sites of vascular injury, and is a well accepted immunohistochemical marker of endothelial cells (Alles and Bosslet, 1988; Pusztaszeri et al., 2006; Yamamoto et al., 1998). Our study revealed that tumors from mice treated with $AACOCF_3$ followed by radiation exhibited a significant reduction in blood vessel number. Upon further immunohistochemical analysis, we found that this attenuation of blood flow and reduction in overall vascularity is associated with the induction of apoptosis within tumor vascular endothelial cells. In addition, immunofluorescence staining revealed that treatment with $AACOCF_3$ followed by 3 Gy suppresses radiation-induced Akt phosphorylation in irradiated tumors. This observation along with increased apoptosis in tumor cells and tumor vasculature suggests the possibility of multiple mechanisms involved in the radiosensitizing effects of the $cPLA_2$ inhibitor $AACOCF_3$. Thus, future investigation of the host-tumor interaction may provide clarification of the molecular events responsible for the increased efficacy of $cPLA_2$ inhibition in irradiated cancer.

The tumor vascular window model allows direct measurement of the vascular response to ionizing radiation *in vivo* (Geng et al., 2001). Our results revealed that, in the absence of irradiation, $AACOCF_3$ alone had no significant effect on existing

vasculature. When treated with $AACOCF_3$ followed by radiation, however, enhanced destruction of tumor blood vessels was observed. Taken together, these data demonstrated that in irradiated mouse tumor models, $AACOCF_3$ disrupts the biological functions of the tumor vasculature, enhances destruction of tumor blood vessels and suppresses tumor growth. Therefore, the $cPLA_2$ inhibitor $AACOCF_3$ is an effective radiosensitizer in mouse lung tumor models.

To provide further *in vitro* validation for our therapeutic strategy, we investigated the effects of $cPLA_2$ inhibition in the 3B11 cell line as well as in primary vascular endothelial cells isolated directly from lung tissue. In selecting the appropriate cell-based models for the pre-clinical development of radiosensitizers, it is ideal to identify a murine vascular endothelial cell line that maintains the expression of traditional endothelial cell markers as well as markers found to be expressed by human tumor endothelial cells (Walter-Yohrling et al., 2004). 3B11 is a murine vascular endothelial cell line that expresses the mouse homologs for five tumor endothelial markers: mTEM1, mTEM3, mTEM5, mTEM7, and mTEM8. Like normal endothelial cells, 3B11 also expresses many of the murine homologs of standard endothelial cell markers including, sialomucin/CD34, GPIIIB/CD36, and VCAMI/CD106 (Walter-Yohrling et al., 2004). Thus, 3B11 has been identified as a relevant murine model for tumor vascular endothelial cells (Carson-Walter et al., 2001; St Croix et al., 2000; Walter-Yohrling et al., 2004). In addition, we also used primary pulmonary vascular endothelial cells, the closest physiological cell culture model for lung cancer vasculature. Our cell culture experiments demonstrated that $cPLA_2$ inhibition with $AACOCF_3$ followed by radiation prevented radiation-induced activation of pro-survival signaling (ERK1/2) and significantly enhanced cell death. This effect was observed in vascular endothelial cells but not in lung tumor cell lines.

This differential response suggests a fundamental regulatory role for radiation-induced $cPLA_2$–dependent activation of pro-survival signal transduction pathways in the viability of irradiated vascular endothelial cells as compared to tumor cells. Additional functional assays revealed that treatment with $AACOCF_3$ reduced migration and attenuated tubule formation in irradiated 3B11 and primary vascular endothelial cells. Taken together, these data indicate that $cPLA_2$ inhibition confers radiosensitivity to tumor vasculature and may disrupt tumor blood vessel function.

These findings identify $cPLA_2$ as a critical component of the tumor vascular response to ionizing radiation. In the present study, we found that $cPLA_2$ inhibition prevents the formation of a functional tumor vascular network both *in vivo* and in cell culture; disrupts already formed tumor blood vessels and significantly delays tumor growth. Thus, $cPLA_2$ inhibition with $AACOCF_3$ enhances the radiation-induced destruction of tumor vasculature and may significantly improve lung tumor response to radiation therapy.

This work was published as:
Linkous AG, Geng L, Lyshchik A, Hallahan DE, Yazlovitskaya EM. Cytosolic Phospholipase A2: Targeting Cancer through the Tumor Vasculature. *Clinical Cancer Research* 2009; 15:1635-1644.

CHAPTER V

THE ROLE OF AUTOTAXIN IN CPLA$_2$-MEDIATED RADIATION-INDUCED SIGNAL TRANSDUCTION

Introduction

Previous work in Chapters III and IV demonstrated key roles for cPLA$_2$ and LPC in the response of tumor vasculature to radiation therapy. Although LPC can independently induce pro-survival signal transduction, this lipid second messenger is frequently hydrolyzed into lysophosphatidic acid (LPA) which has been shown to stimulate cell proliferation, migration, and survival and has been implicated in tumor progression (Ptaszynska et al., 2008; Ren et al., 2006). Signaling of LPA is primarily mediated through classic G protein-coupled receptors belonging to the endothelial differentiation gene (EDG) family (LPA$_1$/EDG-2, and LPA$_2$/EDG-4). However, other receptors such as LPA$_3$/EDG-7, LPA$_4$/GPR23, and LPA$_5$/GPR92 can also play a role in LPA-induced signal transduction.

The primary enzyme responsible for the hydrolysis of LPC to LPA is autotaxin (Hama et al., 2004; Jansen et al., 2005; Tokumura et al., 1986; Umezu-Goto et al., 2002). Secreted as a 103 kDa protein, autotaxin exhibits significant lysophospholipase D activity and is overexpressed in a variety of diseases including lung cancer and glioblastoma (GBM) (Jansen et al., 2005; Kishi et al., 2006; Ptaszynska et al., 2008). In addition, increased secretion of this enzyme is often associated with the stimulation of cell proliferation as well as accelerated tumor invasion and metastasis (Tanaka et al., 2006).

Previous studies indicate that this enhanced tumor progression results from the ability of autotaxin to promote angiogenesis (Nam et al., 2001; Tanaka et al., 2006).

In the absence of autotaxin, the maturation of embryonic vasculature is significantly impaired, suggesting that lysophospholipase D activity is critical for the maturation and stabilization of preformed vascular networks (Tanaka et al., 2006). Furthermore, in addition to stimulating tumor cell proliferation and motility, autotaxin may support an invasive microenvironment for vascular endothelial cells as well as tumor cells. Therefore, the autotaxin-mediated production of LPA may play a critical role not only in angiogenesis, but also in the tumor vascular response to ionizing radiation.

Results

Autotaxin expression is elevated in lung cancer and glioblastoma

In order to determine the expression profile of autotaxin, we performed a western immunoblot using the conditioned medium from endothelial cells as well as tumor cells (GBM and LLC). **Figure 23** shows immunoblots probed with anti-autotaxin purified antiserum (Santa Cruz Biotechnology; Santa Cruz, CA), which recognizes human, rat, and mouse autotaxin. Cells express both ATXt and ATXm splice variants of autotaxin, and both variants are secreted by cells and therefore expressed in the extracellular compartment (van Meeteren and Moolenaar, 2007). Results from this experiment indicate that autotaxin is primarily expressed by tumor cells, and not endothelial cells.

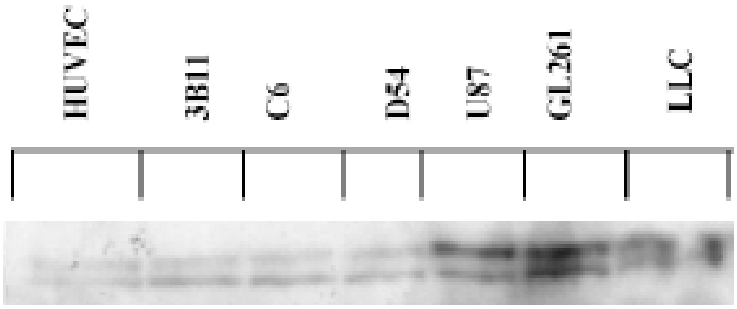

Figure 23. Autotaxin expression. Endothelial Cells (HUVEC and 3B11); Glioblastoma (C6, D54, U87, and GL261); Lung Cancer (LLC).

LPA production is increased following irradiation of HUVEC-GBM co-cultures

To determine whether increased autotaxin expression correlates with increased LPA production, HUVEC were co-cultured either with U87 or D54 GBM cells using 6-well plates with polycarbonate 0.4 μM membrane transwell inserts. Co-cultures were irradiated with 3 Gy. LPA concentration was measured in conditioning medium 60 min after irradiation using a competitive ELISA assay (**Figure 24**). Untreated control cells showed no to little detectable LPA (0 or 5 nM). Following irradiation with 3 Gy, however, LPA levels increased to 160 and 50 nM in U87 and D54 glioma co-cultures respectively ($P < 0.001$).

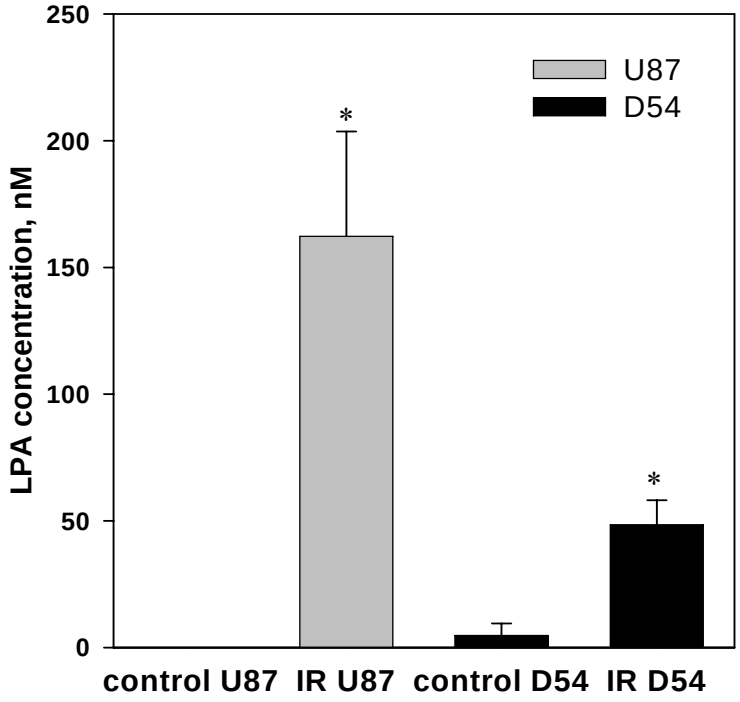

Figure 24. LPA production in conditioning medium of HUVEC co-cultured with U87or D54. Cells were cultured in EGM-2 for 24 h using 6-well plates with polycarbonate 0.4 μM membrane Transwell inserts. Co-cultures were irradiated with 3 Gy. LPA concentration was measured in conditioning medium 60 min after irradiation using a competitive ELISA assay.

Inhibition of LPA1/2 attenuates radiation-induced phosphorylation of Akt and ERK1/2

Signaling of LPA is mediated through classic GPCRs belonging to the EDG family of receptors. To determine if these receptors are involved in the activation of the PI3K/Akt and MAPK pathways, we used Pertussis Toxin to inhibit G-protein signaling. Western immunoblot was used to measure radiation-induced signal transduction, and we found that Pertussis Toxin markedly attenuated radiation-induced phosphorylation of Akt and ERK (data not shown). To further identify which GPCRs may be involved in this signaling cascade, we treated HUVEC with inhibitors (1μM) of either EDG1/3 (S1P1/S1P3) or EDG2/4 (LPA1/2) prior to irradiation with 3 Gy. Interestingly, we found that the inhibition of EDG2/4, not EDG1/3, prevented the radiation-induced phosphorylation of Akt, and ERK (**Figure 25A**). Thus, our results indicate that these signaling pathways may be primarily mediated by the LPA receptors, and not those of S1P. However, future studies are needed to determine if additional receptors are involved.

To determine which receptors are present in our various cell models, we performed western immunoblots using total cell lysates from tumor cells (GBM and LLC) and endothelial cells. Our findings demonstrate that while the S1P receptors are expressed primarily by endothelial cells, the classical LPA receptors are expressed by endothelial cells as well as tumor cells (**Figure 25B**).

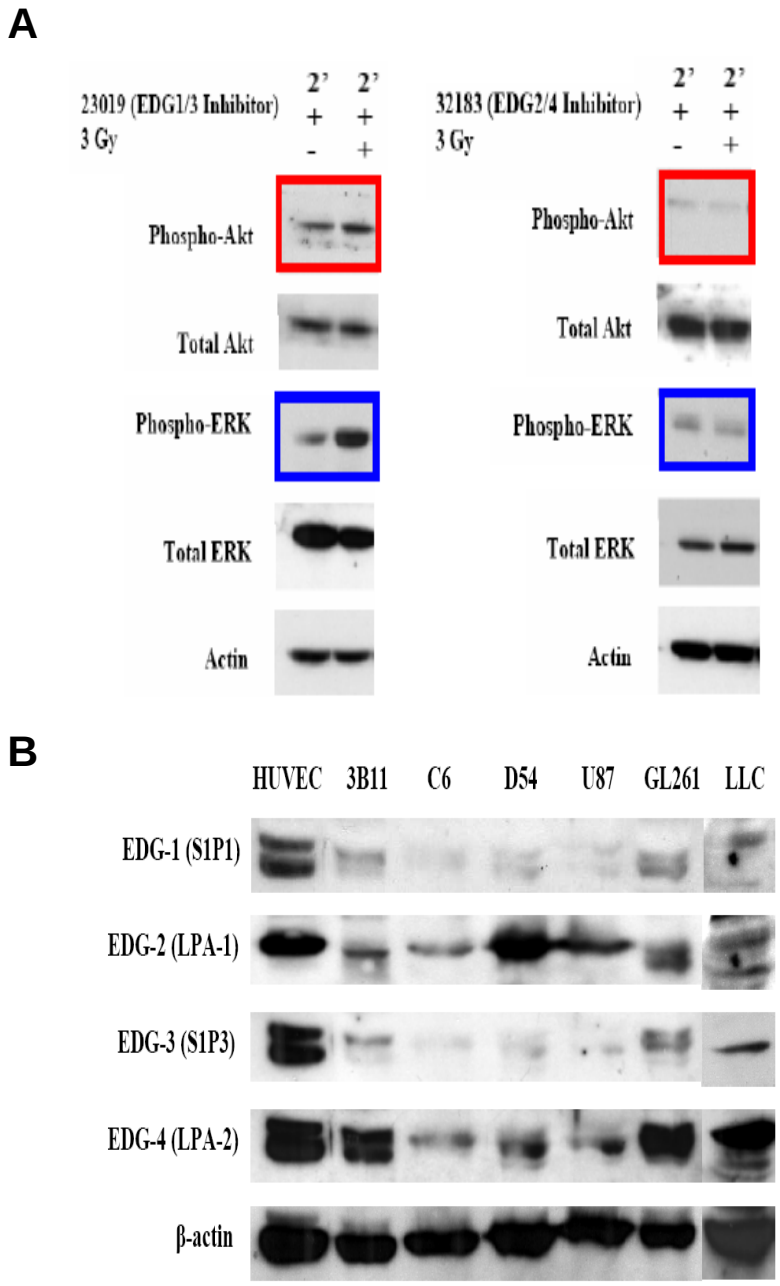

Figure 25. EDG inhibitors affect radiation-induced signaling. (**A**) HUVEC were pretreated with inhibitors of EDG1/3 or EDG2/4 for 30 min prior to irradiation with 3 Gy. Shown is the western immunoblot for phospho-Akt, phospho-ERK1/2, total Akt and ERK1/2, and actin at 2 min after the beginning of irradiation. (**B**)Western immunoblot of EDG1-4 in endothelial and tumor cells.

Inhibition of autotaxin and LPA receptors attenuates endothelial cell migration in HUVEC-A549 co-cultures

To determine whether autotaxin and LPA receptors play a role in the migration of irradiated endothelial cells, co-cultures of HUVEC + HUVEC or HUVEC + A549 cells were pre-treated with the autotaxin inhibitor and LPA receptor antagonist, BrP-LPA (2 μM), for 30 minutes prior to irradiation with 3 Gy. Twenty-four hours after treatment, the migratory ability of BrP-LPA-treated irradiated HUVEC was assessed. Results from the Boyden chamber transwell migration assay revealed that migration of irradiated endothelial cells was not significantly reduced by BrP-LPA treatment in HUVEC + HUVEC co-cultures. In contrast, when HUVEC were cultured with A549 cells, which express elevated levels of autotaxin, BrP-LPA treatment alone and in combination with radiation resulted in a significant reduction of endothelial cell migration (**Figure 26**). Such findings suggest that the autotaxin-LPA signaling axis may contribute to the radioresistance of tumor vasculature through the migratory recruitment of endothelial cells.

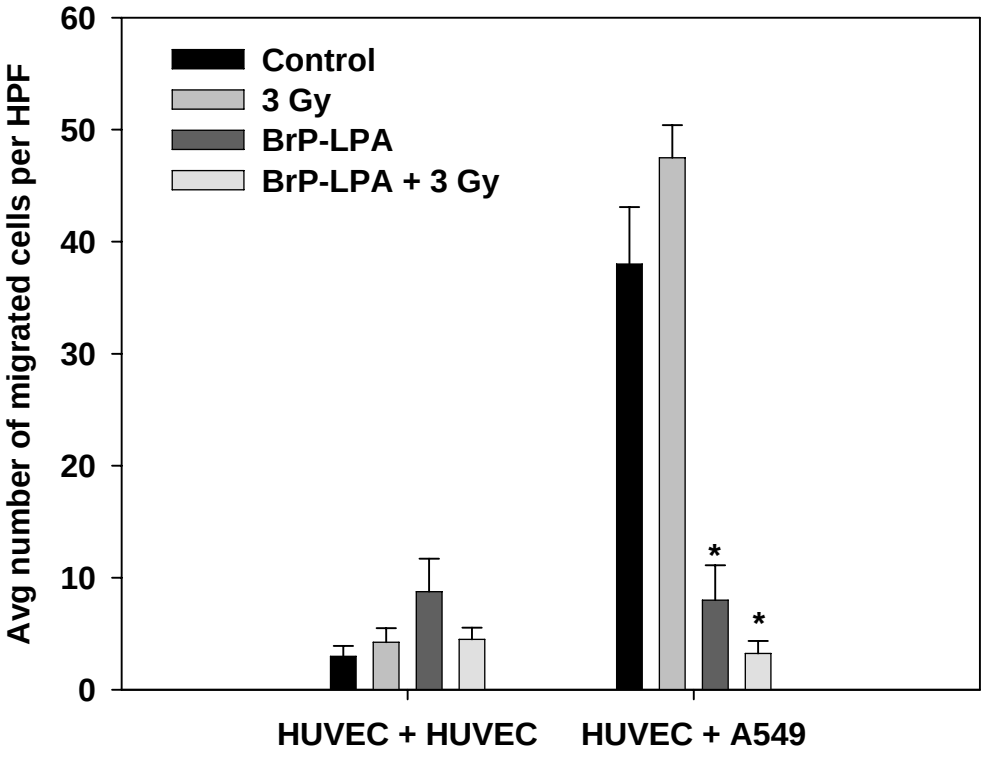

Figure 26. BrP-LPA inhibits migration in irradiated HUVEC-A549 co-cultures. In a Boyden chamber transwell migration assay, HUVEC-HUVEC or HUVEC-A549 co-cultures were pretreated with BrP-LPA for 30 minutes prior to irradiation with 3 Gy. 24 hours after treatment, migrated HUVEC were stained and counted. Shown is a bar graph of the average number of migrated cells per HPF; *, $P < 0.05$.

Inhibition of autotaxin attenuates the migration of A549 tumor cells

Since elevated autotaxin levels are often associated with increased tumor progression and invasiveness, we wanted to determine if autotaxin expression promotes the migration of A549 lung tumor cells. To assess the effects of autotaxin inhibition on the migratory ability of A549 cells, a scratch assay for cell migration was performed. Results from this experiment showed that radiation or BrP-LPA alone reduced A549 migration compared to control cells (**Figure 27A**). However, the most significant reduction was observed in cells treated with BrP-LPA followed by irradiation with 3 Gy (78% vs. 100%; $P < 0.05$, **Figure 27A**).

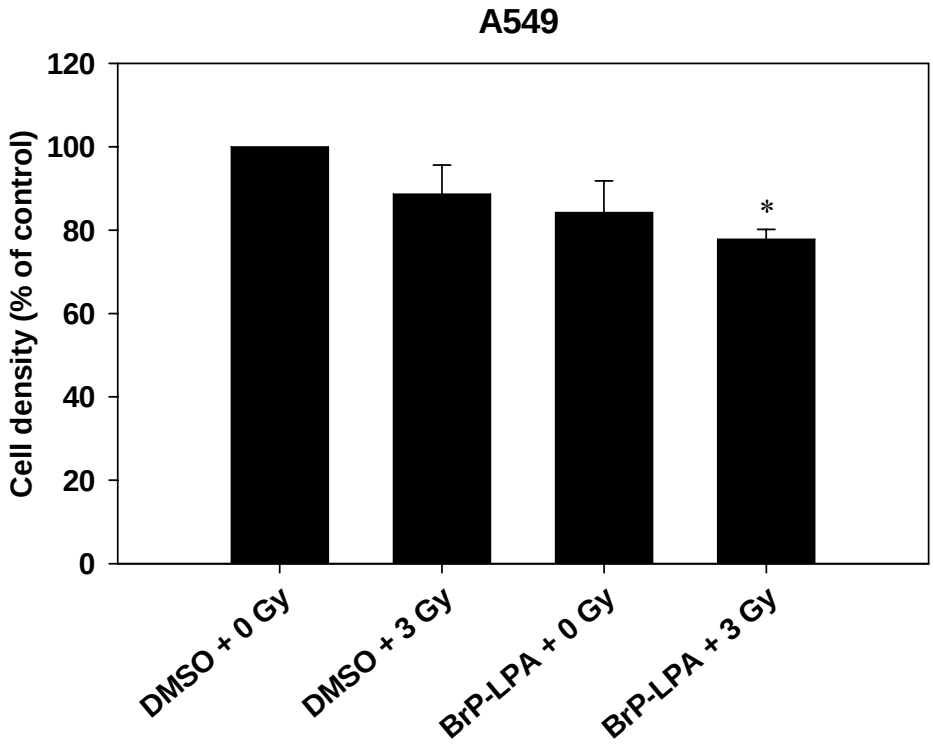

Figure 27. Inhibition of autotaxin attenuates migration of A549 tumor cells. Once A549 cells reached 70-80% confluency, four scratches were made using a 10 L pipette tip. Cells were treated with 2 μM BrP-LPA for 30 minutes prior to irradiation with 3 Gy. Twenty four hours after treatment, migrated cells were stained and counted. Shown is a bar graph of the percent of migrated cells;*, $P < 0.05$.

Discussion

Glioblastoma and lung cancer continue to display resistance to conventional therapies such as radiation, despite recent improvements in treatment protocols. This resistance to therapeutic agents is often determined by the response of the tumor blood vessels. In Chapters III and IV, we identified a key regulatory role for cytosolic phospholipase A2 in radiation-induced pro-survival signal transduction. Upon activation, $cPLA_2$ produces a lipid second messenger known as LPC that can be subsequently converted into LPA by autotaxin. Previous work by a variety of laboratories has shown that autotaxin, LPA, and LPA receptors are frequently expressed at exceedingly high levels in multiple cancers. Such overexpression is often associated with tumor cell invasion, metastasis, and angiogenesis. On the basis of these studies, we hypothesized that the autotaxin-LPA axis may significantly contribute to the increased resistance of lung cancer and glioblastoma to standard radiation therapy.

Using conditioned medium from various endothelial, glioblastoma and lung cancer cell lines, we determined the expression profile of autotaxin by Western immunoblotting. Although autotaxin was secreted at detectable levels in HUVEC and 3B11 endothelial cells, the highest expression of the enzyme was observed in conditioned medium from cancer cells. In addition, LPA production was significantly increased in irradiated co-cultures of HUVEC + glioblastoma cells. Such data suggests that, in response to ionizing radiation, LPC is hydrolyzed to LPA by autotaxin secreted from tumor cells. LPA exerts its multi-faceted biological activities through a variety of G protein-coupled receptors belonging to the EDG family. To determine if these receptors are involved in the activation of the PI3K/Akt and MAPK pathways, we treated HUVEC with inhibitors of EDG2/4 (LPA1/2) prior to irradiation

with 3 Gy. Interestingly, we found that the inhibition of LPA1/2 prevented the radiation-induced phosphorylation of Akt, and ERK1/2. Since LPA1 and LPA2 play a significant role in pro-angiogenic signaling pathways (Liu et al., 2009), these results suggest that these receptors may be important for the vascular endothelial response to radiation.

To assess the effects of autotaxin and LPA receptors on tumor cell migration, cells were treated with the autotaxin inhibitor and pan LPA receptor antagonist, BrP-LPA. Pre-treatment of HUVEC-A549 co-cultures with BrP-LPA resulted in a significant reduction in vascular endothelial cell migration following irradiation with 3 Gy. In addition, results from the scratch assay revealed that BrP-LPA treatment followed by irradiation significantly inhibited A549 tumor cell migration compared to cells treated with vehicle control.

In summary, the work presented in Chapter V implicates the involvement of autotaxin and LPA receptors in the vascular endothelial response to radiation. These findings provide further validation that the autotaxin-LPA axis provides multiple therapeutic candidates for the development of future radiosensitizing agents.

CHAPTER VI

CYTOSOLIC PHOSPHOLIPASE A2 AND LYSOPHOSPHOLIPIDS IN TUMOR ANGIOGENESIS

Introduction

Although recent advancements in therapeutic regimen have improved tumor response, local recurrence in lung cancer and glioblastoma multiforme (GBM) is a persistent problem (Belani et al., 2005; Clamon et al., 1999; DeAngelis, 2001; Lee et al., 1999; Stupp et al., 2009; Wagner, 2000). Both tumors are highly angiogenic and resistant to radiation (Riely and Miller, 2007; Wong and Brem, 2007). Despite aggressive treatment, most patients with unresectable GBM have a median survival of about one year (DeAngelis, 2001; Suh and Barnett, 1999; Videtic et al., 1999). Similarly, unresectable non-small-cell lung cancer also has a poor prognosis (Brock et al., 2008; Hoffman et al., 2000; Martini et al., 1995; Mountain, 1997). Additional treatments are, therefore, needed to provide improved survival benefits for these patients (Amir et al., 2008).

Discerning the molecular events involved in tumor microenvironment signal transduction is imperative for the development of efficient molecular-targeted pharmacological agents (Levy et al., 1995a; Shweiki et al., 1995; Wachsberger et al., 2003). We have recently demonstrated that activation of cytosolic phospholipase A2 ($cPLA_2$) promotes proliferation of vascular endothelial cells, potentiates the formation of a functional tumor vascular network and, therefore, contributes to cancer progression (Linkous et al., 2009; Yazlovitskaya et al., 2008). Activated $cPLA_2$ translocates from the cytosol to the cell membranes (Clark et al., 1991; Hirabayashi and Shimizu, 2000). Once there, $cPLA_2$ then specifically cleaves phosphatidylcholine

(PC) (Farooqui et al., 2006; Grewal et al., 2005; Herbert et al., 2007; Nakanishi and Rosenberg, 2006) to produce lysophosphatidylcholine (LPC) and arachidonic acid (AA) (Linkous et al., 2009; Yazlovitskaya et al., 2008). Another bioactive phospholipid with known tumorigenic and angiogenic properties is lysophosphatidic acid (LPA) (Folkman, 2001; Kishi et al., 2006; Ptaszynska et al., 2008). Two major pathways of LPA production depend upon $cPLA_2$ activity: 1) lysophospholipids generated by $cPLA_2$ (such as LPC) are subsequently converted to LPA by lysophospholipase D; 2) phosphatidic acid generated by phospholipase D or diacylglycerol kinase is subsequently converted to LPA by $cPLA_2$ (Aoki, 2004; Aoki et al., 2008). Therefore, $cPLA_2$ is involved in the regulation of the levels of at least three potent tumorigenic/angiogenic lipid mediators, LPC, AA and LPA. The role of AA and LPA in tumorigenesis has been extensively studied. There is a broad literature linking these two lipids, their turnover and signaling to cancer progression (Ambesi and McKeown-Longo, 2009; Herbert et al., 2009; Nakanishi and Rosenberg, 2006; Zhang et al., 2009) There is also a vivid discussion about AA and LPA signaling pathways being molecular targets for controlling cancer and several companies are developing drugs for this purpose (Murph and Mills, 2007; Peyruchaud, 2009). In contrast, relatively little is known about the role of LPC in tumor progression. Recent studies by our laboratory and others have shown that LPC is a lipid-derived second messenger that triggers the downstream phosphorylation of both PI3K/Akt and MAPK/ERK pro-survival signal transduction pathways resulting in an increased cellular viability within tumor vascular endothelium (Fujita et al., 2006; Linkous et al., 2009; Yazlovitskaya et al., 2008).

To investigate the effects of $cPLA_2$ on lung carcinoma and glioblastoma growth, we utilized C57/BL6 mice deficient in $cPLA_2$-alpha (α), the predominant

isoform of $cPLA_2$ in endothelium. The $cPLA_2\alpha^{-/-}$ mouse model allowed us to determine how the deficiency in $cPLA_2$ within host-derived vascular endothelium affects tumor maintenance and progression. In addition, Murine Pulmonary Microvascular Endothelial Cells (MPMEC) from $cPLA_2\alpha^{-/-}$ mice were used to investigate the addback of LPC, LPA and AA on cell viability and functions.

To further inhibit $cPLA_2$ in cell culture models and wild-type animal studies, we incorporated the use of the $cPLA_2\alpha$ inhibitor CDIBA. Through its potent inhibition of the enzyme, CDIBA has been shown to significantly attenuate arachidonic acid release and PGE_2 production in a wide variety of enzymatic and cell-based assays (McKew et al., 2006). We showed that $cPLA_2$ deficiency was associated with impaired tumor growth and blood vessel formation *in vivo*. In cell culture models, $cPLA_2$ inhibition significantly reduced the proliferation, invasion, migration, and tubule formation of vascular endothelial cells. Following the addition of lysophospholipids LPC and LPA, however, restoration of the angiogenic phenotype was observed. Since LPC and LPA are regulators of migration and cellular growth in a variety of cell systems, these lipid mediators may play a critical role in $cPLA_2$-mediated angiogenesis.

Results

Lysophospholipids restore proliferation in $cPLA_2$-deficient and CDIBA-treated vascular endothelial cells

Since new vessel formation requires vascular endothelial cell proliferation, primary MPMEC isolated from $cPLA_2\alpha^{+/+}$ or $cPLA_2\alpha^{-/-}$ mice were used to assess the effects of $cPLA_2$ deficiency on the growth and proliferation of cells in culture. MPMEC were stained with an antibody to Ki67, an established proliferation marker. Interestingly, in $cPLA_2\alpha^{-/-}$ cells, Ki-67 staining was reduced by 59% compared to

$cPLA_2\alpha^{+/+}$ cells (**Figure 28A**). The ability of $cPLA_2$ to promote endothelial cell proliferation was further evident when 3B11 vascular endothelial cells and LLC tumor cells were treated with the $cPLA_2$ inhibitor, CDIBA (2 μM), and assessed for proliferation. Immunofluorescence staining for Ki-67 revealed a significant decrease in endothelial cell proliferation as a result of $cPLA_2$ inhibition (44% for 3B11, **Figure 28B, D**). Furthermore, inhibition of $cPLA_2$ had no significant effect on LLC cell proliferation (92% for LLC, **Figure 28D**). Similarly to Ki-67 staining, BrdU incorporation was reduced by 50% in 3B11 cells treated with CDIBA compared to control (**Figure 28C**). Conversely, an MTS assay for metabolic activity revealed no significant difference between CDIBA-treated 3B11 cells and cells treated with vehicle alone (data not shown), suggesting that $cPLA_2$ inhibition affects the proliferative status but not cellular viability of vascular endothelial cells.

Studies have shown that $cPLA_2$ is essential for the production of three bioactive lipid mediators, arachidonic acid (AA), lysophosphatidylcholine (LPC) and lysophosphatidic acid (LPA). To determine which of these three lipids contribute to vascular endothelial cell proliferation, MPMEC from $cPLA_2\alpha^{+/+}$ and $cPLA_2\alpha^{-/-}$ mice and CDIBA-treated 3B11 cells were incubated with 10 μM LPC, LPA, or AA for 24 hours and then assessed for changes in Ki-67 staining. In $cPLA_2\alpha^{-/-}$ cells, the addition of LPC or LPA alone did not significantly increase proliferation. In comparison, $cPLA_2\alpha^{-/-}$ cells treated with a combination of both lysophospholipids (LPC + LPA) demonstrated a statistically significant increase of Ki-67 positive staining from 41% to 75% (**Figure 28A**). Interestingly, exogenous AA contributed little to proliferation (**Figure 28A**). In 3B11 cells, treatment with LPC or LPA resulted in slightly enhanced Ki-67 staining in comparison to cells treated with CDIBA alone (56% and 58% *vs.* 44%, **Figure 28B**). The addition of AA produced a similar increase (56% *vs.*

44%, **Figure 28B**). A combined treatment of LPC and AA further enhanced proliferation, with 62% of cells staining positive for Ki-67 (**Figure 28B**). However, a statistically significant increase in endothelial cell proliferation was observed in 3B11 cells that received a combination of both LPC and LPA (81% *vs.* 44%, **Figure 28B**). Similar results were obtained in the BrdU incorporation assay, in which the addition of exogenous LPC and LPA to CDIBA-treated cells resulted in increased proliferation compared to cells treated with CDIBA alone (**Figure 28C**). These results indicate that, in addition to AA, both $cPLA_2$-dependent LPC and LPA may be involved in vascular endothelial cell proliferation.

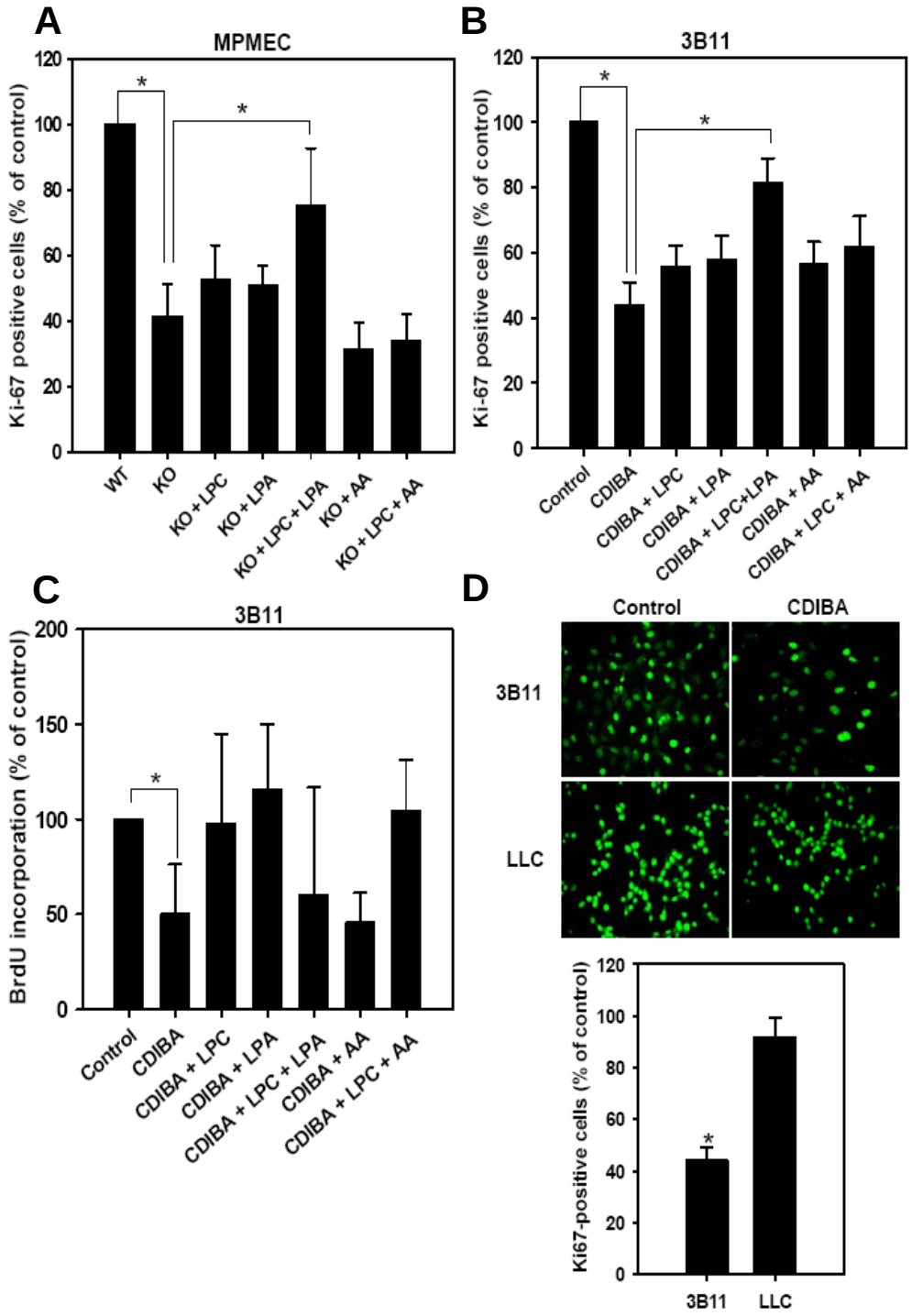

Figure 28. Lysophospholipids restore proliferation in cPLA$_2$-deficient and CDIBA-treated vascular endothelial cells. cPLA$_2\alpha^{+/+}$ and cPLA$_2\alpha^{-/-}$ MPMEC (**A**), 3B11 (**B-D**), or LLC cells (**D**) were grown to 60–70% confluency. Cultures were treated with 2 μM CDIBA (3B11 and LLC only) in the absence or presence of 10 μM LPC, LPA, or AA for 24 hours. Proliferation was assayed using anti-Ki67 immunofluorescence (**A-B**, **D**) or BrdU incorporation (**C**). Shown are micrographs and corresponding bar graphs of the percentage of MPMEC (**A**), 3B11 (**B**, **D**), or LLC tumor cells (**D**) exhibiting positive Ki-67 staining with SEM from three experiments, *, $P < 0.05$. (**C**) Shown is a bar graph of BrdU incorporation in 3B11 cells (% of control with SEM from three experiments, *, $P < 0.05$.

Lysophospholipids restore invasion and migration in cPLA$_2$-deficient and CDIBA-treated vascular endothelial cells

To facilitate blood vessel formation, matrix degradation and endothelial cell invasion is required. Therefore, to determine if lysophospholipids affect endothelial cell invasion and migration, MPMEC or 3B11 cells were plated onto matrigel-coated transwell inserts and treated for 24 hours with vehicle or 2 μM CDIBA ± 10 μM LPC, LPA, or AA. Once the incubation was complete, migrated cells were stained with DAPI and counted using fluorescence microscopy. As shown in **Figure 29**, the average number of migrated cells was reduced by 78% in cPLA$_2\alpha^{-/-}$ cells compared to cPLA$_2\alpha^{+/+}$ cells (**Figure 29A**). In addition, although treatment with LPC + AA produced a slight increase in the average number of migrated cells, the statistically significant increase in endothelial migration was observed following the addition of LPC + LPA (34 *vs.* 10 migrated cells, **Figure 29A**). In the 3B11 vascular endothelial cells, treatment with CDIBA alone reduced migration by 71% compared to control cells (**Figure 29B, C**). As expected, introduction of AA, a known stimulus for cell migration, enhanced the number of migrated cells by 58% in CDIBA-treated cells (24 *vs*. 10, **Figure 29B**). Interestingly, a similar increase in the total number of migrated cells per HPF was observed with the addition of either LPC or LPA (24 or 21 *vs.* 10, **Figure 29B**). The most pronounced increase in transwell migration, however, was observed in the cells that received a combined treatment of LPC + LPA or LPC + AA (31 or 28 *vs.* 10, **Figure 29B**). Thus, the ability of vascular endothelial cells MPMEC and 3B11 to invade and migrate may be dependent upon lysophospholipids in addition to the well-characterized AA pathway.

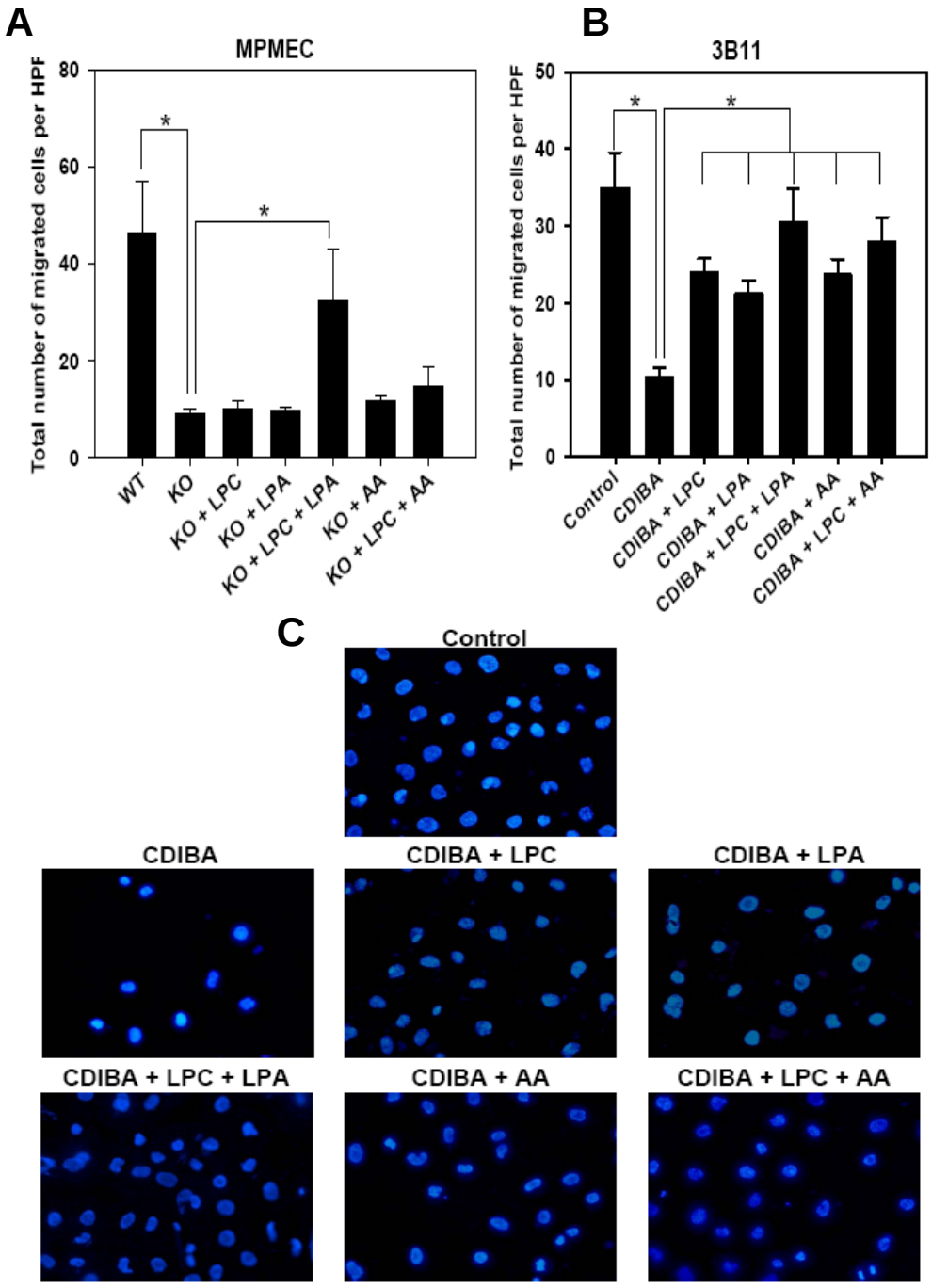

Figure 29. Lysophospholipids restore invasion and migration in cPLA$_2$-deficient and CDIBA-treated vascular endothelial cells. MPMEC (**A**) or 3B11 (**B, C**) endothelial cells were added to the top chambers of 24 transwell Boyden chamber plates with 8 μm matrigel-coated inserts. Fresh medium was added to the bottom chambers, and both chambers were treated for 24 hr with vehicle or 2 μM CDIBA (3B11 only) in the absence or presence of 10 μM LPC, LPA, or AA. After 24 hours, the insert chambers were stained with DAPI and migrated cells were counted (4 HPF per sample). (**A, B**) Shown are bar graphs of the average number of migrated cells per HPF for cPLA$_2\alpha^{-/-}$ MPMEC (**A**) or 3B11 (**B**) with SEM from three experiments, *, $P < 0.05$. (**C**) Shown are representative micrographs of migrated 3B11 cells obtained 24 hr after treatment;*, $P < 0.05$.

Inhibition of cPLA$_2$ decreases migration of vascular endothelial cells but not lung tumor cells

To determine if cPLA$_2$ inhibition affects the migratory ability of cells, a scratch assay for cell migration was performed using both 3B11 and LLC cells. Once cultures reached 70–80% confluency, four parallel scratches were created on each plate using a 10 µl pipette tip. Cells were then treated with DMSO or CDIBA (2 µM) for 24 hours. In the 3B11 vascular endothelial cell line, cPLA$_2$ inhibition significantly reduced migration by 75% compared to control cells ($P < 0.05$, **Figure 30**). In contrast, no statistically significant reduction in migratory ability was observed in LLC cells treated with the cPLA$_2$ inhibitor (**Figure 30**).

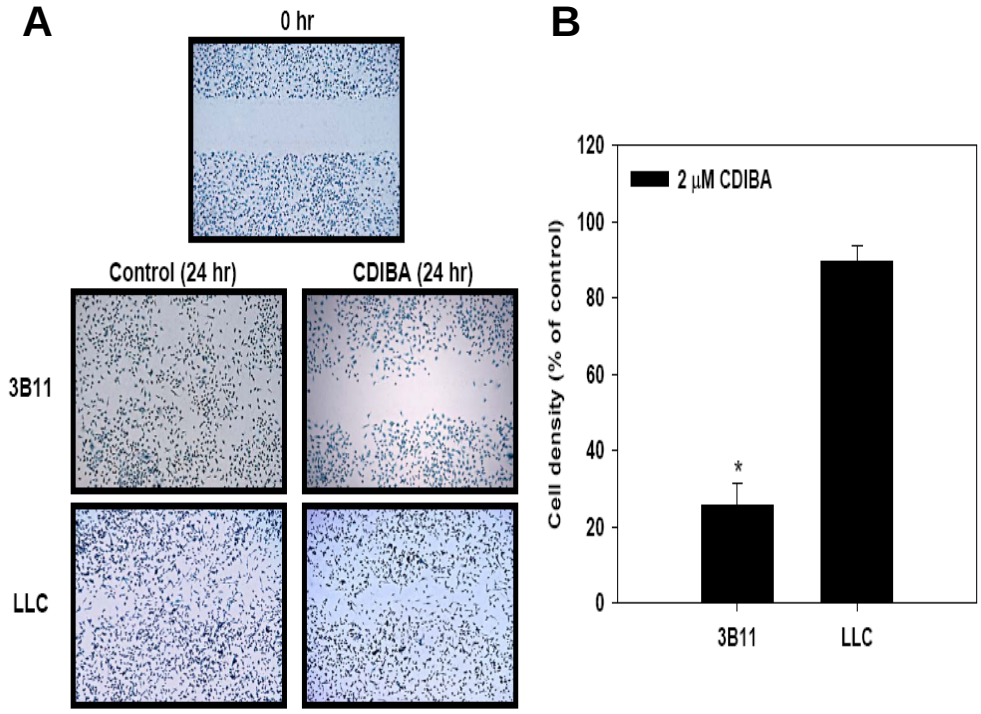

Figure 30. Inhibition of cPLA$_2$ decreases vascular endothelial cell migration. A scratch assay for cell migration was performed on 3B11 or LLC cells grown to 70–80% confluency. Four parallel wounds were created on each plate using a 10 µl pipette tip, and cells were treated with DMSO or the cPLA$_2$ inhibitor CDIBA (2 µM) for 24 hours. Cells were then stained with 1% methylene blue and counted. Shown are representative micrographs of stained cells (**A**) and a bar graph of the corresponding average percentage of migrated cells with SEM. from three experiments, *, $P < 0.05$ (**B**).

Inhibition of cPLA$_2$ with CDIBA attenuates tubule formation in vascular endothelial cells

One of the primary stages in angiogenesis is the assembly of vascular endothelial cells into tubular vessels. To determine if cPLA$_2$ plays a role in this angiogenic process, we performed a capillary-like tubule formation assay. 3B11 and HUVEC were plated onto Matrigel-coated 24-well plates in the absence or presence of the cPLA$_2$ inhibitor CDIBA (2 μM). In 3B11 cells, treatment with 2 μM CDIBA reduced tubule formation by 64% compared to cells treated with vehicle alone (**Figure 31**). A similar effect was observed in HUVEC in which cPLA$_2$ inhibition attenuated tubule formation by 40% (**Figure 31**).

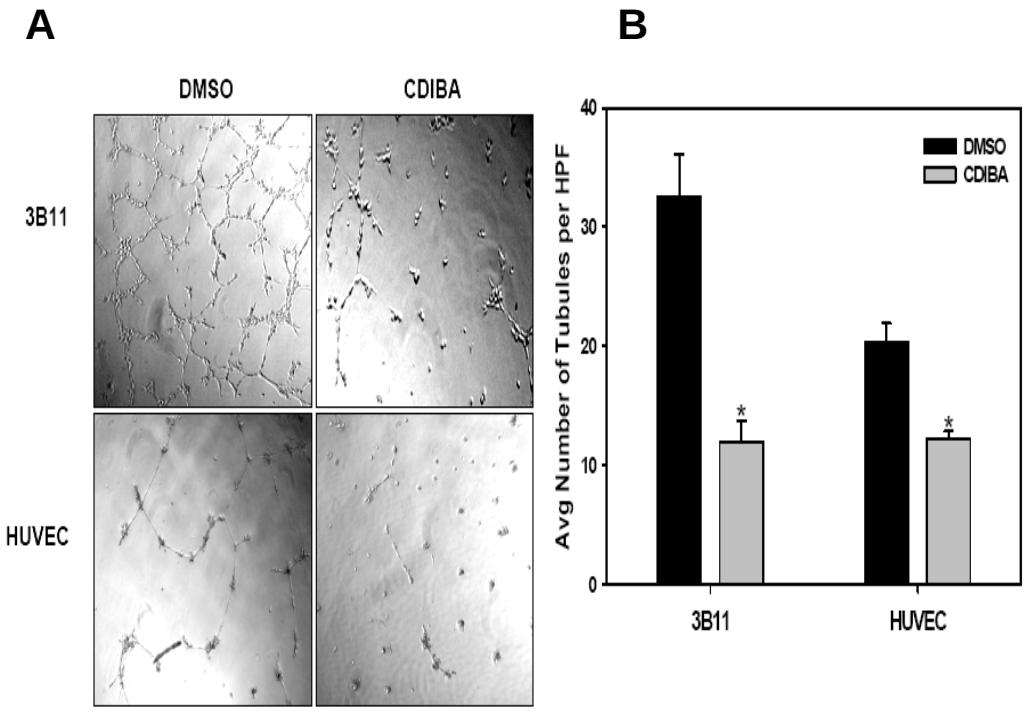

Figure 31. cPLA$_2$ inhibition attenuates vascular endothelial cell tubule formation. 3B11 or HUVEC were cultured onto Matrigel in the absence (DMSO) or presence of 2 μM CDIBA. Capillary tubule formation was evaluated at 6 hours (3B11) or 24 hours (HUVEC) after treatment. Tubule formation was quantified as the number of tubule branches per high power field (4 HPF per sample). Shown are representative micrographs (**A**) and a bar graph of the average tubule formation for 3B11 and HUVEC with SEM from three independent experiments; *, $P < 0.05$ (**B**).

Inhibition of cPLA$_2$ suppresses tumor growth

To determine whether cPLA$_2$ inhibition is sufficient to suppress tumor growth, syngeneic heterotopic tumor models of Lewis Lung Carcinoma (LLC) and glioblastoma (GL261) were studied. To inhibit cPLA$_2$, tumor-bearing mice were treated with CDIBA (0.5-1.0 mg/kg) once daily for 5 or 7 consecutive days, and tumor volume was monitored over time. **Figure 32A, B** demonstrates that in mice treated with CDIBA, LLC tumor growth was significantly delayed by approximately 5 days. Tumor growth suppression was further increased among GL261 tumors (**Figure 32C**). Interestingly, complete GL261 tumor regression was observed in 50% of CDIBA-treated mice. Moreover, volume calculations from remaining tumors on Day 21 revealed a statistically significant decrease in GL261 tumor size in mice treated with CDIBA (**Figure 32D**).

Plasma LPA levels were measured in LLC- or GL261-tumor bearing mice before treatment and immediately following the final treatment with vehicle or CDIBA. There was no statistical difference in plasma LPA levels among treatment groups in either of the two tumor models, suggesting that CDIBA treatment may affect the production of LPC, but not the overall generation of LPA (**Figure 32E**).

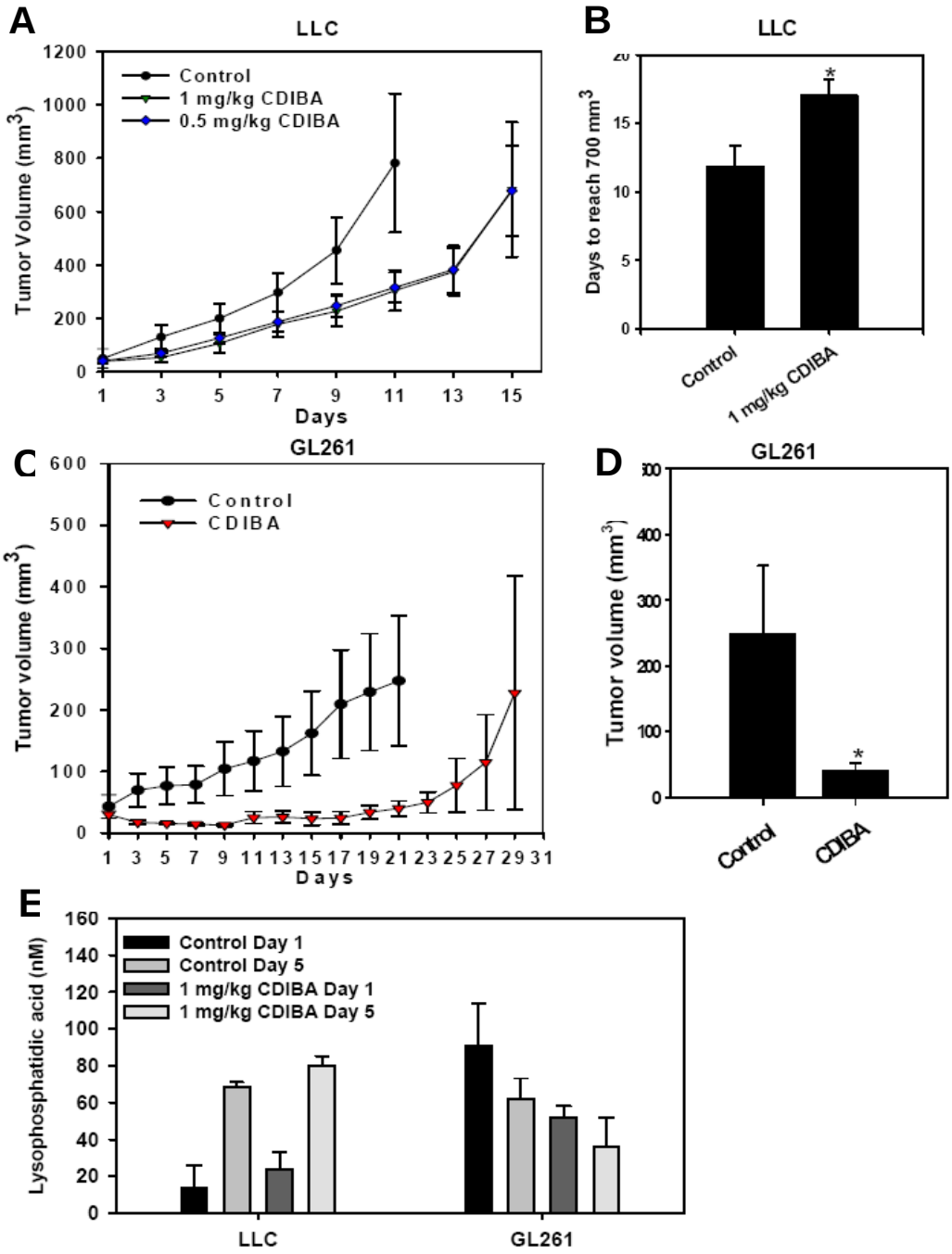

Figure 32. Inhibition of $cPLA_2$ suppresses tumor growth. LLC (**A, B**) or GL261 cells (**C, D**) were injected s.c. into the hindlimbs of C57/BL6 mice. Mice received i.p. injections of 0.5 mg/kg-1.0 mg/kg CDIBA once per day for 5 and 7 consecutive days (LLC and GL261, respectively). (**A**) Shown are mean LLC tumor volumes with SEM. (**B**) Shown is the bar graph of the average number of days for LLC tumors to reach 700 mm^3 in mice treated with 1.0 mg/kg CDIBA in comparison to control mice with SEM,*, $P < 0.05$. (**C**) Shown are mean GL261 tumor volumes with SEM. (**D**) Shown is the average GL261 tumor volume for each treatment group at Day 21 with SEM,*, $P < 0.05$. Each treatment group in all experiments included at least 6 mice. (**E**) LPA was measured in plasma from tumor-bearing mice before treatment initiation (Day 1) and immediately after the final treatment (Day 5). Shown is a bar graph of LPA plasma levels (nM).

Mice deficient in cPLA$_2$α exhibit suppressed tumor growth

To further examine the role of cPLA$_2$ in angiogenesis and tumor progression, LLC and GL261 tumor growth was monitored in cPLA$_2\alpha^{+/+}$ and cPLA$_2\alpha^{-/-}$ mice. Mice were injected with 10^6 LLC cells or 2 x 10^6 GL261 cells, and tumor volume was monitored using Power Doppler Sonography. Interestingly, at 14 days post-injection, spontaneous LLC tumor regression was observed in 50% of cPLA$_2\alpha^{-/-}$ mice with no regression of tumors in wild-type mice. Furthermore, measurements from Day 16 revealed that tumor volume was significantly reduced in remaining tumors from cPLA$_2\alpha^{-/-}$ mice compared to tumors from cPLA$_2\alpha^{+/+}$ mice (**Figure 33A**). The effects of cPLA$_2$ deficiency on tumor growth were even more pronounced in the GL261 model. Results from the glioblastoma study revealed that while cPLA$_2\alpha^{+/+}$ mice exhibited normal tumor growth progression (tumor take rate = 100%, **Figure 33B**), GL261 tumor formation in cPLA$_2\alpha^{-/-}$ mice remained undetectable one month after the injection of tumor cells (tumor take rate = 0 %, **Figure 33B**).

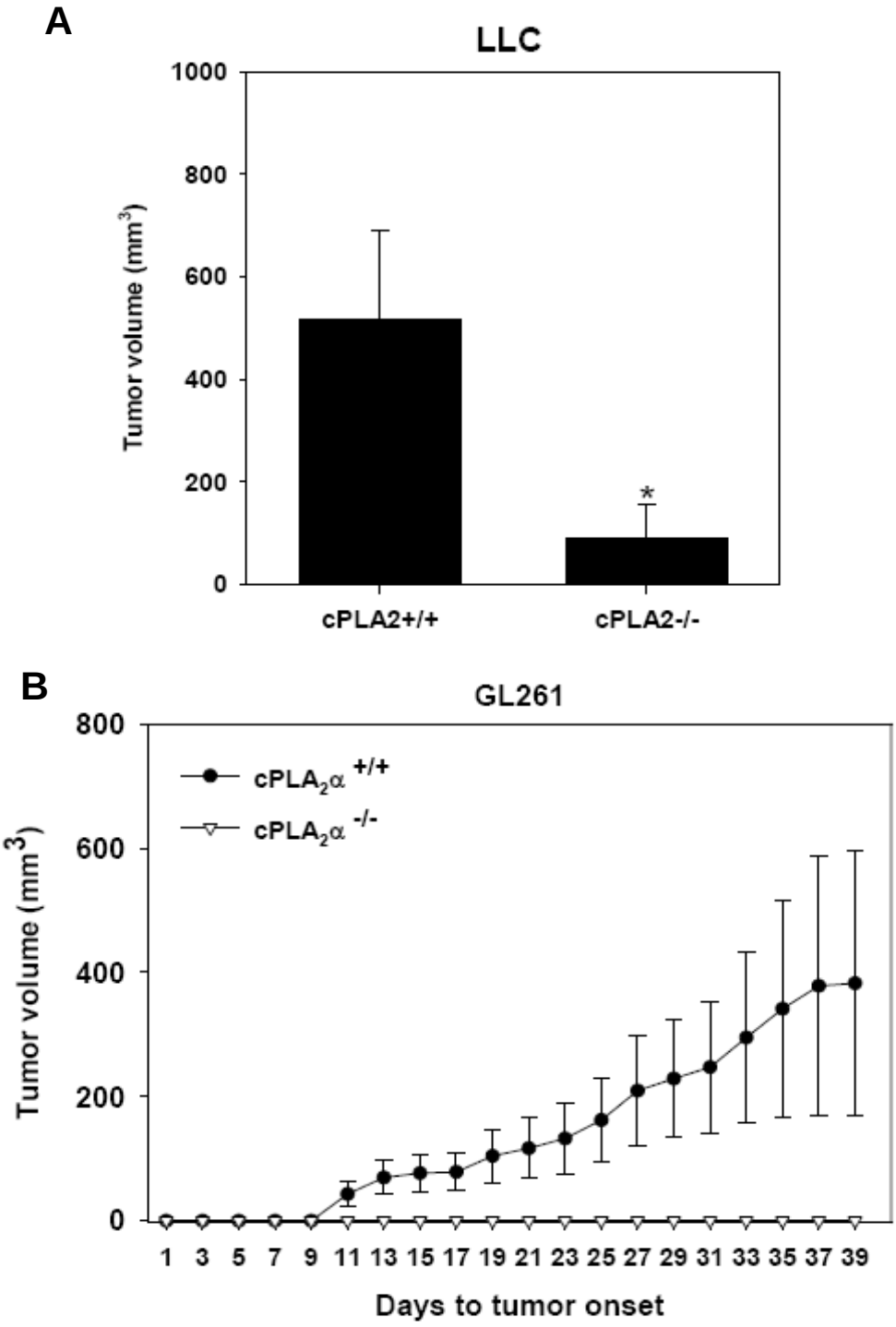

Figure 33. Mice deficient in cPLA$_2\alpha$ exhibit suppressed tumor growth. LLC or GL261 cells were injected subcutaneously into the hind limbs of cPLA$_2\alpha^{+/+}$ or cPLA$_2\alpha^{-/-}$ C57/BL6 mice. Tumor volume was measured using Power Doppler Sonography. (**A**) Shown is the average LLC tumor volume for each group at Day 16 with SEM,*, $P < 0.05$. (**B**) Shown are the mean GL261 tumor volumes with SEM in cPLA$_2\alpha^{-/-}$ and wild-type mice. Each group in all experiments included at least 6 mice.

Tumors from cPLA$_2\alpha^{-/-}$ mice exhibit decreased vascularity, attenuated pericyte coverage, and elevated necrosis

To determine the effects of cPLA$_2$ deficiency on tumor vascularity, formalin-fixed LLC tumors from cPLA$_2\alpha^{+/+}$ and cPLA$_2\alpha^{-/-}$ mice were sectioned and examined for microvascular density using an antibody against von Willebrand Factor (vWF), a known vascular endothelial cell marker (**Figure 34A**). Immunohistochemical examination showed a significant decrease in the average vessel number per HPF in tumors from cPLA$_2\alpha^{-/-}$ mice as compared to wild-type mice (2.3 *vs.* 5.4, **Figure 34A, B**). Hematoxylin and eosin staining revealed multiple necrotic areas in tumors from cPLA$_2\alpha^{-/-}$ mice, but only minimal necrosis in tumors from cPLA$_2\alpha^{+/+}$ mice, thus implicating cPLA$_2$ as an important factor for tumor formation, growth and maintenance of vascularity (**Figure 34C**). To investigate whether cPLA$_2$ is involved in tumor blood vessel maturation, LLC tumor sections were co-stained with antibodies to vWF and alpha-smooth muscle actin (α-SMA) or desmin, two known pericyte markers used to detect stages of vascular development. Results from α-SMA immunofluorescence demonstrated significant pericyte coverage of the tumor vasculature in LLC tumors from cPLA$_2\alpha^{+/+}$ mice (**Figure 35A**). In tumors from cPLA$_2\alpha^{-/-}$ mice, however, vessel-encircling pericytes were undetectable. Since α-SMA expression may be dependent upon the maturation stage of pericytes, tumor sections were also examined for the presence of desmin which is expressed by mature and immature pericytes. Although desmin was detected in tumor vasculature from cPLA$_2\alpha^{+/+}$ mice, no desmin-positive cells were observed within tumor blood vessels from cPLA$_2\alpha^{-/-}$ mice (**Figure 35B**). These marked differences in pericyte coverage suggest that, in addition to its role in endothelial cell function, cPLA$_2$ may also be responsible for pericyte recruitment and vessel maturation.

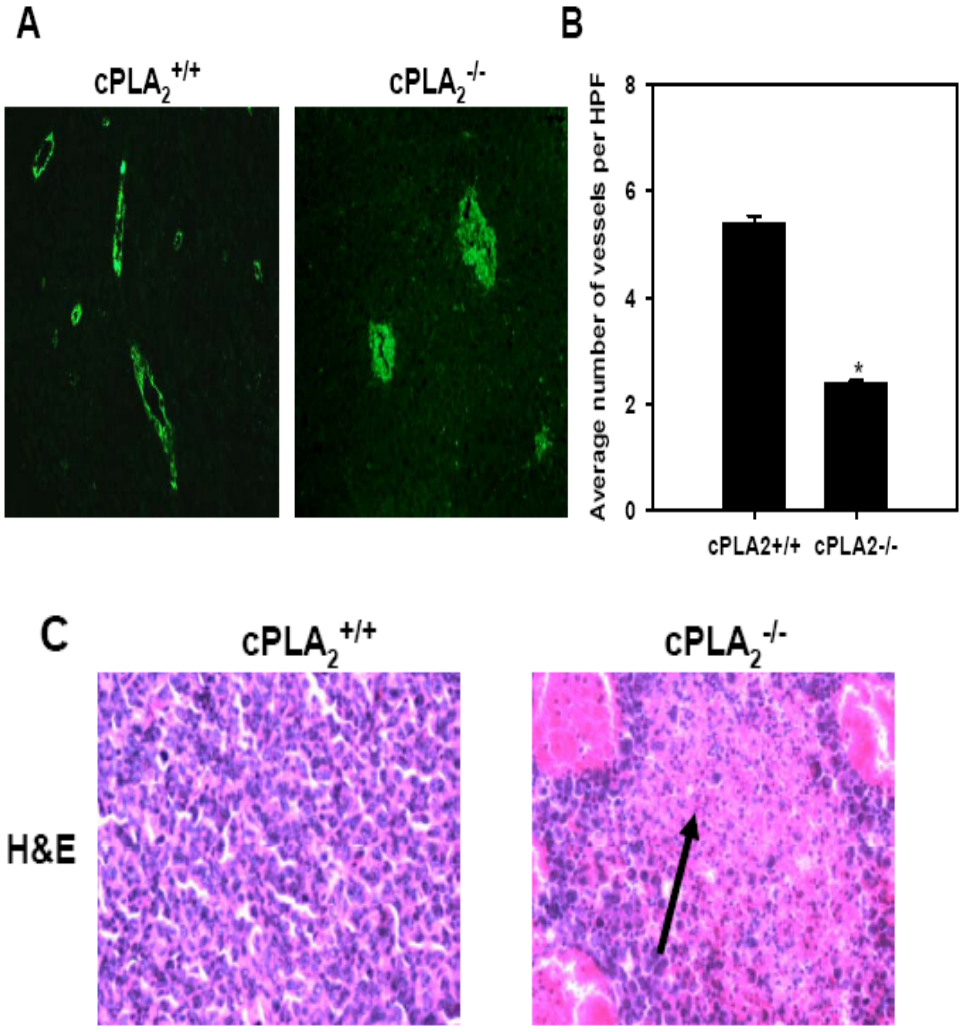

Figure 34. Tumors in cPLA$_2\alpha^{-/-}$ mice exhibit decreased vascularity and elevated necrosis. Formalin-fixed LLC tumors from cPLA$_2\alpha^{+/+}$ and cPLA$_2\alpha^{-/-}$ mice were sectioned and stained with anti-von Willebrand Factor (vWF) antibody or hematoxylin and eosin (H and E). Shown are microscopic photographs of positive vWF staining (**A**) and a bar graph of the average number of tumor blood vessels per high power field with SEM (**B**),*, $P < 0.05$. (**C**) Shown are microscopic photographs of H and E staining in tumors from cPLA$_2\alpha^{+/+}$ and cPLA$_2\alpha^{-/-}$ mice. Black arrow indicates necrosis. Each group in all experiments included at least 6 mice.

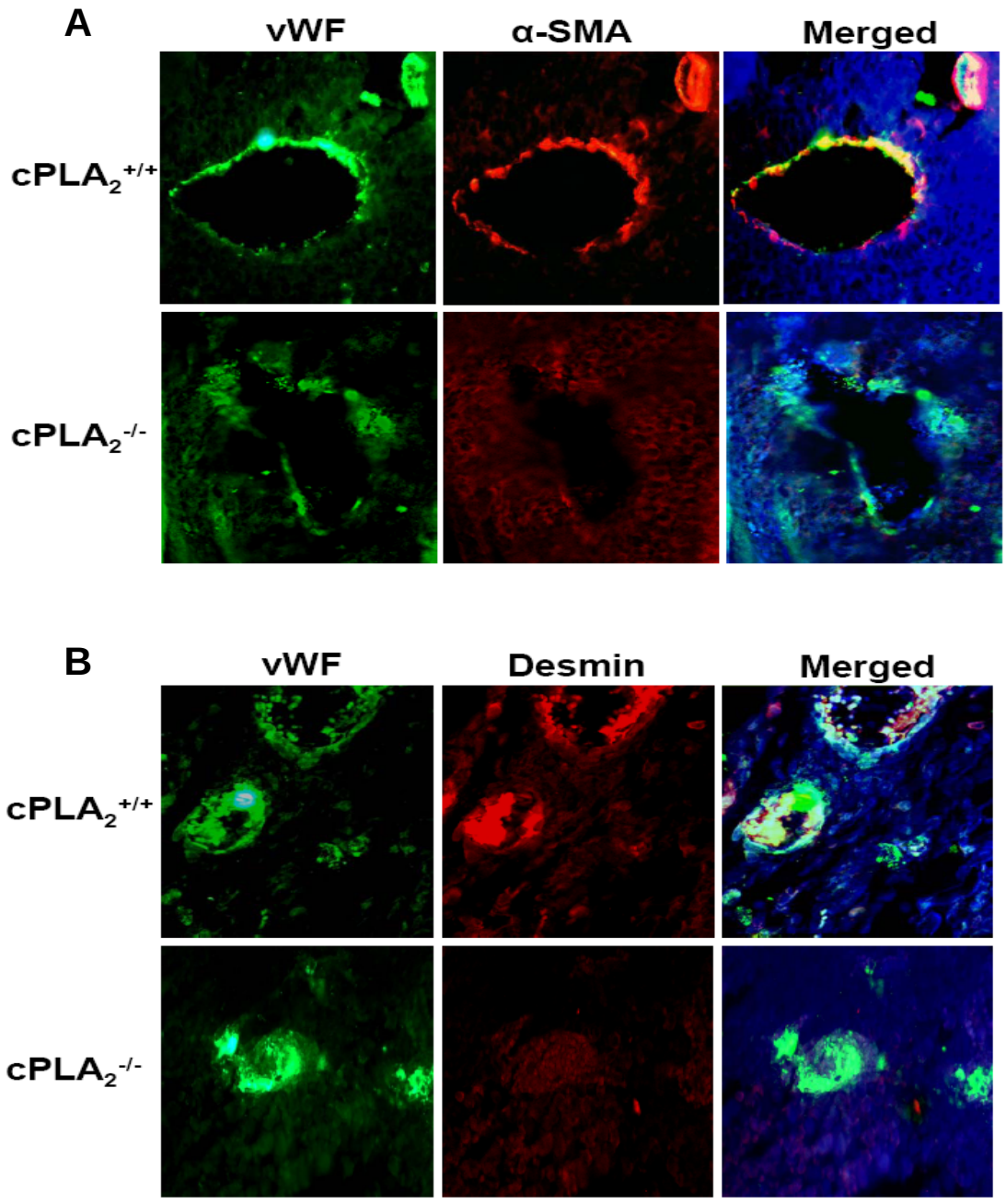

Figure 35. Tumors in cPLA$_2\alpha^{-/-}$ mice exhibit attenuated pericyte coverage. Formalin-fixed LLC tumors from cPLA$_2\alpha^{+/+}$ and cPLA$_2\alpha^{-/-}$ mice were sectioned and co-stained with anti-von Willebrand Factor (vWF) antibody and anti-alpha-smooth muscle actin antibody or anti-desmin antibody. (**A**) Shown are microscopic photographs of immunofluorescence staining for vWF (green), alpha-smooth muscle actin (red) and DAPI (blue) in tumors from cPLA$_2\alpha^{+/+}$ and cPLA$_2\alpha^{-/-}$ mice. (**B**) Shown are microscopic photographs of immunofluorescence staining for vWF (green), desmin (red) and DAPI (blue) in tumors from cPLA$_2\alpha^{+/+}$ and cPLA$_2\alpha^{-/-}$ mice.

Discussion

Blood vessel formation is a fundamental process that occurs during both normal and pathologic periods of tissue growth. Vascularization is often excessive and associated with tumor progression in malignancies such as lung cancer and glioblastoma (Goodwin, 2007). In an effort to inhibit this tumor growth, multiple anti-angiogenic agents have been developed. However, although several angiogenesis inhibitors have produced an enhanced clinical benefit, many of these pharmacologic agents only result in transitory improvements followed by increased tumor resistance (Bergers and Hanahan, 2008). Thus, the development of novel, effective anti-angiogenic therapies could improve tumor control in treatment-resistant cancers like lung carcinoma and glioblastoma. In the present study, we identify a key regulatory role for cytosolic phospholipase A2 in tumor angiogenesis and provide evidence that $cPLA_2$ inhibition may prevent the formation of a functional tumor vascular network.

We found that $cPLA_2$ inhibition significantly attenuated capillary-like tubule formation in two vascular endothelial cell models. In addition, treatment with the $cPLA_2$ inhibitor CDIBA reduced endothelial cell migration by 75%, but had no significant effect on lung tumor cells. Thus, these data suggest that $cPLA_2$ contributes to both the migratory ability and morphogenesis of vascular endothelial cells during tumor vascularization.

Migration and tubule formation are dependent upon the ability of endothelial cells to degrade both the basement membrane and the extracellular matrix of the surrounding connective tissue (Goodwin, 2007). Our experiments using multiple models of cultured vascular endothelial cells have shown that $cPLA_2$ inhibition dramatically reduced the ability of these cells to degrade the matrigel and migrate through the filter. These results suggest an essential role of $cPLA_2$ in the migratory

function of vascular endothelial cells. Since $cPLA_2$ is responsible for the production of bioactive lipid mediators, LPC, AA, and LPA, we wanted to determine which of these products contributes to the promotion of vascular endothelial cell migration. Although the restoration of LPC, LPA, and AA alone resulted in increased migration, the most pronounced effect was observed with the addition of LPC + LPA or LPC + AA to $cPLA_2\alpha^{-/-}$ cells or cells treated with CDIBA. These results indicate that, in addition to AA and LPA, which regulate endothelial cell migration (Folkman, 2001; Herbert et al., 2009; Kishi et al., 2006; Ptaszynska et al., 2008), the less-characterized LPC pathway may also play a significant role in this process.

In addition to migration, tumor vascularization requires the multiplication of endothelial cell populations. To determine the effects of CDIBA on cellular proliferation, we assessed staining intensity for Ki67, a well-known proliferative marker, (Grosse-Wilde et al., 2008; Teplyuk et al., 2008) in MPMEC, 3B11 and LLC cells. Ki67 immunofluorescence was significantly reduced in MPMEC from $cPLA_2\alpha^{-/-}$ mice and in 3B11 cells treated with CDIBA. Furthermore, BrdU incorporation, but not metabolic activity, was also reduced in CDIBA-treated 3B11 cells, suggesting that $cPLA_2$ inhibition affects proliferation rather than cellular viability. Tumor cell (LLC) proliferation, however, remained unchanged by $cPLA_2$ inhibition. Addition of LPC + AA resulted in a modest increase in Ki67 staining, but the most significant restorative effect was observed in endothelial cells treated with LPC + LPA. These findings were further supported by evidence from primary cultures in which the most pronounced increase in cellular proliferation was observed in $cPLA_2\alpha^{-/-}$ cells treated with a combination of LPC and LPA. These data demonstrate a key role for $cPLA_2$ in endothelial cell proliferation and indicate that lysophospholipids, LPC and LPA, may serve as effectors for this stage of angiogenesis.

To determine the role of $cPLA_2$ in tumor growth, we studied both lung carcinoma and glioblastoma tumor models. Using the $cPLA_2$ inhibitor CDIBA, we found that chemical inhibition of $cPLA_2$ significantly delayed tumor growth in both tumor models. In the glioblastoma model, specifically, we observed tumor regression during administration of the drug. Given the high level of vascularity in GBM tumors, this unexpected biological response may be due to impaired blood flow which can ultimately prevent cancer growth (de Bouard et al., 2007; Dewhirst et al., 2008; Folkman, 1971; Keshet and Ben-Sasson, 1999; Plate and Risau, 1995). Moreover, tumor growth suppression was sustained for several days following treatment cessation, suggesting that CDIBA exhibits a prolonged pharmacodynamic profile. Analysis of plasma LPA concentrations from LLC- or GL261-tumor bearing mice before and immediately following treatment revealed no statistical difference in LPA levels among mice treated with vehicle or the $cPLA_2$ inhibitor, CDIBA. These results indicate that the inhibition of $cPLA_2$ may directly attenuate LPC production, rather than LPA generation. In addition, since LPA can also be generated independently of LPC by a variety of other than $cPLA_2$ enzymes including PLD, PLA_1, and secretory PLA_2, reduced LPC levels do not always correlate with decreased LPA production (Aoki et al., 2008; Gaits et al., 1997). Thus, the investigation of CDIBA treatment on LPC production *in vivo* may serve as a new direction for future studies.

These findings support previous studies that showed decreased tumorigenesis in the absence of $cPLA_2$ (Meyer et al., 2004; Weiser-Evans et al., 2009). In a recent study, $cPLA_2\alpha^{-/-}$ mice were shown to exhibit decreased lung tumor metastasis as a result of attenuated levels of IL-6 and tumor-associated macrophages surrounding the tumor (Weiser-Evans et al., 2009). However, tumor blood vessel formation was not considered in that impaired tumorigenesis. Thus, we analyzed the role of $cPLA_2$ in

tumor vascularization in $cPLA_2\alpha^{+/+}$ and $cPLA_2\alpha^{-/-}$ mice. In the syngeneic heterotopic lung tumor model, we observed a significant reduction in tumor volume in $cPLA_2\alpha^{-/-}$ mice compared to $cPLA_2\alpha^{+/+}$ mice. Furthermore, spontaneous lung tumor regression was observed in 50% of $cPLA_2\alpha^{-/-}$ mice with no regression in wild-type mice. Upon histological examination of the remaining tumors, a significant reduction in vascularity was observed in tumors from $cPLA_2\alpha^{-/-}$ mice. Furthermore, immunofluorescence staining revealed a distinct clustered pattern of desmin-positive cells and a striking absence of α-SMA pericyte coverage in the tumor vasculature of $cPLA_2\alpha^{-/-}$ mice. Since previous studies have shown that tumor pericytes can regulate vessel integrity, maintenance, and function, the observed alterations in desmin and α-SMA staining in the tumor vasculature of $cPLA_2\alpha^{-/-}$ mice may indicate that $cPLA_2$ is also involved in pericyte recruitment and tumor vessel maturation (Bergers and Song, 2005; Gerhardt and Betsholtz, 2003; Morikawa et al., 2002; Rucker et al., 2000; Sennino et al., 2007). In addition, multiple areas of necrosis were present in tumors from $cPLA_2\alpha^{-/-}$ mice, but only minimal necrosis was detected in lung tumors from $cPLA_2\alpha^{+/+}$ mice, confirming that $cPLA_2$ contributes to tumor vascularization and its deficiency leads to massive necrosis of tumor tissue. An even greater suppression of tumor growth was observed in the glioblastoma tumor model. In the GL261 study, normal tumor progression occurred in $cPLA_2\alpha^{+/+}$ mice, however, tumor formation in $cPLA_2\alpha^{-/-}$ mice remained undetectable one month after the injection of tumor cells. Thus, these results suggest that the presence of $cPLA_2$ within the host component of cancer contributes to efficient tumor development. However, since $cPLA_2$ is also responsible for the production of arachidonic acid, future studies regarding the role of eicosanoids in $cPLA_2$-mediated tumor progression are needed to determine the mechanism *in vivo*.

These findings implicate a key role for $cPLA_2$ and lysophospholipids in the invasive migration, proliferation, and morphogenesis of vascular endothelial cells. In addition, we found that in mouse tumor models, despite the presence of $cPLA_2$ within tumor cells, $cPLA_2$ deficiency within the host component resulted in a delayed tumor growth and impaired tumor vascularization. Thus, these data identify $cPLA_2$ as an important factor in tumor angiogenesis and suggest that $cPLA_2$ may be a novel molecular target for anti-angiogenesis cancer therapy.

This work is submitted as:
Linkous AG, Hallahan DE, Yazlovitskaya EM. Cytosolic phospholipase A2 and lysophospholipids in tumor angiogenesis. *Journal of the National Cancer Institute*; (Resubmitted).

CHAPTER VII

CONCLUDING REMARKS

This dissertation describes novel findings in the fields of radiation biology and tumor angiogenesis. Results from this study identify $cPLA_2$ as a critical component in the formation, development, and radioresistance of tumor vasculature. Moreover, these significant findings are specifically applicable to poor prognosis cancers such as lung cancer and glioblastoma.

While previous studies have shown that $cPLA_2$ and arachidonic acid are associated with tumor progression, the present study provides evidence that $cPLA_2$ promotes tumor angiogenesis and resistance to radiation through a lysophospholipid-mediated mechanism. These data implicate key regulatory roles for $cPLA_2$ and the lysophospholipids LPC and LPA in the invasive migration, proliferation, and morphogenesis of vascular endothelial cells. In addition, we show that, despite the presence of $cPLA_2$ within tumor cells, $cPLA_2$ deficiency within the host component results in delayed tumor growth, impaired tumor vascularization, and decreased pericyte development in tumor blood vessels. Thus, these clinically-relevant findings identify $cPLA_2$ and lysophospholipids as important molecular targets for angiogenic blockade and tumor sensitization to radiation therapy.

In recent years, several angiogenesis inhibitors have enhanced cancer outcomes. However, the transitory improvement provided by these agents is often followed by increased tumor resistance and metastasis. The observed resistance may be partially explained by the complex network of signal transduction that constitutes the angiogenic process. The frequent interconnectivity of these signaling pathways

often results in redundancy during the formation of tumor blood vessels. As a result, when one pro-angiogenic target is inhibited, other pathways can be upregulated so that the tumor's requirement for vascularization is once again fulfilled. Thus, the most effective therapeutic strategy may be to target multiple angiogenic pathways using combined therapies. Work from this dissertation provides extensive evidence that $cPLA_2$, LPC, and LPA may serve as effective molecular targets for the combined inhibition of tumor angiogenesis.

In addition to its role in angiogenesis, $cPLA_2$ also contributes to the radioresistance of tumor vasculature. This decreased sensitivity to radiation therapy significantly diminishes treatment success rates in two poor prognosis malignancies, lung cancer and glioblastoma. The work presented in this dissertation helped elucidate the molecular mechanism by which the bioactive lipid second messenger LPC contributes to the radiation-dependent activation of the PI3K/Akt and ERK1/2 pathways. Furthermore, work performed in Chapter V illustrated that the autotaxin-mediated conversion of LPC to LPA may also activate pro-survival signaling through the LPA1 and LPA2 receptors. However, due to the variety of ligands that bind to the EDG family of receptors, future studies are needed to determine which receptors are involved in the radiation response. For example, signal transduction from the LPA receptors following irradiation must be studied. Secondly, the role of arachidonic acid and downstream signaling (COX2) must be considered in concert with LPC and LPA signaling.

One other potential area of research is the study of the normal tissue response to radiation therapy in the $cPLA_2$ knockout mouse. We expect that normal vascular endothelium within the lungs, intestine and other organs will demonstrate greater radiosensitivity in these knockout mice. This unanswered question has clinical

implications when considering $cPLA_2$ as a molecular target for development of radiation sensitizing drugs.

In summary, the work described in this dissertation has shown that, in addition to its role in inflammation and the well-characterized arachidonic acid pathway, $cPLA_2$ is also important for radiation-induced signal transduction and tumor vasculature development. These findings have significantly contributed to the mechanistic understanding of vascular endothelial radioresistance and tumor angiogenesis, and have identified a variety of novel molecular targets for future therapeutic intervention.

REFERENCES

Alles JU, and Bosslet K (**1988**) Immunocytochemistry of angiosarcomas. A study of 19 cases with special emphasis on the applicability of endothelial cell specific markers to routinely prepared tissues. **American journal of clinical pathology**. 89, 463-471

Ambesi A, and McKeown-Longo PJ (**2009**) Anastellin, the angiostatic fibronectin peptide, is a selective inhibitor of lysophospholipid signaling. **Mol Cancer Res**. 7, 255-265

Amir E, Hughes S, Blackhall F, Thatcher N, Ostoros G, Timar J, Tovari J, Kovacs G, and Dome B (**2008**) Targeting blood vessels for the treatment of non-small cell lung cancer. **Current cancer drug targets**. 8, 392-403

Aoki J (**2004**) Mechanisms of lysophosphatidic acid production. **Semin Cell Dev Biol**. 15, 477-489

Aoki J, Inoue A, and Okudaira S (**2008**) Two pathways for lysophosphatidic acid production. **Biochimica et biophysica acta**. 1781, 513-518

Arany I, and Safirstein RL (**2003**) Cisplatin nephrotoxicity. **Seminars in nephrology**. 23, 460-464

Belani CP, Choy H, Bonomi P, Scott C, Travis P, Haluschak J, and Curran WJ, Jr. (**2005**) Combined chemoradiotherapy regimens of paclitaxel and carboplatin for locally advanced non-small-cell lung cancer: a randomized phase II locally advanced multi-modality protocol. **J Clin Oncol**. 23, 5883-5891

Bergers G, and Hanahan D (**2008**) Modes of resistance to anti-angiogenic therapy. **Nat Rev Cancer**. 8, 592-603

Bergers G, and Song S (**2005**) The role of pericytes in blood-vessel formation and maintenance. **Neuro Oncol**. 7, 452-464

Berns JS, and Ford PA (**1997**) Renal toxicities of antineoplastic drugs and bone marrow transplantation. **Seminars in nephrology**. 17, 54-66

Bligh EG, and Dyer WJ (**1959**) A rapid method of total lipid extraction and purification. **Canadian journal of biochemistry and physiology**. 37, 911-917

Bonventre JV (**1999**) The 85-kD cytosolic phospholipase A2 knockout mouse: a new tool for physiology and cell biology. **J Am Soc Nephrol**. 10, 404-412

Brock MV, Hooker CM, Ota-Machida E, Han Y, Guo M, Ames S, Glockner S, Piantadosi S, Gabrielson E, Pridham G, Pelosky K, Belinsky SA, Yang SC, Baylin SB, and Herman JG (**2008**) DNA methylation markers and early recurrence in stage I lung cancer. **The New England journal of medicine**. 358, 1118-1128

Cabral GA (**2005**) Lipids as bioeffectors in the immune system. **Life Sci**. 77, 1699-1710

Calzada C, Vericel E, Mitel B, Coulon L, and Lagarde M (**2001**) 12(S)-Hydroperoxy-eicosatetraenoic acid increases arachidonic acid availability in collagen-primed platelets. **Journal of lipid research**. 42, 1467-1473

Carson-Walter EB, Watkins DN, Nanda A, Vogelstein B, Kinzler KW, and St Croix B (**2001**) Cell surface tumor endothelial markers are conserved in mice and humans. **Cancer research**. 61, 6649-6655

Castedo M, Perfettini JL, Roumier T, Andreau K, Medema R, and Kroemer G (**2004**) Cell death by mitotic catastrophe: a molecular definition. **Oncogene**. 23, 2825-2837

Castedo M, Perfettini JL, Roumier T, and Kroemer G (**2002**) Cyclin-dependent kinase-1: linking apoptosis to cell cycle and mitotic catastrophe. **Cell Death Differ**. 9, 1287-1293

Chakraborti S (**2003**) Phospholipase A(2) isoforms: a perspective. **Cell Signal**. 15, 637-665

Clamon G, Herndon J, Cooper R, Chang AY, Rosenman J, and Green MR (**1999**) Radiosensitization with carboplatin for patients with unresectable stage III non-small-cell lung cancer: a phase III trial of the Cancer and Leukemia Group B and the Eastern Cooperative Oncology Group. **J Clin Oncol**. 17, 4-11

Clark JD, Lin LL, Kriz RW, Ramesha CS, Sultzman LA, Lin AY, Milona N, and Knopf JL (**1991**) A novel arachidonic acid-selective cytosolic PLA2 contains a Ca(2+)-dependent translocation domain with homology to PKC and GAP. **Cell**. 65, 1043-1051

de Bouard S, Herlin P, Christensen JG, Lemoisson E, Gauduchon P, Raymond E, and Guillamo JS (**2007**) Antiangiogenic and anti-invasive effects of sunitinib on experimental human glioblastoma. **Neuro Oncol**. 9, 412-423

DeAngelis LM (**2001**) Brain tumors. **The New England journal of medicine**. 344, 114-123

Dent P, Yacoub A, Contessa J, Caron R, Amorino G, Valerie K, Hagan MP, Grant S, and Schmidt-Ullrich R (**2003a**) Stress and radiation-induced activation of multiple intracellular signaling pathways. **Radiation Research**. 159, 283-300

Dent P, Yacoub A, Contessa J, Caron R, Amorino G, Valerie K, Hagan MP, Grant S, and Schmidt-Ullrich R (**2003b**) Stress and radiation-induced activation of multiple intracellular signaling pathways. **Radiat Res**. 159, 283-300

Dent P, Yacoub A, Fisher PB, Hagan MP, and Grant S (**2003c**) MAPK pathways in radiation responses. **Oncogene**. 22, 5885-5896

Dewhirst MW, Cao Y, and Moeller B (**2008**) Cycling hypoxia and free radicals regulate angiogenesis and radiotherapy response. **Nature reviews**. 8, 425-437

Dietz A, Boehm A, Mozet C, Wichmann G, and Giannis A (**2008**) Current aspects of targeted therapy in head and neck tumors. **Eur Arch Otorhinolaryngol**

Duan L, Gan H, Arm J, and Remold HG (**2001**) Cytosolic phospholipase A2 participates with TNF-alpha in the induction of apoptosis of human macrophages infected with Mycobacterium tuberculosis H37Ra. **J Immunol**. 166, 7469-7476

Edwards E, Geng L, Tan J, Onishko H, Donnelly E, and Hallahan DE (**2002**) Phosphatidylinositol 3-kinase/Akt signaling in the response of vascular endothelium to ionizing radiation. **Cancer Res**. 62, 4671-4677

Fabisiak JP, Kagan VE, Tyurina YY, Tyurin VA, and Lazo JS (**1998**) Paraquat-induced phosphatidylserine oxidation and apoptosis are independent of activation of PLA2. **The American journal of physiology**. 274, L793-802

Farooqui AA, and Horrocks LA (**2006**) Phospholipase A2-generated lipid mediators in the brain: the good, the bad, and the ugly. **Neuroscientist**. 12, 245-260

Farooqui AA, Ong WY, and Horrocks LA (**2006**) Inhibitors of brain phospholipase A2 activity: their neuropharmacological effects and therapeutic importance for the treatment of neurologic disorders. **Pharmacological reviews**. 58, 591-620

Folkman J (**1971**) Tumor angiogenesis: therapeutic implications. **The New England journal of medicine**. 285, 1182-1186

Folkman J (**2001**) A new link in ovarian cancer angiogenesis: lysophosphatidic acid and vascular endothelial growth factor expression. **J Natl Cancer Inst**. 93, 734-735

Forastiere AA, Trotti A, Pfister DG, and Grandis JR (**2006**) Head and neck cancer: recent advances and new standards of care. **Journal of Clinical Oncology**. 24, 2603-2605

Fujita Y, Yoshizumi M, Izawa Y, Ali N, Ohnishi H, Kanematsu Y, Ishizawa K, Tsuchiya K, and Tamaki T (**2006**) Transactivation of fetal liver kinase-1/kinase-insert domain-containing receptor by lysophosphatidylcholine induces vascular endothelial cell proliferation. **Endocrinology**. 147, 1377-1385

Gaits F, Fourcade O, Le Balle F, Gueguen G, Gaige B, Gassama-Diagne A, Fauvel J, Salles JP, Mauco G, Simon MF, and Chap H (**1997**) Lysophosphatidic acid as a phospholipid mediator: pathways of synthesis. **FEBS letters**. 410, 54-58

Geng L, Donnelly E, McMahon G, Lin PC, Sierra-Rivera E, Oshinka H, and Hallahan DE (**2001**) Inhibition of vascular endothelial growth factor receptor signaling leads to reversal of tumor resistance to radiotherapy. **Cancer Res**. 61, 2413-2419

Geng L, Tan J, Himmelfarb E, Schueneman A, Niermann K, Brousal J, Fu A, Cuneo K, Kesicki EA, Treiberg J, Hayflick JS, and Hallahan DE (**2004**) A specific antagonist of the p110delta catalytic component of phosphatidylinositol 3'-kinase, IC486068, enhances radiation-induced tumor vascular destruction. **Cancer Res**. 64, 4893-4899

Gerhardt H, and Betsholtz C (**2003**) Endothelial-pericyte interactions in angiogenesis. **Cell Tissue Res**. 314, 15-23

Goertz DE, Yu JL, Kerbel RS, Burns PN, and Foster FS (**2002**) High-frequency Doppler ultrasound monitors the effects of antivascular therapy on tumor blood flow. **Cancer research**. 62, 6371-6375

Goldstein RS, and Mayor GH (**1983**) Minireview. The nephrotoxicity of cisplatin. **Life sciences**. 32, 685-690

Goodwin AM (**2007**) In vitro assays of angiogenesis for assessment of angiogenic and anti-angiogenic agents. **Microvasc Res**. 74, 172-183

Grewal S, Herbert SP, Ponnambalam S, and Walker JH (**2005**) Cytosolic phospholipase A2-alpha and cyclooxygenase-2 localize to intracellular membranes of

EA.hy.926 endothelial cells that are distinct from the endoplasmic reticulum and the Golgi apparatus. **The FEBS journal**. 272, 1278-1290

Grosse-Wilde A, Voloshanenko O, Bailey SL, Longton GM, Schaefer U, Csernok AI, Schutz G, Greiner EF, Kemp CJ, and Walczak H (**2008**) TRAIL-R deficiency in mice enhances lymph node metastasis without affecting primary tumor development. **J Clin Invest**. 118, 100-110

Haimovitz-Friedman A, Kan CC, Ehleiter D, Persaud RS, McLoughlin M, Fuks Z, and Kolesnick RN (**1994**) Ionizing radiation acts on cellular membranes to generate ceramide and initiate apoptosis. **J Exp Med**. 180, 525-535

Hama K, Aoki J, Fukaya M, Kishi Y, Sakai T, Suzuki R, Ohta H, Yamori T, Watanabe M, Chun J, and Arai H (**2004**) Lysophosphatidic acid and autotaxin stimulate cell motility of neoplastic and non-neoplastic cells through LPA1. **The Journal of biological chemistry**. 279, 17634-17639

Herbert SP, Odell AF, Ponnambalam S, and Walker JH (**2007**) The confluence-dependent interaction of cytosolic phospholipase A2-alpha with annexin A1 regulates endothelial cell prostaglandin E2 generation. **The Journal of biological chemistry**. 282, 34468-34478

Herbert SP, Odell AF, Ponnambalam S, and Walker JH (**2009**) Activation of Cytosolic Phospholipase A2-{alpha} as a Novel Mechanism Regulating Endothelial Cell Cycle Progression and Angiogenesis. **J Biol Chem**. 284, 5784-5796

Herbert SP, Ponnambalam S, and Walker JH (**2005**) Cytosolic phospholipase A2-alpha mediates endothelial cell proliferation and is inactivated by association with the Golgi apparatus. **Molecular biology of the cell**. 16, 3800-3809

Hirabayashi T, Murayama T, and Shimizu T (**2004**) Regulatory mechanism and physiological role of cytosolic phospholipase A2. **Biol Pharm Bull**. 27, 1168-1173

Hirabayashi T, and Shimizu T (**2000**) Localization and regulation of cytosolic phospholipase A(2). **Biochimica et biophysica acta**. 1488, 124-138

Hoffman PC, Mauer AM, and Vokes EE (**2000**) Lung cancer. **Lancet**. 355, 479-485

Hwang A, and Muschel RJ (**1998**) Radiation and the G2 phase of the cell cycle. **Radiat Res**. 150, S52-59

Ianzini F, Bertoldo A, Kosmacek EA, Phillips SL, and Mackey MA (**2006**) Lack of p53 function promotes radiation-induced mitotic catastrophe in mouse embryonic fibroblast cells. **Cancer Cell Int**. 6, 11

Iranzo V, Bremnes RM, Almendros P, Gavila J, Blasco A, Sirera R, and Camps C (**2008**) Induction chemotherapy followed by concurrent chemoradiation for patients with non-operable stage III non-small-cell lung cancer. **Lung cancer (Amsterdam, Netherlands)**

Jansen S, Stefan C, Creemers JW, Waelkens E, Van Eynde A, Stalmans W, and Bollen M (**2005**) Proteolytic maturation and activation of autotaxin (NPP2), a secreted metastasis-enhancing lysophospholipase D. **Journal of cell science**. 118, 3081-3089

Keshet E, and Ben-Sasson SA (**1999**) Anticancer drug targets: approaching angiogenesis. **J Clin Invest**. 104, 1497-1501

Kirschnek S, and Gulbins E (**2006**) Phospholipase A2 functions in Pseudomonas aeruginosa-induced apoptosis. **Infection and immunity**. 74, 850-860

Kishi Y, Okudaira S, Tanaka M, Hama K, Shida D, Kitayama J, Yamori T, Aoki J, Fujimaki T, and Arai H (**2006**) Autotaxin is overexpressed in glioblastoma multiforme and contributes to cell motility of glioblastoma by converting lysophosphatidylcholine to lysophosphatidic acid. **The Journal of biological chemistry**. 281, 17492-17500

Kolesnick R, and Fuks Z (**2003**) Radiation and ceramide-induced apoptosis. **Oncogene**. 22, 5897-5906

Kramer A, Lukas J, and Bartek J (**2004**) Checking out the centrosome. **Cell Cycle**. 3, 1390-1393

Kufe D, and Weichselbaum R (**2003**) Radiation therapy: activation for gene transcription and the development of genetic radiotherapy-therapeutic strategies in oncology. **Cancer Biol Ther**. 2, 326-329

Lee JH, Machtay M, Kaiser LR, Friedberg JS, Hahn SM, McKenna MG, and McKenna WG (**1999**) Non-small cell lung cancer: prognostic factors in patients treated with surgery and postoperative radiation therapy. **Radiology**. 213, 845-852

Levy AP, Levy NS, Wegner S, and Goldberg MA (**1995a**) Transcriptional regulation of the rat vascular endothelial growth factor gene by hypoxia. **J Biol Chem**. 270, 13333-13340

Levy AP, Levy NS, Wegner S, and Goldberg MA (**1995b**) Transcriptional regulation of the rat vascular endothelial growth factor gene by hypoxia. **Journal of Biological Chemistry**. 270, 13333-13340

Linkous A, Geng L, Lyshchik A, Hallahan DE, and Yazlovitskaya EM (**2009**) Cytosolic Phospholipase A2: Targeting Cancer through the Tumor Vasculature. **Clin Cancer Res**. 15, 1635-1644

Mackall CL (**2000**) T-cell immunodeficiency following cytotoxic antineoplastic therapy: a review. **Stem cells (Dayton, Ohio)**. 18, 10-18

Maclachlan T, Narayanan B, Gerlach VL, Smithson G, Gerwien RW, Folkerts O, Fey EG, Watkins B, Seed T, and Alvarez E (**2005**) Human fibroblast growth factor 20 (FGF-20; CG53135-05): a novel cytoprotectant with radioprotective potential. **Int J Radiat Biol**. 81, 567-579

Marathe GK, Silva AR, de Castro Faria Neto HC, Tjoelker LW, Prescott SM, Zimmerman GA, and McIntyre TM (**2001**) Lysophosphatidylcholine and lyso-PAF display PAF-like activity derived from contaminating phospholipids. **Journal of lipid research**. 42, 1430-1437

Martini N, Bains MS, Burt ME, Zakowski MF, McCormack P, Rusch VW, and Ginsberg RJ (**1995**) Incidence of local recurrence and second primary tumors in resected stage I lung cancer. **J Thorac Cardiovasc Surg**. 109, 120-129

McGinn CJ, Shewach DS, and Lawrence TS (**1996**) Radiosensitizing nucleosides. **Journal of the National Cancer Institute**. 88, 1193-1203

McKew JC, Foley MA, Thakker P, Behnke ML, Lovering FE, Sum FW, Tam S, Wu K, Shen MW, Zhang W, Gonzalez M, Liu S, Mahadevan A, Sard H, Khor SP, and Clark JD (**2006**) Inhibition of cytosolic phospholipase A2alpha: hit to lead optimization. **J Med Chem**. 49, 135-158

Meyer AM, Dwyer-Nield LD, Hurteau GJ, Keith RL, O'Leary E, You M, Bonventre JV, Nemenoff RA, and Malkinson AM (**2004**) Decreased lung tumorigenesis in mice genetically deficient in cytosolic phospholipase A2. **Carcinogenesis**. 25, 1517-1524

Mikkelsen RB, and Wardman P (**2003**) Biological chemistry of reactive oxygen and nitrogen and radiation-induced signal transduction mechanisms. **Oncogene**. 22, 5734-5754

Morikawa S, Baluk P, Kaidoh T, Haskell A, Jain RK, and McDonald DM (**2002**) Abnormalities in pericytes on blood vessels and endothelial sprouts in tumors. **Am J Pathol**. 160, 985-1000

Mountain CF (**1997**) Revisions in the International System for Staging Lung Cancer. **Chest**. 111, 1710-1717

Murph M, and Mills GB (**2007**) Targeting the lipids LPA and S1P and their signalling pathways to inhibit tumour progression. **Expert Rev Mol Med**. 9, 1-18

Murugesan G, Sandhya Rani MR, Gerber CE, Mukhopadhyay C, Ransohoff RM, Chisolm GM, and Kottke-Marchant K (**2003**) Lysophosphatidylcholine regulates human microvascular endothelial cell expression of chemokines. **J Mol Cell Cardiol**. 35, 1375-1384

Nakanishi M, and Rosenberg DW (**2006**) Roles of cPLA2alpha and arachidonic acid in cancer. **Biochimica et Biophysica Acta**. 1761, 1335-1343

Nam SW, Clair T, Kim YS, McMarlin A, Schiffmann E, Liotta LA, and Stracke ML (**2001**) Autotaxin (NPP-2), a metastasis-enhancing motogen, is an angiogenic factor. **Cancer research**. 61, 6938-6944

Pelevina, II, Gotlib V, and Konradov AA (**2006**) [20 years after Chernobyl accident--is it a lot or not for the estimation its characteristics ?]. **Radiats Biol Radioecol**. 46, 240-247

Peyruchaud O (**2009**) Novel implications for lysophospholipids, lysophosphatidic acid and sphingosine 1-phosphate, as drug targets in cancer. **Anticancer Agents Med Chem**. 9, 381-391

Pierce DA, Shimizu Y, Preston DL, Vaeth M, and Mabuchi K (**1996**) Studies of the mortality of atomic bomb survivors. Report 12, Part I. Cancer: 1950-1990. **Radiat Res**. 146, 1-27

Plate KH, and Risau W (**1995**) Angiogenesis in malignant gliomas. **Glia**. 15, 339-347

Pozzi A, Moberg PE, Miles LA, Wagner S, Soloway P, and Gardner HA (**2000**) Elevated matrix metalloprotease and angiostatin levels in integrin alpha 1 knockout mice cause reduced tumor vascularization. **Proceedings of the National Academy of Sciences of the United States of America**. 97, 2202-2207

Prokazova NV, Zvezdina ND, and Korotaeva AA (**1998**) Effect of lysophosphatidylcholine on transmembrane signal transduction. **Biochemistry (Mosc)**. 63, 31-37

Ptaszynska MM, Pendrak ML, Bandle RW, Stracke ML, and Roberts DD (**2008**) Positive feedback between vascular endothelial growth factor-A and autotaxin in ovarian cancer cells. **Mol Cancer Res**. 6, 352-363

Pusztaszeri MP, Seelentag W, and Bosman FT (**2006**) Immunohistochemical expression of endothelial markers CD31, CD34, von Willebrand factor, and Fli-1 in normal human tissues. **J Histochem Cytochem**. 54, 385-395

Ren J, Xiao YJ, Singh LS, Zhao X, Zhao Z, Feng L, Rose TM, Prestwich GD, and Xu Y (**2006**) Lysophosphatidic acid is constitutively produced by human peritoneal mesothelial cells and enhances adhesion, migration, and invasion of ovarian cancer cells. **Cancer research**. 66, 3006-3014

Ricci MS, and Zong WX (**2006**) Chemotherapeutic approaches for targeting cell death pathways. **Oncologist**. 11, 342-357

Riely GJ, and Miller VA (**2007**) Vascular endothelial growth factor trap in non small cell lung cancer. **Clin Cancer Res**. 13, s4623-4627

Rodel F, Keilholz L, Herrmann M, Sauer R, and Hildebrandt G (**2007**) Radiobiological mechanisms in inflammatory diseases of low-dose radiation therapy. **Int J Radiat Biol**. 83, 357-366

Rucker HK, Wynder HJ, and Thomas WE (**2000**) Cellular mechanisms of CNS pericytes. **Brain Res Bull**. 51, 363-369

Sennino B, Falcon BL, McCauley D, Le T, McCauley T, Kurz JC, Haskell A, Epstein DM, and McDonald DM (**2007**) Sequential loss of tumor vessel pericytes and endothelial cells after inhibition of platelet-derived growth factor B by selective aptamer AX102. **Cancer research**. 67, 7358-7367

Shweiki D, Neeman M, Itin A, and Keshet E (**1995**) Induction of vascular endothelial growth factor expression by hypoxia and by glucose deficiency in multicell spheroids: implications for tumor angiogenesis. **Proceedings of the National Academy of Sciences of the United States of America**. 92, 768-772

St Croix B, Rago C, Velculescu V, Traverso G, Romans KE, Montgomery E, Lal A, Riggins GJ, Lengauer C, Vogelstein B, and Kinzler KW (**2000**) Genes expressed in human tumor endothelium. **Science (New York, NY**. 289, 1197-1202

Stracke ML, Krutzsch HC, Unsworth EJ, Arestad A, Cioce V, Schiffmann E, and Liotta LA (**1992**) Identification, purification, and partial sequence analysis of autotaxin, a novel motility-stimulating protein. **The Journal of biological chemistry**. 267, 2524-2529

Stratford IJ (**1992**) Concepts and developments in radiosensitization of mammalian cells. **International journal of radiation oncology, biology, physics**. 22, 529-532

Street IP, Lin HK, Laliberte F, Ghomashchi F, Wang Z, Perrier H, Tremblay NM, Huang Z, Weech PK, and Gelb MH (**1993**) Slow- and tight-binding inhibitors of the 85-kDa human phospholipase A2. **Biochemistry**. 32, 5935-5940

Strijbos MH, Gratama JW, Kraan J, Lamers CH, den Bakker MA, and Sleijfer S (**2008**) Circulating endothelial cells in oncology: pitfalls and promises. **British journal of cancer**. 98, 1731-1735

Stupp R, Hegi ME, Mason WP, van den Bent MJ, Taphoorn MJ, Janzer RC, Ludwin SK, Allgeier A, Fisher B, Belanger K, Hau P, Brandes AA, Gijtenbeek J, Marosi C, Vecht CJ, Mokhtari K, Wesseling P, Villa S, Eisenhauer E, Gorlia T, Weller M, Lacombe D, Cairncross JG, and Mirimanoff RO (**2009**) Effects of radiotherapy with concomitant and adjuvant temozolomide versus radiotherapy alone on survival in glioblastoma in a randomised phase III study: 5-year analysis of the EORTC-NCIC trial. **The lancet oncology**. 10, 459-466

Sugiyama S, Kugiyama K, Ogata N, Doi H, Ota Y, Ohgushi M, Matsumura T, Oka H, and Yasue H (**1998**) Biphasic regulation of transcription factor nuclear factor-kappaB activity in human endothelial cells by lysophosphatidylcholine through protein kinase C-mediated pathway. **Arterioscler Thromb Vasc Biol**. 18, 568-576

Suh JH, and Barnett GH (**1999**) Brachytherapy for brain tumor. **Hematology/oncology clinics of North America**. 13, 635-650, viii-ix

Tan J, Geng L, Yazlovitskaya EM, and Hallahan DE (**2006**) Protein kinase B/Akt-dependent phosphorylation of glycogen synthase kinase-3beta in irradiated vascular endothelium. **Cancer Res**. 66, 2320-2327

Tan J, and Hallahan DE (**2003**) Growth factor-independent activation of protein kinase B contributes to the inherent resistance of vascular endothelium to radiation-induced apoptotic response. **Cancer Res**. 63, 7663-7667

Tanaka M, Okudaira S, Kishi Y, Ohkawa R, Iseki S, Ota M, Noji S, Yatomi Y, Aoki J, and Arai H (**2006**) Autotaxin stabilizes blood vessels and is required for embryonic vasculature by producing lysophosphatidic acid. **J Biol Chem**. 281, 25822-25830

Teplyuk NM, Galindo M, Teplyuk VI, Pratap J, Young DW, Lapointe D, Javed A, Stein JL, Lian JB, Stein GS, and van Wijnen AJ (**2008**) Runx2 regulates G protein-coupled signaling pathways to control growth of osteoblast progenitors. **J Biol Chem**. 283, 27585-27597

Tokumura A, Harada K, Fukuzawa K, and Tsukatani H (**1986**) Involvement of lysophospholipase D in the production of lysophosphatidic acid in rat plasma. **Biochimica et Biophysica Acta**. 875, 31-38

Tokuuye K, Akine Y, Sumi M, Kagami Y, Ikeda H, Oyama H, Inou Y, Shibui S, and Nomura K (**1998**) Reirradiation of brain and skull base tumors with fractionated stereotactic radiotherapy. **International journal of radiation oncology, biology, physics**. 40, 1151-1155

Trimble LA, Street IP, Perrier H, Tremblay NM, Weech PK, and Bernstein MA (**1993**) NMR structural studies of the tight complex between a trifluoromethyl ketone inhibitor and the 85-kDa human phospholipase A2. **Biochemistry**. 32, 12560-12565

Truman JP, Gueven N, Lavin M, Leibel S, Kolesnick R, Fuks Z, and Haimovitz-Friedman A (**2005**) Down-regulation of ATM protein sensitizes human prostate cancer cells to radiation-induced apoptosis. **J Biol Chem**. 280, 23262-23272

Tsutsumi H, Kumagai T, Naitoo S, Ebina K, and Yokota K (**2006**) Synthetic peptide (P-21) derived from Asp-hemolysin inhibits the induction of apoptosis on HUVECs by lysophosphatidylcholine. **Biol Pharm Bull**. 29, 907-910

Umezu-Goto M, Kishi Y, Taira A, Hama K, Dohmae N, Takio K, Yamori T, Mills GB, Inoue K, Aoki J, and Arai H (**2002**) Autotaxin has lysophospholipase D activity leading to tumor cell growth and motility by lysophosphatidic acid production. **The Journal of cell biology**. 158, 227-233

Upton AC (**1990**) Carcinogenic effects of low-level ionizing radiation. **J Natl Cancer Inst**. 82, 448-449

Valerie K, Yacoub A, Hagan MP, Curiel DT, Fisher PB, Grant S, and Dent P (**2007**) Radiation-induced cell signaling: inside-out and outside-in. **Mol Cancer Ther**. 6, 789-801

Valko M, Leibfritz D, Moncol J, Cronin MT, Mazur M, and Telser J (**2007**) Free radicals and antioxidants in normal physiological functions and human disease. **Int J Biochem Cell Biol**. 39, 44-84

van Meeteren LA, and Moolenaar WH (**2007**) Regulation and biological activities of the autotaxin-LPA axis. **Prog Lipid Res**. 46, 145-160

Videtic GM, Gaspar LE, Zamorano L, Fontanesi J, Levin KJ, Kupsky WJ, and Tekyi-Mensah S (**1999**) Use of the RTOG recursive partitioning analysis to validate the benefit of iodine-125 implants in the primary treatment of malignant gliomas. **International journal of radiation oncology, biology, physics**. 45, 687-692

Wachsberger P, Burd R, and Dicker AP (**2003**) Tumor response to ionizing radiation combined with antiangiogenesis or vascular targeting agents: exploring mechanisms of interaction. **Clin Cancer Res**. 9, 1957-1971

Wagner H, Jr. (**2000**) Postoperative adjuvant therapy for patients with resected non-small cell lung cancer: still controversial after all these years. **Chest**. 117, 110S-118S

Walter-Yohrling J, Morgenbesser S, Rouleau C, Bagley R, Callahan M, Weber W, and Teicher BA (**2004**) Murine endothelial cell lines as models of tumor endothelial cells. **Clin Cancer Res**. 10, 2179-2189

Wang H, Li M, Rinehart JJ, and Zhang R (**2004**) Pretreatment with dexamethasone increases antitumor activity of carboplatin and gemcitabine in mice bearing human cancer xenografts: in vivo activity, pharmacokinetics, and clinical implications for cancer chemotherapy. **Clin Cancer Res**. 10, 1633-1644

Weiser-Evans MC, Wang XQ, Amin J, Van Putten V, Choudhary R, Winn RA, Scheinman R, Simpson P, Geraci MW, and Nemenoff RA (**2009**) Depletion of Cytosolic Phospholipase A2 in Bone Marrow-Derived Macrophages Protects against Lung Cancer Progression and Metastasis. **Cancer research**. 69, 1733-1738

Wong ET, and Brem S (**2007**) Taming glioblastoma: targeting angiogenesis. **J Clin Oncol**. 25, 4705-4706

Yamamoto K, de Waard V, Fearns C, and Loskutoff DJ (**1998**) Tissue distribution and regulation of murine von Willebrand factor gene expression in vivo. **Blood**. 92, 2791-2801

Yazlovitskaya EM, Linkous AG, Thotala DK, Cuneo KC, and Hallahan DE (**2008**) Cytosolic phospholipase A2 regulates viability of irradiated vascular endothelium. **Cell death and differentiation**. 15, 1641-1653

Zhan M, and Han ZC (**2004**) Phosphatidylinositide 3-kinase/AKT in radiation responses. **Histology and histopathology**. 19, 915-923

Zhang H, Xu X, Gajewiak J, Tsukahara R, Fujiwara Y, Liu J, Fells JI, Perygin D, Parrill AL, Tigyi G, and Prestwich GD (**2009**) Dual activity lysophosphatidic acid receptor pan-antagonist/autotaxin inhibitor reduces breast cancer cell migration in vitro and causes tumor regression in vivo. **Cancer research**. 69, 5441-5449

Zingg D, Riesterer O, Fabbro D, Glanzmann C, Bodis S, and Pruschy M (**2004**) Differential activation of the phosphatidylinositol 3'-kinase/Akt survival pathway by ionizing radiation in tumor and primary endothelial cells. **Cancer research**. 64, 5398-5406